

---

# Analytical Methods

Alexander Heuser, Anne-Désirée Schmitt,  
Nikolaus Gussone and Frank Wombacher

---

## Abstract

Despite the large relative mass difference between different Ca isotopes, the isotopic variability of Ca in natural materials is relatively small. Consequently, high-precision Ca isotope analyses are required to accurately resolve Ca isotope fractionation prior to data interpretation. This chapter summarises techniques which are successfully used to digest samples and to purify different types of sample material. The basic principles of different mass spectrometric methods for the accurate and precise determination of Ca isotope compositions are presented with a focus on thermal ionisation mass spectrometry (TIMS) and multi-collector inductively coupled plasma mass spectrometry (MC-ICP-MS). We also present an overview about other, less frequently applied techniques used so far. Additionally, we provide useful information on how to report Ca isotope data (e.g. different notations and reference materials) and explain how to convert literature data based on different reference materials and/or given in different notations.

---

## Keywords

Reference materials • Chemical separation • Digestion • Isotope fractionation • Mass spectrometry • TIMS • MC-ICP-MS • Double spike

---

A. Heuser  
Steinmann-Institut für Geologie, Mineralogie und  
Paläontologie, Universität Bonn, Bonn, Germany  
e-mail: aheuser@uni-bonn.de

A.-D. Schmitt  
LHyGeS/EOST, Université de Strasbourg,  
Strasbourg, France  
e-mail: adschmitt@unistra.fr

A.-D. Schmitt  
Laboratoire Chrono-Environnement, Université  
Bourgogne Franche-Comté, Besançon, France

---

N. Gussone (✉)  
Institut für Mineralogie, Universität Münster,  
Münster, Germany  
e-mail: nguss\_01@uni-muenster.de

F. Wombacher  
Institut für Geologie und Mineralogie, Universität zu  
Köln, Köln, Germany  
e-mail: fwombach@uni-koeln.de

## 1 Introduction

Russell et al. (1978) developed a reliable measurement protocol for calcium isotopes using thermal ionization mass spectrometry (TIMS) and a double spike technique. They observed that the natural fractionation of Ca isotopes is generally low (<1.3 ‰ per amu) and that high analytical precision and accuracy is necessary to resolve natural differences in calcium isotope ratios. Despite further advancements in analytical methods, the precision of stable isotope analysis remains a major limitation for Ca stable isotope research.

Accurate mass spectrometry often requests the purification of the sample before Ca isotope analysis. This purification is commonly achieved by ion exchange using column chemistry. Both, column chemistry and mass spectrometry can induce artefacts that have to be avoided or corrected for in order to accurately resolve the natural or experimentally induced Ca isotope fractionation.

In this chapter we provide the basic principles of the applied techniques along with detailed descriptions of methods applied to analyze Ca isotope ratios in different kinds of geological, biological and extraterrestrial samples. These methods include sample specific preparation (cleaning, digestion, and column chemistry), mass spectrometry protocols and data reduction, including the double spike technique.

## 2 Notations and Data Presentation

Looking through the Ca isotope literature shows that different authors use slightly different notations to present their data. This can lead to confusion and makes it difficult to compare literature data. We recommend to follow the IUPAC/IUPAP “guidelines recommended terms for expression of stable-isotope-ratio and gas-ratio measurement results” (Coplen 2011).

### 2.1 $\delta$ -Notation

Variations of the Ca isotopic compositions are very small and thus variations of Ca isotopes are normally expressed using the  $\delta$ -notation. The  $\delta$ -value refers to the deviation of the isotope composition of a sample from that of the reference material (Coplen 2011):

$$\delta^a X = \left( \frac{(^aX/^bX)_{\text{sample}}}{(^aX/^bX)_{\text{reference}}} - 1 \right) \quad (1)$$

where  $^aX$  and  $^bX$  are the isotopes with nominal mass  $a$  and  $b$  of the element  $X$ . By convention, isotope  $^aX$  is always heavier than  $^bX$ . Therefore, positive  $\delta$ -values thus refer to samples being enriched in the heavy isotopes relative to the reference standard; negative values denote light isotope enrichment in the sample relative to the standard. As the variations of the isotopic compositions are small,  $\delta$ -values are typically reported as per mil (‰).

$\delta$  values for Ca isotope variations are typically based on either  $^{44}\text{Ca}/^{40}\text{Ca}$  or  $^{44}\text{Ca}/^{42}\text{Ca}$ . The latter ratio is commonly used if Ca isotope ratios are determined by MC-ICP-MS, where  $^{40}\text{Ar}$  interferes with  $^{40}\text{Ca}$  (cf. Sect. 5.3.3).

Using the common  $\delta$ -notation (Eq. 1) both ratios would be reported as  $\delta^{44}\text{Ca}$ -values. But the stable isotope fractionation in  $^{44}\text{Ca}/^{42}\text{Ca}$  is only about half of the fractionation in  $^{44}\text{Ca}/^{40}\text{Ca}$  (see Eqs. 5 and 7). To circumvent this problem Hippler et al. (2003) and Eisenhauer et al. (2004) defined a  $\delta^{44/4x}\text{Ca}$  ratio which clearly indicates which Ca isotope ratio is used in the  $\delta$ -notation:

$$\delta^{44/40}\text{Ca} = \left( \frac{(^{44}\text{Ca}/^{40}\text{Ca})_{\text{sample}}}{(^{44}\text{Ca}/^{40}\text{Ca})_{\text{reference}}} - 1 \right) \quad (2)$$

$$\delta^{44/42}\text{Ca} = \left( \frac{(^{44}\text{Ca}/^{42}\text{Ca})_{\text{sample}}}{(^{44}\text{Ca}/^{42}\text{Ca})_{\text{reference}}} - 1 \right) \quad (3)$$

These  $\delta$ -notations follow the recommendations of the IUPAC (Coplen 2011). Typically,

$\delta^{44/40}\text{Ca}$  and  $\delta^{44/42}\text{Ca}$  values are reported in per mil (‰, parts per thousand) which means that the  $\delta$ -value obtained by Eqs. 2 and 3 are then multiplied by 1000.  $\delta$ -values reported as parts per ten thousand (pptt) or even parts per million (ppm) can also be found in the literature.

The existence of two different  $\delta$ -notations for Ca with different degrees of fractionation hampers a direct comparison of  $\delta^{44/40}\text{Ca}$  and  $\delta^{44/42}\text{Ca}$  literature values. Fortunately, it is possible to convert  $\delta^{44/40}\text{Ca}$  values to  $\delta^{44/42}\text{Ca}$  values and vice versa. There are three potential problems concerning the conversion of  $\delta$ -values (e.g. from  $\delta^{44/42}\text{Ca}$  to  $\delta^{44/40}\text{Ca}$ ) which can be ignored in many cases:

- (1) The exact relationship between two different  $\delta$ -values depends on the assumed fractionation mechanism.

If one assumes kinetic fractionation based on atomic masses of Ca isotopes (see Young et al. 2002 and Chapter “[Introduction](#)” for discussion),  $\delta^{44/40}\text{Ca}$  values can be converted into  $\delta^{44/42}\text{Ca}$  values and vice versa using the following equation:

$$\delta^{44/40}\text{Ca} \approx \delta^{44/42}\text{Ca} \times \frac{\ln(m^{44}\text{Ca}/m^{40}\text{Ca})}{\ln(m^{44}\text{Ca}/m^{42}\text{Ca})} \quad (4)$$

where  $m^x\text{Ca}$  is the exact atomic mass (given in Chapter “[Introduction](#)”) of the respective isotope. In a good approximation Eq. 4 can be rewritten to:

$$\delta^{44/40}\text{Ca} \approx \delta^{44/42}\text{Ca} \times 2.05 \quad (5)$$

If one assumes equilibrium isotope fractionation for Ca isotopes:

$$\delta^{44/40}\text{Ca} \approx \delta^{44/42}\text{Ca} \times \frac{1/m^{44}\text{Ca} - 1/m^{40}\text{Ca}}{1/m^{44}\text{Ca} - 1/m^{42}\text{Ca}} \quad (6)$$

with  $m^x\text{Ca}$  being the exact atomic mass of the respective isotope. In a good approximation we obtain:

$$\delta^{44/40}\text{Ca} \approx \delta^{44/42}\text{Ca} \times 2.10 \quad (7)$$

Given a  $\delta^{44/42}\text{Ca}$  of 1 ‰, recalculated  $\delta^{44/40}\text{Ca}$  values amount to 2.05 or 2.1 ‰ respectively depending whether Eq. 5 for kinetic isotope fractionation or Eq. 7 for equilibrium isotope fractionation is used. This difference of 0.05 ‰ appears acceptable given current analytical precisions of typically larger than 0.02 ‰ *per u* and the fact that Ca isotope fractionation in nature is usually <1 ‰ for  $\delta^{44/42}\text{Ca}$ .

- (2) The relationship between two  $\delta$ -values is not linear.

The above equations assume a linear relationship between  $\delta^{44/40}\text{Ca}$  and  $\delta^{44/42}\text{Ca}$ , while fractionation lines in conventional three isotope space are curved. However, the error introduced by this linear approximation is negligible. Only extremely large Ca isotope fractionations of more than 6.6 ‰ for  $\delta^{44/42}\text{Ca}$  would result in systematic errors approaching −0.05 for recalculated  $\delta^{44/40}\text{Ca}$ . The error introduced by this linear approximation is not only negligible, it is also much less than the uncertainty introduced by variations in the fractionation mechanism.

- (3)  $^{40}\text{Ca}$  can be variable due to ingrowth from radioactive  $^{40}\text{K}$ .

While  $\delta^{44/42}\text{Ca}$  represents exclusively mass fractionation processes,  $\delta^{44/40}\text{Ca}$  may also be affected by  $^{40}\text{Ca}$  excess (see Sect. 3 in Chapter “[High Temperature Geochemistry and Cosmochemistry](#)”). If radiogenic ingrowth is larger than the analytical precision and more significant than differences introduced by the fractionation mechanism, then it is possible to deconvolute both processes by measuring and representing  $\delta^{44/40}\text{Ca}$  versus  $\delta^{44/42}\text{Ca}$  (Schmitt et al. 2003a, b; Schmitt and Stille 2005; Ryu et al. 2011).

Because of the ambiguity of the  $\delta^{44}\text{Ca}$  notation ( $\delta^{44/40}\text{Ca}$  or  $\delta^{44/42}\text{Ca}$ ), Gussone et al. (2005) proposed an alternative notation and introduced a  $\delta^{\text{mu}}\text{Ca}$  (ppm/amu) such that  $\delta$ -values from different Ca isotope ratios can be directly compared without further recalculation. The superscript *mu*

refers to the fractionation per one atomic mass unit.  $\delta^{\text{mu}}\text{Ca}$  is defined as:

$$\delta^{\text{mu}}\text{Ca} \left( \frac{\text{ppm}}{\text{amu}} \right) = \left( \frac{(^a\text{Ca}/^b\text{Ca})_{\text{sample}}}{(^a\text{Ca}/^b\text{Ca})_{\text{reference}}} - 1 \right) \times 10^6 / (a - b) \quad (8)$$

where  $a$  and  $b$  refer to the exact masses of the isotopes used. Note that unlike in Eqs. 1–3, the conversion factor is considered in order to report the  $\delta$ -value in parts per million. As with  $\delta^{44/42}\text{Ca}$  and  $\delta^{44/40}\text{Ca}$ ,  $\delta^{\text{mu}}\text{Ca}$  obtained from different Ca isotope ratios may differ depending on the fractionation mechanism. The use of  $\delta^{\text{mu}}\text{Ca}$  has not become accepted and should be avoided. The same applies to reporting Ca isotope data as  $\delta^{44/42}\text{Ca}$  in ‰/amu i.e. the calculated  $\delta^{44/42}\text{Ca}$  is divided by two (Tacail et al. 2014).

## 2.2 Fractionation Factor ( $\alpha$ )

When comparing the isotopic signature of two substances or compartments where the isotopic composition of a compartment remains constant, the usage of the fractionation factor ( $\alpha$ ) instead of  $\delta$ -values is preferred. The fractionation factor is defined as the ratio of two isotopes in the compound A divided by the ratio of the same isotopes in the compound B:

$$\alpha_{A-B} = \frac{R_A}{R_B} \quad (9)$$

Normally, the isotope ratios  $R$  are not reported in the literature which prevents the direct calculation of fractionation factors from isotope ratios. However,  $\alpha$  can be calculated from the reported  $\delta$ -values (given in ‰):

$$\alpha_{A-B} = \frac{\delta_A + 1000}{\delta_B + 1000} \quad (10)$$

It is obvious that the usage of  $\delta^{44/40}\text{Ca}$  and  $\delta^{44/42}\text{Ca}$  in Eq. 10 will result in different fractionation factors. Therefore, fractionation factors calculated from  $\delta^{44/42}\text{Ca}$  (or  $^{44}\text{Ca}/^{42}\text{Ca}$  in Eq. 9) have to be converted to fractionation factors for

$^{44}\text{Ca}/^{40}\text{Ca}$  or vice versa using the same factors as given in Eqs. 5 and 7.

## 2.3 $\Delta$ -Notation

The capital delta notation ( $\Delta$ ) describes the difference between the  $\delta$ -values of two phases A and B and relates to the fractionation factor  $\alpha$  according to:

$$\Delta_{A-B} = \delta_A - \delta_B \approx 1000 \ln \alpha_{A-B} \quad (11)$$

## 2.4 $\epsilon_{\text{Ca}}$ -Notation for Radiogenic $^{40}\text{Ca}$ Ingrowth

Isotope  $^{40}\text{Ca}$  plays a special role within the Ca isotope system as ratios involving  $^{40}\text{Ca}$  are not only affected by mass-dependent fractionation, but also by radiogenic ingrowth. Radiogenic  $^{40}\text{Ca}$  is produced by a  $\beta^-$  decay of  $^{40}\text{K}$  (half-life  $1.397 \times 10^9$  y, Steiger and Jäger 1977). The K–Ca system can be used to date K-rich rocks, which has been shown by several authors (Heumann et al. 1977, 1979; Marshall and DePaolo 1982, 1989; Marshall et al. 1986; Baadsgaard 1987; Nelson and McCulloch 1989; Shih et al. 1994; Fletcher et al. 1997; Nägler and Villa 2000; Kreissig and Elliot 2005). In analogy to other radiogenic isotope systems (e.g. Hf, Nd, Sr), a  $\epsilon$ -notation, representing deviations (excesses) in the abundance of  $^{40}\text{Ca}$  from a reference compositions in parts per  $10^4$  is used. Again, two different  $\epsilon_{\text{Ca}}$  notations exist, depending on the denominator isotope chosen:

$$\epsilon_{\text{Ca}} = \left( \frac{(^{40}\text{Ca}/^{42}\text{Ca})_{\text{sample}}}{(^{40}\text{Ca}/^{42}\text{Ca})_{\text{mantle}}} - 1 \right) \times 10^4 \quad (12)$$

$$\epsilon_{\text{Ca}} = \left( \frac{(^{40}\text{Ca}/^{44}\text{Ca})_{\text{sample}}}{(^{40}\text{Ca}/^{44}\text{Ca})_{\text{mantle}}} - 1 \right) \times 10^4 \quad (13)$$

The  $\epsilon_{\text{Ca}}$  values are commonly calculated from isotope ratios that are first corrected for the instrumental mass discrimination by the exponential law, using  $^{42}\text{Ca}/^{44}\text{Ca} = 0.31221$

(Marshall and DePaolo 1982) (see Sect. 5.2.1, and note Sect. 5.2.2 for a routine where both the stable isotope fractionation and  $\epsilon_{\text{Ca}}$  are determined). Because of the low  $^{40}\text{K}/^{40}\text{Ca}$  ratio of the mantle, radiogenic ingrowth is negligible such that  $(^{40}\text{Ca}/^{42}\text{Ca})_{\text{mantle}}$  can be applied without time-correction. The  $(^{40}\text{Ca}/^{44}\text{Ca})_{\text{mantle}}$  and  $(^{40}\text{Ca}/^{42}\text{Ca})_{\text{mantle}}$  values correspond to about 47.16 and 151.0, respectively. Since the measured absolute Ca isotope ratios vary between different laboratories, the precise reference value for the mantle (=bulk Earth) may be determined by repeated analysis of mantle derived samples in the respective laboratory or even during the particular measurement session (e.g. Kreissig and Elliot 2005; Caro et al. 2010). In contrast to common practice in geosciences, the IUPAC/IUPAP guidelines recommend to use  $\delta^{40}\text{Ca}^*$  (pptt) as an alternative for  $\epsilon_{\text{Ca}}$  to denote radiogenic ingrowth of  $^{40}\text{Ca}$  (Coplen 2011).

Note that natural Ca stable isotope fractionation can systematically bias  $\epsilon_{\text{Ca}}$  values if the mass discrimination correction does not accurately describe the mass-scaling of the natural isotope fractionation process. Likewise, ingrowth of  $^{40}\text{Ca}$  can affect the determination of  $\delta^{44/40}\text{Ca}$ . These issues are discussed below (Sect. 5.2.2).

For several other non-traditional stable isotope systems,  $\epsilon$  is often used to denote mass-dependent stable isotope effects. For example,  $\epsilon^{44/40}\text{Ca}$  would refer to the deviation from a reference material in pptt (in analogy to Eq. 2). Furthermore,  $\epsilon$  is also applied to denote a separation factor to express stable isotope fractionations in stable isotope systems:

$$\epsilon = \alpha - 1 \quad (14)$$

## 2.5 $\epsilon$ - and $\mu$ -Notations in Cosmochemistry

In addition to mass-dependent and potentially radiogenic effects, Ca isotopes in extraterrestrial samples also exhibit nucleosynthetic anomalies that attest to the production of Ca isotopes at different stellar environments (Chapter “High Temperature

Geochemistry and Cosmochemistry”). Although different formats are in use, they all give deviations from terrestrial Ca isotope compositions (i.e. NIST SRM 915) in pptt or parts per million using  $\epsilon$ - or  $\mu$ -notations:

$$\epsilon^{43/44}\text{Ca} = \left( \frac{(^{43}\text{Ca}/^{44}\text{Ca})_{\text{sample}}}{(^{43}\text{Ca}/^{44}\text{Ca})_{\text{reference}}} - 1 \right) \times 10^4 \quad (15)$$

$$\mu^{48/44}\text{Ca} = \left( \frac{(^{48}\text{Ca}/^{44}\text{Ca})_{\text{sample}}}{(^{48}\text{Ca}/^{44}\text{Ca})_{\text{reference}}} - 1 \right) \times 10^6 \quad (16)$$

Although in terms of nucleosynthesis all Ca isotope ratios are of interest,  $^{44}\text{Ca}$  is commonly chosen as the denominator isotope. Please note, that these  $\epsilon$ - and  $\mu$ -notations do not follow the recommendations of Coplen (2011). Following the recommendations of Coplen  $\delta^{43/44}\text{Ca}$  and  $\delta^{48/44}\text{Ca}$  should be used and the results should be reported as either pptt or ppm (cf. Eq. 1).

## 3 Reference Materials

### 3.1 Used Reference Materials

The variability of stable isotope ratios is regularly expressed relative to an international standard, to allow the comparison of results obtained from different studies. Unlike many isotopic systems there is no universal agreement on what reference material should be used as international standard for Ca isotopes. Consequently, published Ca isotope data are reported relative to several different reference materials, which add further complications to the different isotope ratios used ( $^{44}\text{Ca}/^{42}\text{Ca}$  and  $^{44}\text{Ca}/^{40}\text{Ca}$ ). A lookup table (Table 1) summarizing the most frequently used reference materials and equations for the conversion of Ca isotope data from different studies are provided at the end of this section.

In order to achieve better comparability of published Ca isotope data, the IUPAC suggested to use the SRM 915a carbonate standard provided by NIST as a primary standard, and natural

**Table 1** Conversion of standards relative to SRM 915a (in ‰)

Standard	$\delta^{44/40}\text{Ca}_{\text{SRM915a}}$	$\delta^{44/42}\text{Ca}_{\text{SRM915a}}$
SRM915a	0.00	0.00
Seawater	1.88	0.92
SRM915b	0.72	0.35
CaF <sub>2</sub>	1.44	0.70
SRM1486	−1.01	−0.49
BSE	1.03	0.50
CaCO <sub>3</sub>	1.02	0.50
HPSCa	0.34	0.17
Bone powder	−0.84	0.41

seawater (e.g. IAPSO) as a secondary standard (Coplen et al. 2002). Both reference materials were already isotopically well characterized and had been used in earlier studies. Since then most data are presented relative to one of the two standards, or at least studies provide  $\delta$ -values of one of these standards to allow renormalization of the data. Nevertheless, the debate concerning the best suited Ca isotope standard is still ongoing. A short overview below provides background information about different standards and discusses their pros and cons:

Zhu and Macdougall (1998) and Schmitt et al. (2001) proposed to use seawater as a common standard, since seawater was the only common and comparable sample reported in several Ca isotopic studies. In particular, it has been shown that, within uncertainties, the Ca isotopic composition of modern seawater is homogenous (Zhu and MacDougall 1998; De La Rocha and DePaolo 2000; Schmitt et al. 2001; Hippler et al. 2003). This is due to the long Ca residence time of 0.5–1 Myr which is long compared to the mixing time of ocean water ( $10^3$  years). Therefore, seawater seems to be a very suitable reservoir to serve as a reference material. Seawater has a relatively high Ca concentration of 400 mg l<sup>−1</sup> (Taylor and MacLennan 1985) and is furthermore widely available. A minor disadvantage is that a chemical procedure is necessary to separate Ca from the matrix prior to the analysis. Moreover, DePaolo and co-workers (cf. DePaolo 2004) recommend not to use seawater

as a standard because its calcium isotopic composition changes with time (see Chapter “Global Ca Cycles: Coupling of Continental and Oceanic Processes”). Although <sup>40</sup>Ca excess from continental weathering is introduced into the ocean, the radiogenic enrichment of <sup>40</sup>Ca in ocean water throughout Earth history relative to bulk Earth is smaller than the analytical uncertainties of 0.035 ‰, and thus negligible (Caro et al. 2010, Chapter “High Temperature Geochemistry and Cosmochemistry”).

The CaCO<sub>3</sub> reference powder of the National Institute of standards SRM 915a, first used by Halicz et al. (1999), is not related to a specific geological reservoir, but has been proposed as future reference standard (Hippler et al. 2003; Eisenhauer et al. 2004; Coplen et al. 2002). However, since 2006 this reference material is out of stock and replaced by NIST SRM 915b. Since this standard is a solid standard, small isotopic differences could occur between different batches. Therefore the use of this standard as an international Ca standard first necessitates verification of its homogeneity (Wombacher et al. 2009). NIST SRM 915b is presently only sparsely employed (Heuser and Eisenhauer 2008; Wombacher et al. 2009; Hindshaw et al. 2011; Silva-Tamayo et al. 2010; Heuser et al. 2011; Reynard et al. 2011; Valdes et al. 2014; Brazier et al. 2015).

Published Ca isotope ratios of other CaCO<sub>3</sub> salts used so far as standards can only be considered as internal laboratory values. Russell et al. (1978) furthermore showed that industrially produced CaCO<sub>3</sub> salts may have a strongly fractionated composition. This was confirmed by Schmitt et al. (2001) and Hippler et al. (2003) ( $\Delta_{\text{Johnson Matthey Lot 4064-Lot 9912}} = -11.95$  ‰).

Russell et al. (1978) gave a precisely defined absolute reference value for the <sup>42</sup>Ca/<sup>44</sup>Ca of  $0.31221 \pm 0.00002$  (2 $\sigma$ ) deduced from two Ca terrestrial standards, two lunar samples and four meteorites. Marshall and DePaolo (1989) proposed for their part to use the <sup>40</sup>Ca/<sup>42</sup>Ca value of the mantle, estimated by measuring four terrestrial basaltic lavas and obtained a value equal to 151.016 (Marshall and DePaolo 1982) as a reference. The mantle is indeed considered to have a constant Ca isotopic composition throughout

geologic time within reproducibility (see Sect. 3 in Chapter “[High Temperature Geochemistry and Cosmochemistry](#)”). This is due to its low K/Ca ratio ( $\approx 0.01$ ). More recently, Simon et al. (2009) re-evaluated this value by determining the Ca isotopic composition of oceanic basalts and four differentiated meteorites. They determined a weighted average for  $^{40}\text{Ca}/^{44}\text{Ca}$  equal to  $47.1480 \pm 0.0004$  ( $2\sigma$ ), equivalent to a  $^{40}\text{Ca}/^{42}\text{Ca}$  value of  $151.0150 \pm 0.0013$  ( $2\sigma$ ), consistent with the values of Russell et al. (1978) and Marshall and DePaolo (1989).

Skulan et al. (1997) set an arbitrary but reasonable value for their  $^{40}\text{Ca}/^{44}\text{Ca}$  ultrapure  $\text{CaCO}_3$  standard ratio of 47.144 and referred all data to this value. They found that their  $^{40}\text{Ca}/^{44}\text{Ca}$  ratios are very close to that of the average value measured in igneous rocks and minerals, and thus suggested that it should be close to that of bulk silicate Earth.

In order to avoid industrially produced  $\text{CaCO}_3$  salts with fractionated initial isotopic compositions, other studies used a natural  $\text{CaF}_2$  as reference material free of technical or biological isotopic fractionation (cf. Russell et al. 1978; Nagler and Villa 2000; Nagler et al. 2000; Heuser et al. 2002).

Added to these more or less recognized standards, additional standards have also been used by some authors, such as NIST SRM 1486 bone meal (Heuser and Eisenhauer 2008), in-house “HPSCa” solution (Blattler et al. 2011), bone powder (Reynard et al. 2011) or an ICP Ca standard solution (ICP1; Channon et al. 2015; Morgan et al. 2012). In the latter studies  $\delta$ -values were presented using the inhouse standard as reference material. At least the ICP1 based  $\delta$ -value of SRM915a was presented which allows converting the published data to SRM915a based values. A MORB glass (PH 78-2) has also been used as a standard to express  $^{40}\text{Ca}$  excess measurements (Kreissig and Elliott 2005).

A cross calibration of several reference materials between three laboratories (Institute of Geological Sciences of Berne, Geomar from Kiel and Centre de Geochimie de la Surface from Strasbourg) has enabled calibrations independent of laboratory specific biases (Hippler et al. 2003). The main result

of this study is that, despite a range of chemical processing protocols, loading techniques and isotopic measurement protocols have been employed, no inter-laboratory bias correction is necessary and that the Ca isotope data are directly comparable with each-other when expressed in  $\delta^{44/40}\text{Ca}$  notation relative to a common standard.

### 3.2 Conversion of $\delta$ -Values Based on Different Reference Materials

It is possible to convert the  $\delta$ -values based on exotic or outdated reference materials into  $\delta$ -values based on commonly used reference materials if the isotopic composition of the commonly used reference material relative to the exotic reference material is known. The  $\delta$ -value of a sample relative to the “old” reference material is given by

$$\delta_{\text{old}} = (R_{\text{sample}}/R_{\text{ref\_old}} - 1) \cdot 1000 \quad (17)$$

and the  $\delta$ -value of a sample based on the “new” reference material is

$$\delta_{\text{new}} = (R_{\text{sample}}/R_{\text{ref\_new}} - 1) \cdot 1000 \quad (18)$$

The  $\delta$ -value of the “old” reference material based on the “new” reference material is

$$\delta_{\text{ref}} = (R_{\text{ref\_old}}/R_{\text{ref\_new}} - 1) \cdot 1000 \quad (19)$$

Solving Eq. 17 for  $R_{\text{sample}}$  and Eq. 19 for  $R_{\text{ref\_new}}$  and applying to Eq. 18 results in:

$$\delta_{\text{new}} = \left( \frac{\frac{\delta_{\text{old}} + 1000}{1000} \cdot R_{\text{ref\_old}}}{\frac{1000}{\delta_{\text{ref}} + 1000} \cdot R_{\text{ref\_old}}} - 1 \right) \cdot 1000 \quad (20)$$

Solving Eq. 20 leads to:

$$\delta_{\text{new}} = \frac{\delta_{\text{old}} \cdot \delta_{\text{ref}}}{1000} + \delta_{\text{ref}} + \delta_{\text{old}} \quad (21)$$

If the product  $\delta_{\text{old}} \cdot \delta_{\text{ref}}$  is small ( $< 10$ ) the first term is negligible and  $\delta_{\text{new}}$  is in good approximation:

$$\delta_{\text{new}} \approx \delta_{\text{ref}} + \delta_{\text{old}} \quad (22)$$



In the following we present convenient ways to convert data expressed relative to different standards used in the literature, relative to NIST SRM 915a, the most commonly used standard and the common reference of all chapters of this book. When no reference is indicated after the conversion equation, it means that the values are compiled from different laboratories-weighted averages.

*National Institute of Standards and Technology (NIST) SRM 915a and SRM 915b*

NIST SRM 915a is the presently most commonly used standard. As mentioned above this SRM is out of stock and was replaced by SRM 915b.

$$\begin{aligned} \delta^{44/40} Ca_{sample/NISTSRM915a} \\ = \delta^{44/40} Ca_{sample/NISTSRM915b} + 0.72 (‰) \end{aligned} \quad (23)$$

*Seawater standard*

Due to the modern seawater  $\delta^{44/40}Ca$  homogeneity, either an aliquot of seawater available in different laboratories (e.g. seawater from San Diego in Skulan et al. 1997 or from the Atlantic in Schmitt et al. 2001) or IAPSO (International Association for the Physical Sciences of the Ocean) seawater salinity standard available from OSIL (Ocean Scientific International Ltd) have been employed (Hippler et al. 2003):

$$\begin{aligned} \delta^{44/40} Ca_{sample/NISTSRM915a} \\ = \delta^{44/40} Ca_{sample/sw} + 1.88 (‰) \end{aligned} \quad (24)$$

*Bulk Silicate Earth (BSE) standard*

This standard is linked to an Earth reservoir that is not subjected to variation through time. The geological significance of this approach is undoubted. Increasing evidence for Ca isotope fractionation occurring at high temperatures and pressures call for a reliable determination of BSEs Ca isotope composition, which is however not a straightforward task and still pending further verification:

$$\begin{aligned} \delta^{44/40} Ca_{sample/NISTSRM915a} \\ = \delta^{44/40} Ca_{sample/BSE} + 1.03 (‰) \end{aligned} \quad (25)$$

*Further used phosphate,  $CaF_2$  and  $CaCO_3$  standards*

$CaF_2$  and ultra-pure  $CaCO_3$  have only been measured few times and are presently more or less abandoned. Other reference materials reported so far are SRM 1486 (bone ash), bone powder and HFSCa (Heuser and Eisenhauer 2008 (Eq. 28); Reynard et al. 2011 (Eq. 29); Blättler et al. 2011 (Eq. 30); Russel et al. 1978 (Eq. 31)).

$$\begin{aligned} \delta^{44/40} Ca_{sample/NISTSRM915a} \\ = \delta^{44/40} Ca_{sample/CaF_2} + 1.45 (‰) \end{aligned} \quad (26)$$

$$\begin{aligned} \delta^{44/40} Ca_{sample/NISTSRM915a} \\ = \delta^{44/40} Ca_{sample/CaCO_3} + 1.02 (‰) \end{aligned} \quad (27)$$

$$\begin{aligned} \delta^{44/40} Ca_{sample/NISTSRM915a} \\ = \delta^{44/40} Ca_{sample/NISTSRM1486} - 1.01 (‰) \end{aligned} \quad (28)$$

$$\begin{aligned} \delta^{44/40} Ca_{sample/NISTSRM915a} \\ = \delta^{44/40} Ca_{sample/bonepowder} - 0.84 (‰) \end{aligned} \quad (29)$$

$$\begin{aligned} \delta^{44/40} Ca_{sample/NISTSRM915a} \\ = \delta^{44/40} Ca_{sample/HPSCa} + 0.68 (‰) \end{aligned} \quad (30)$$

$$\begin{aligned} \delta^{44/40} Ca_{sample/NISTSRM915a} \\ = -\delta^{40/44} Ca_{sample/std} + 0.98 (‰) \end{aligned} \quad (31)$$

Factors used for the conversion between different standards are summarized in Table 1.

Another way to rapidly convert Ca isotopic data expressed against one standard to another is to renormalize data from “source” to “target” standard following (Table 2):

$$\delta^{44/40} Ca_{sample/target} = \delta^{44/40} Ca_{sample/source} - (\text{correction value}) \quad (32)$$

For example, renormalisation from seawater to SRM915a:  $\delta^{44/40} Ca_{sa/SRM915a} = \delta^{44/40} Ca_{sa/seawater} - (-1.88)‰$  additional standard values can be found in the GeoReM database (<http://georem.mpch-mainz.gwdg.de>; 2016-01-02).



**Table 2**  $\delta^{44/40}\text{Ca}$  conversions between different standards (‰)

from source To target	Seawater	SRM 915a	SRM 915b	SRM 1486
Seawater		1.88	1.14	2.88
SRM 915a	−1.88		−0.74	1.01
SRM 915b	−1.14	0.74		1.74
SRM 1486	−2.88	−1.01	−1.74	

## 4 Sample Preparation

Different preparation protocols have been developed for Ca isotope analysis on various types of samples. The following sections contain detailed descriptions of sample preparation and cleaning protocols for different kinds of materials and matrices.

### 4.1 Digestion and Cleaning Techniques

#### 4.1.1 Carbonates

Digestion techniques for carbonates depend on the mineralogy and the sample matrix. Pure  $\text{CaCO}_3$  as found for instance in marine microfossils, or experimentally precipitated carbonates is easily dissolved in diluted acids. Most commonly hydrochloric acid (HCl), nitric acid ( $\text{HNO}_3$ ) or acetic acid ( $\text{CH}_3\text{COOH}$ ) are used, depending on the further sample treatment (e.g. taking aliquots for trace-element work, column chemistry and presence of matrix minerals which dissolution or leaching should be avoided). To eliminate any organic impurities the dissolved fraction is treated with a  $\text{H}_2\text{O}_2$ – $\text{HNO}_3$  mixture (Hippler et al. 2003, 2006) or is ultrasonically cleaned with ultrapure water and  $\text{H}_2\text{O}_2$  (Heuser et al. 2005; Farkaš et al. 2006). Depending on the carbonate minerals and matrix several protocols have been proposed:

#### **$\text{CaCO}_3$ shells**

Biogenic  $\text{CaCO}_3$  shells collected from the environment normally need to be cleaned prior to Ca isotope analysis, mainly for two reasons, removing of detritus and organic compounds. Two different methods have been used, depending on the sample material:

#### **$\text{H}_2\text{O}_2$ –NaOH method: For shell fragments (recommended for planktic and benthonic foraminifers):**

The sample is first gently crushed and transferred into acid pre-cleaned 1.5 ml polypropylene (PP) reaction vials and ultrasonicated for 2 min in ultrapure water, the pH of which was elevated to 8–9 by the addition of  $\text{NH}_4\text{OH}$ -solution to prevent partial dissolution of the calcareous samples during the cleaning process. This procedure is repeated twice with ultrapure water, once with methanol and two more times with water. Then the sample is heated to about 80 °C for 30 min in a  $\text{NaOH}$ – $\text{H}_2\text{O}_2$  (0.1 and 0.01 M, respectively) solution in a heated ultrasonic bath. Finally, the tests are washed three times and ultrasonicated with ultrapure water. The cleaned sample is dissolved in 0.5 N HCl (cf. Gussone et al. 2004; Gussone and Filipsson 2010).

#### **NaClO method: suited for powdered samples (e.g. corals, mollusks) and nanofossils (coccolithophores and calcareous dinoflagellates):**

Samples are transferred into acid-cleaned polypropylene (PP) reaction vials and bleached for 24 h in a 10 % NaClO solution ( $\sim 1$  % active chlorine), to remove organic compounds with potentially deviating composition or which might influence the ionization in the mass spectrometer. Samples are ultrasonicated several times during the bleaching. The bleach is subsequently removed and the samples are washed 6 times in distilled water, the pH of which was elevated to 8–9 by the addition of  $\text{NH}_4\text{OH}$ -solution to prevent partial dissolution of the calcareous samples during the cleaning process. The samples are finally dissolved in 0.5 N HCl (cf. Gussone et al. 2006; Böhm et al. 2006).

### Dolomite—limestone

Fine grained dolomite powder dissolves readily in 2.5 N HCl or HNO<sub>3</sub>. Different published protocols dissolve 1 g of dolomite and limestone in 6 N ultrapure HCl (Fantle and DePaolo 2007; Jacobson and Holmden 2008), 3 M HCl (Halicz et al. 1999), at room temperature or 2.5 N HCl heated at 70 °C (Wang et al. 2012). 2N acetic acid (Brazier et al. 2015) was also proposed. Whatever the protocol, the dissolved samples are centrifuged and the insoluble residues are discarded.

For the selective dissolution of carbonate minerals in the presence of non-carbonate matrix, potential leaching of e.g. clay minerals need to be considered and taken into account for selection of the used type and strength of acid.

### 4.1.2 Phosphates

#### Peloidal phosphates

For analyses of sedimentary peloidal phosphates it can be necessary to remove Sr-rich calcite overgrowths by a treatment with 0.5 N acetic acid and subsequent washing with distilled water prior to dissolution in 6N HCl (Schmitt et al. 2003a, b; Cobert et al. 2011a). An alternative treatment includes a facultative heating to remove any free MgO and CaO, decalcification with tri ammonium citrate (TAC) and washing with deionized water and dissolution in 1.3M HCl (Soudry et al. 2006).

#### Bone and teeth

Samples of bones (cortex) and teeth (enamel and dentin) are obtained using hand-operated drills. To obtain fresh unaltered material, their surface layer is removed. For digesting the samples, two different techniques are then applied:

- (1) The samples are bleached overnight in 2 % NaClO to break down organic molecules, rinsed with water and dissolved in 1.5 mL 2.5 N HCl (Clementz et al. 2003), warm 5 M HNO<sub>3</sub> (Chu et al. 2006) or 2 M HCl (Reynard et al. 2010).
- (2) The samples are dissolved in 1 mL high-purity concentrated HNO<sub>3</sub> and 30 µL of H<sub>2</sub>O<sub>2</sub> over 12 h on a hot plate at 140 °C (Heuser et al. 2011).

### 4.1.3 Sulfates

#### Gypsum and anhydrite

Gypsum and anhydrite samples are first washed, depending on their origin and potential contamination, dried and powdered. A few mg are digested in a Teflon beaker in 0.5 ml of 4.5 N HCl. Dissolution takes place within a few days (Hensley 2006).

#### Barite

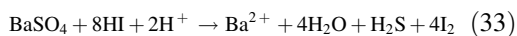
Three different methods have been published to digest barite samples:

- (1) Na<sub>2</sub>CO<sub>3</sub> digestion method (von Allmen et al. 2010a) for Ba-isotope analysis based on Breit et al. (1985)

Barite powder (~5 mg) is mixed with 50 mg sodium carbonate (Na<sub>2</sub>CO<sub>3</sub>) and 1 ml distilled water in a Teflon beaker, and subsequently heated for 4 h on a hotplate at 95 °C. In order to keep the fluid volume at about 1 ml deionized water is intermittently added. A chemical reaction in the beaker leads to the formation of strongly alkaline Na<sub>2</sub>SO<sub>4</sub> in the liquid phase and solid BaCO<sub>3</sub>. To ensure complete dissolution of barite, the liquid is decanted and again 50 mg Na<sub>2</sub>CO<sub>3</sub> are added together with 1 ml H<sub>2</sub>O to the residue and heated for 4 h at 95 °C. After that, the fluid is decanted and the solid residue is several times rinsed with H<sub>2</sub>O, and finally dissolved in 2.5 N HCl.

- (2) HI digestion based on Takano and Watanuki (1972)

About 10–30 mg of powdered barite is mixed with 2 ml of HI in Teflon beakers and placed in pressure bombs in an oven at 180 °C for at least 4 h. The solution is dried down and recovered in 2 ml 2 N HCl. This is repeated (up to 6 times) until all HI is removed. The basic principle of this digestion is the following reaction:



- (3) Chelate method (cf. Griffith et al. 2008)

Purified barite (10 mg) is mixed with pure water and 1 ml pre-cleaned cation exchange resin (pH ~5.5) (Mitsubishi Chemical Industries, MCI Gel-CK08P) following

Church (1979) and Paytan et al. (1993) and heated for about 10 days to 90 °C. The cations bind to the resin while the sulfate goes into the fluid phase. To achieve complete dissolution the water is decanted daily. After dissolution, the cations are extracted from the resin by 2 rinses of 2 ml 6 N HCl.

#### 4.1.4 Silicate Minerals, Rocks and Soils

Most digestion protocols use significantly larger amounts of sample material for digestion (~100 mg on average) compared to what is required and utilised for Ca isotope analysis in the mass spectrometer. On one hand, this procedure minimizes potential blanks during handling, but on the other hand, double spike cannot be added to the sample before digestion. Instead it is added to an aliquot of the sample right after dissolution. This requires a protocol that provides complete dissolution and prevents the formation of insoluble Ca fluorides in the case of silicate samples.

##### Felsic and mafic rocks

Approximately 50–100 mg whole rock powder are weighed into 15 ml pre-cleaned Teflon screwtop vials and digested with closed caps in different mixtures of HF and HNO<sub>3</sub> (Zhu and MacDougall 1998, 2:1; John et al. 2012, 1:4; Kreissig and Elliott 2005, 3:1; Wiegand et al. 2005, 1:1; Huang et al. 2010, 5:3; Ryu et al. 2011) to break-down any Si-bond, for several days on a hotplate at ~120 °C. Afterwards 1 ml HClO<sub>4</sub> is usually added to break down organics and dissolve secondary Ca-fluorites and the solution is evaporated at ~190 °C. The dried sample is re-dissolved in a mixture of 6 N HCl and H<sub>3</sub>BO<sub>3</sub> to dissolve secondary Ca-fluorides, heated at 140 °C on a hotplate for 12 h with closed caps. Afterwards, the sample is evaporated at 125 °C. The dried samples is then re-dissolved in 6 ml 6 N HCl and heated with closed caps for 45 min at 100 °C. The cooled solution is then checked for precipitates. While residual refractory compounds (e.g. Al<sub>2</sub>O<sub>3</sub>, TiO<sub>2</sub>...) are not problematic for Ca isotope analyses, because they do not contain significant

amount of Ca and can be removed by centrifuging, the presence of any fluorides in the residue is not acceptable for stable isotope analyses.

Besides these table-top protocols, samples can also be dissolved under higher pressure using Parr bombs with a HF-HNO<sub>3</sub> mixture (Simon et al. 2009).

##### Ultramafic rocks

Ultramafic rock samples can be pre-treated by leaching in 8.8 mol L<sup>-1</sup> HBr at ~160 °C for 72 h in closed vessels and repeated ultrasonical treatment to promote the release of cations from the crystal cage, before HF-HNO<sub>3</sub> digestion (Amini et al. 2009).

##### Mineral separates

For Ca isotope work on pure mineral fractions standard procedures for mineral separation are used, e.g. based on the density (heavy liquids), magnetic susceptibility of the mineral grains, and hand-picking (Hindshaw et al. 2011; Ryu et al. 2011). Depending on the studied mineral, one of the above described digestion protocols is applied.

##### Extra-terrestrial material

Chondrite samples are hand powdered, dissolved in hot HF-HClO<sub>4</sub> mixtures, dried down, dissolved again in HNO<sub>3</sub> or HCl and centrifuged (Valdez et al. 2014). Some samples were dissolved under higher pressure in Parr bombs without HClO<sub>4</sub> (Simon et al. 2009; Simon and DePaolo 2010). Alternatively, chondrites were dissolved in HF-HNO<sub>3</sub> during 24 h at 120 °C, dried down and fumed in HClO<sub>4</sub> to eliminate any CaF<sub>2</sub> precipitate (Caro et al. 2010).

#### 4.1.5 Organic Samples

##### Plants

The vegetation samples are washed with deionised water. Root samples are especially cleared of soil particles by repeated rinsing and sonication in ultra-pure water, and checked for cleanliness using a binocular microscope (Holmden

and Bélanger 2010). Tree-rings can be collected with an increment drill from living trees and dissected based on tree-rings counting (Farkaš et al. 2011). The plant samples are dried in an oven at  $\sim 30$ – $60$  °C, reduced to powder using either an agate mortar or a tungsten carbide rotary disc mill or a zirconium oxide mixer mill, depending on the sample size. About 50–150 mg powder can be digested within several days in 5 mL concentrated  $\text{HNO}_3$  and 1 mL 30 %  $\text{H}_2\text{O}_2$ . In order to avoid a too intense reaction, the dissolution is started at room temperature and later heated to 70 °C. To promote the reaction, the sample acid mixture is regularly ultrasonicated. After evaporation the process is repeated with a concentrated  $\text{HNO}_3$ – $\text{HCl}$ – $\text{H}_2\text{O}_2$  mixture, evaporated to dryness, dissolved in dilute  $\text{HNO}_3$ , and centrifuged (Cenki-Tok et al. 2009; Hindshaw et al. 2011; Cobert et al. 2011b; Bagard et al. 2013; Schmitt et al. 2013). Undissolved siliceous fractions (e.g. phytoliths) are removed by filtration and centrifugation (Chu et al. 2006).

Alternative protocols use hot ( $\sim 150$  °C) concentrated  $\text{HNO}_3$  (Bullen et al. 2004; Wiegand et al. 2005; Holmden and Bélanger 2010), or high-pressure microwave  $\text{HNO}_3$ – $\text{HCl}$  digestion in reinforced Teflon (PTFE) vessels for digestion (Hindshaw et al. 2012). The solution is evaporated to dryness, dissolved in ultrapure 5 %  $\text{HNO}_3$  (Blum et al. 2008). A further approach is ashing of samples in nickel crucibles in an oven at 500 °C for 8 h, transferring the ashes to Teflon beakers and digesting them in concentrated hot (160 °C)  $\text{HNO}_3$  acid.

#### **Animal soft and hard tissues**

Soft and hard tissues of organisms are ashed for 12–72 h at 450 °C in acid-washed quartz or platinum crucibles, before being dissolved in 1.5 M  $\text{HCl}$ . If the dissolution is incomplete, the samples are further treated with  $\text{HClO}_4$ ,  $\text{HNO}_3$ ,  $\text{HCl}$  and  $\text{HF}$ , before being dried at  $\sim 150$  °C (Skulan and DePaolo 1999).

#### **Animal/human excretes, blood**

Milk and feces are reduced to ash in a muffle furnace at 550 °C for at least 24 h. Then they are

digested in various strengths of  $\text{HNO}_3$ / $\text{HCl}$  mixtures (Chu et al. 2006).

Urine samples are digested in a mixture of 2 mL concentrated  $\text{HNO}_3$  and 250  $\mu\text{L}$   $\text{HClO}_4$  at 150 °C during 12 h. Then the sample-acid mixture is heated to 180 °C. Once evaporated, 1 mL  $\text{HNO}_3$  is added to the residue, which is slowly heated up to 180 °C again, until complete dryness. This step should be repeated twice in order to remove relicts of  $\text{HClO}_4$ . Blood samples (plasma or whole blood) are digested similar to urine using an 8:1 mixture of concentrated  $\text{HNO}_3$  and  $\text{HClO}_4$ .

### **4.1.6 Liquid Samples**

Liquid samples (e.g. rainwater, seawater, snow, soil solutions, throughfall) are filtered if necessary [with 0.22  $\mu\text{m}$  (Schmitt et al. 2003a; Schmitt and Stille 2005; Bagard et al. 2013; Wiegand and Schwendenmann 2013), 0.40  $\mu\text{m}$  (Holmden and Bélanger 2010) or 0.45  $\mu\text{m}$  (Cenki-Tok et al. 2009; Tipper et al. 2010) cellulose acetate filters] or centrifuged. Water samples are acidified to pH 1 with  $\text{HCl}$  (Schmitt and Stille 2005) or to pH 2 with  $\text{HNO}_3$  (Jacobson and Holmden 2008; Bagard et al. 2013) and stored in precleaned polypropylene (PP), polyethylene (PE) or Teflon bottles. Once evaporated, the solid residues of waters are redissolved in concentrated nitric acid, dried down again and re-dissolved in 3 M  $\text{HNO}_3$  (Hindshaw et al. 2013).

### **4.1.7 Leachates**

#### **Carbonates in silicate rock matrix**

For carbonate leachates whole rock powders are treated with dilute 1 M  $\text{CH}_3\text{COOH}$  (Ewing et al. 2008; Teichert et al. 2009; Ryu et al. 2011). Centrifugation allows removing any non-carbonate residue, such as quartz, feldspar or clay minerals and organic compounds (Blättler et al. 2011).

#### **Soil sequential extractions**

Successive leaching steps are usually performed in order to have access to the nutrient pools that are available to fine roots in soils: generally the

soil's exchangeable cations and the acid-leachable fraction. The soil-exchangeable fraction is obtained by leaching 1–5 g soil sample with 1 N  $\text{NH}_4\text{OAc}$  (Bullen et al. 2004; Perakis et al. 2006; Page et al. 2008), 0.1 N  $\text{NH}_4\text{OAc}$  (Wiegand et al. 2005), 1 N  $\text{NH}_4\text{Cl}$  (Hindshaw et al. 2011), or 0.1 N  $\text{BaCl}_2$  (Holmden and Bélanger 2010; Farkaš et al. 2011).

The soil acid-leachable fraction is obtained by leaching the residue from the soil-exchangeable fraction leachate once rinsed with ultra-pure water with 1 N  $\text{HNO}_3$  (Bullen et al. 2004; Perakis et al. 2006; Holmden and Bélanger 2010; Farkaš et al. 2011). The same acid is used by Hindshaw et al. (2011) to extract the phyllosilicates. An intermediate step was also introduced by the latter authors: a  $\text{H}_2\text{O}_2/\text{HNO}_3$  mixture allows them to extract organically-bound Ca. After each step the solutions are centrifuged, the supernatant are stored and the solid residues are carried forward to the next step. Less resistant silicate minerals (biotite and hornblende) are leached in a further step using hot (70 °C) 15 N  $\text{HNO}_3$  acid during several hours (Holmden and Bélanger 2010; Farkaš et al. 2011).

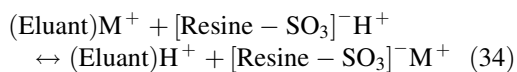
For their part, Hindshaw et al. (2011) published a five-step sequential extraction procedure in order to extract exchangeable, organically-bound, phyllosilicates and two residual soil pools. More recently, Bagard et al. (2013) performed three successive extractions, in order to (1) dissolve carbonates and remove metals adsorbed on the soil particles as outerspheric complexes with 1 N  $\text{CH}_3\text{COOH}$ , (2) dissolve remaining adsorbed trace metals and Fe–Mn oxides and hydroxides with 1 N  $\text{HCl}$ , and (3) digest organic matter with 1 N  $\text{HNO}_3$ .

Leachates must always be interpreted with care because there is always a continuum between leachable and residual phases (Stille and Clauer 1994; Steinmann and Stille 1997, 2006). It can also be noted that  $\text{BaCl}_2$  is a more powerful ion exchanger than e.g.  $\text{NH}_4\text{Cl}$ . As a result, based on  $^{87}\text{Sr}/^{86}\text{Sr}$  values from Nezat et al. (2010), Farkaš et al. (2011) suggested that  $\text{BaCl}_2$  can also weather cations from interlayered biotite phases, complicating the interpretation of leachates.

## 4.2 Chemical Separation

The determination of Ca isotope compositions using mass spectrometry implies a chromatographic clean-up for Ca to remove the sample matrix and elements that form interferences with Ca isotopes (see Sect. 5.3.3). Russell and Papanastassiou (1978) were the first to use such a chemical clean-up. They adapted their elution protocol to separate alkaline and alkaline-earth elements from Tera et al. (1970). The main result of their study is the identification of stable isotope fractionation occurring during the chemical separation; the first eluted Ca fractions are enriched in heavy Ca isotopes, whereas the later eluted Ca fractions are enriched in light Ca isotopes. To avoid this isotope fractionation, digested sample aliquots are mixed with a Ca-double spike before the chemical protocol (see Sect. 5.4). Unspiked aliquots are commonly taken to analyse radiogenic  $^{40}\text{Ca}$  or nucleosynthetic anomalies, which implies a near quantitative recovery from the column to avoid any large chromatographically-induced fractionation. Moreover, *pure* Ca carbonates do not need any chemical clean-up and can be directly measured in the spectrometer (Halicz et al. 1999; Nägler et al. 2000; Clementz et al. 2003; Marriott et al. 2004; Fantle and DePaolo 2005, 2007; Hippler et al. 2006; Heuser et al. 2005; Gussone et al. 2007, 2009; Gussone and Filipsson 2010; Reynard et al. 2011).

Calcium purification protocols are based on  $\text{Ca}^{2+}$ – $\text{H}^{+}$  exchange processes between the solution and ion exchange resins. Cation exchange resins consist of sulfonic acid functional groups in the hydrogen form ( $\text{R}-\text{SO}_3\text{H}$ ), attached to a styrene divinylbenzene copolymer of variable crosslinkage.



The variable affinity of the resin for different cations (Ca, Mg, Fe, Al, Sr...) determines the efficiency of the separation, which is based on the distribution coefficient of the cations between the resin and different acids ( $\text{HNO}_3$ ,  $\text{HCl}$ ,  $\text{HBr}$ ). It



can be noted that Ca presents high distribution coefficients at high HCl or HBr molarities (Nelson 1964). However such high-molarity acids do not provide a good separation of Ca from Sr, Ba and some REE (e.g. Wombacher et al. 2009). Several different lab-specific Ca purification protocols, which are summarized below, are applied.

Commercially available resins are normally not clean enough for direct usage and need a thorough pre-cleaning, with several H<sub>2</sub>O and acid washing steps. The degree of contamination can vary for each batch of resin and the cleaning protocol might be adapted and blanks need to be regularly tested.

Cation exchange resin (AG50W-X8, 200–400 mesh) is often employed for the selective separation of Ca from the other cations, using as eluent diluted HCl (Russell and Papanastassiou 1978; Schmitt et al. 2001, 2003a, b, 2009; Kasemann et al. 2005; Schmitt and Stille 2005; Perakis et al. 2006; Cenki-Tok et al. 2009; Caro et al. 2010; Hindshaw et al. 2011; Heuser et al. 2011; Wiegand and Schwendenmann 2013), HNO<sub>3</sub> (Fig. 1; Fantle and DePaolo 2007; Ewing et al. 2008; Simon et al. 2009) or HBr (Kreissig and Elliott 2005; Heuser and Eisenhauer 2008, 2010). Another particle size (100–200 mesh) of this resin and HCl as an eluent was also employed (Soudry et al. 2006). In addition the higher cross-linked AG50W-X12 (200–400 mesh) with HCl as an eluent was also often used to perform Ca purification (Chang et al. 2004;

Wieser et al. 2004; Chu et al. 2006; Farkaš et al. 2006, 2011; Tipper et al. 2006, 2008a, 2010; Komiya et al. 2008; Teichert et al. 2009; Huang et al. 2010; Reynard et al. 2010; Blättler et al. 2011; Hippler et al. 2009). Macroporous (AGMP50, 100–200 mesh; HCl as eluent) (Jacobson and Holmden 2008; Amini et al. 2009; Holmden and Bélanger 2010; Fantle et al. 2012; Holmden et al. 2012; Lehn et al. 2013) and the Mitsubishi (MCI Gel-CK08P; 75–100 mesh; HCl as eluent) (Zhu and McDougall 1998; Amini et al. 2008, 2009; Griffith et al. 2008; Harouaka et al. 2014) cation exchange resins were also applied.

During these chemical separation protocols Ca and Sr peaks can overlap, which may cause interferences during mass spectrometer measurements. Added to that, Fe and Al need also to be removed. For instance, samples with high Al/Ca ratios cause short-term beam instabilities or lower Ca ionization efficiency (Boulyga 2010). Several techniques have been employed to avoid these drawbacks. Strontium was separated from Ca using a Sr specific resin (Sr spec SPS, 50–100 mesh) (Chang et al. 2004; Chu et al. 2006; Tipper et al. 2006; Simon et al. 2009; Hindshaw et al. 2011; Reynard et al. 2010; Blättler et al. 2011). Another way to avoid Ca–Sr peak overlap is to truncate the elution curve, leading to a recovery yield of about 70 % (Cenki-Tok et al. 2009) or greater than 80 % (Amini et al. 2008). Aluminium, Fe and Ti were removed by passing the eluted aliquot a second time through the same column employing the same cleaning and separating process (Skulan and DePaolo 1999; Kreissig and Elliott 2005; Simon et al. 2009; Simon and DePaolo 2010) or using small cation resin columns and HCl as an eluent (Caro et al. 2010). Hindshaw et al. (2011) proposed for their part to employ AG1-X4 anion resin to retain Fe as FeCl<sub>4</sub><sup>−</sup> together with the anion matrix. Aluminium was removed by elution in 0.1 N HF and 1 N HNO<sub>3</sub> through AG50W-X8 cation resin (based on Schiller et al. 2012). Another way to remove Fe and Al is to co-precipitate them with NH<sub>3</sub> at pH 7 (Tipper et al. 2006).

To avoid multiple-step chromatographic clean-up (up to four-step separation chemistry,

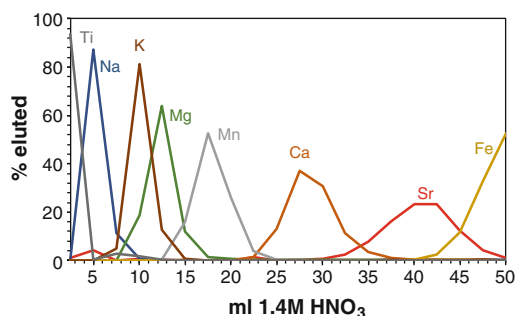


**Fig. 1** Example for the chemical separation of Ca from a chondrite sample using 1.4 M HNO<sub>3</sub> and 1 ml of AG50W-X12 cation exchanger. F. Wombacher, unpublished data



Hindshaw et al. 2010), Wombacher et al. (2009) developed a new procedure allowing the combined chemical separation of Mg, Ca and Fe for most studied matrices (water, bone, carbonate and sediment samples, igneous and sedimentary rocks, chondritic meteorites). By using AG50 W-X8 (200–400 mesh) Ca was selectively eluted using either HBr or HCl.

A further approach to isolate Ca from the matrix is the use of a high selectivity automated ionic chromatography separation protocol (Schmitt et al. 2009). It is applicable to multiple natural matrices (waters, mineral and organic samples) and ensures a complete separation of Ca from K, Mg and Sr. This protocol was initially developed to avoid K-tailing into the Ca fraction for vegetation samples, occurring with traditional column procedures. Indeed, K and Sr are the closest elements to Ca in terms of chemical behavior during the various separation steps, so that satisfactorily separation often cannot be achieved for these cations. More recently Romaniello et al. (2015) published a protocol describing a fully automated chromatographic purification of Sr and Ca for isotopic analysis. It relies on a commercially available platform combined to a highly reusable Sr–Ca column. For the moment this protocol has only been tested for rock, bone and seawater standard samples.

In order to oxidize organic functional groups that may have leached from ion-exchange resins during chemical processing, H<sub>2</sub>O<sub>2</sub> (Holmden and Bélanger 2010) or HNO<sub>3</sub>–H<sub>2</sub>O<sub>2</sub> mixtures (Schmitt et al. 2009; Cobert et al. 2011a, b) have been added to the processed samples and heated in closed Teflon (PTFE) vessels. This can help to avoid isobaric interferences or variation in the ionization behavior during mass spectrometric measurements.

Chemical blank values are highly variable from one laboratory to the other, ranging from <1 ng (Caro et al. 2010) to 100 ng (Jacobson and Holmden 2008). Generally these values are low compared to the Ca processed through the columns and can thus be neglected.

## 5 Mass Spectrometry

### 5.1 Introduction to Mass Spectrometry for Ca Isotope Analysis

Precise Ca isotope analysis requires mass spectrometry. Mass spectrometers consist of three principle units: an ion source, an analyzer for mass separation and an ion detection unit. Up to now, most Ca isotope analysis have been performed using thermal ionization mass spectrometry (TIMS), followed by multi-collector inductively coupled plasma mass spectrometry (MC-ICP-MS) and occasionally secondary ion mass spectrometry (SIMS). SIMS offers high spatial resolution, as does MC-ICP-MS if coupled to a laser ablation system. Due to matrix effects and interferences, *in situ* analysis, however, is usually limited to samples that are dominated by Ca, such as calcite or apatite.

Calcium atoms need to be ionized in order to be accelerated and focused inside the mass spectrometer. TIMS, MC-ICP-MS and SIMS differ fundamentally in regard to their ion sources. In TIMS, Ca is ionized at the surface of a metal filament that is heated by an electrical current. The filaments are made from metals characterized by high melting points e.g. W and Re. In SIMS, atoms are sputtered from the sample using a primary ion beam (such as <sup>16</sup>O<sup>−</sup> ions) whereby only a fraction of the analyte atoms liberated is ionized. The Ar plasma source in MC-ICP-MS ionizes Ca atoms very efficiently, but suffers from interferences, in particular from abundant <sup>40</sup>Ar<sup>+</sup> ions (99.6 %) that interfere with <sup>40</sup>Ca<sup>+</sup> ions. In contrast, thermal ionization is rather element specific and thus generates less interferences.

Once formed, Ca<sup>+</sup> ions are accelerated by a negative potential and the ion beam is focused and aligned by a set of electrostatic lenses. When passing through the magnetic field of the mass analyzer, ions are dispersed depending on their mass to charge ratio (*m/z*) and their kinetic

energy (velocity). Unlike thermal ion sources, plasma and secondary ion sources generate ions with a spread in kinetic energy. To compensate for the ion energy spread, MC-ICP-MS and SIMS instruments are commonly equipped with an electrostatic analyzer that is dispersive for ion energy only. In order to compensate the energy discrimination of the magnetic sector field, energy discrimination of the electrostatic analyzer is of the same magnitude, but opposite in sign. Thus, the combination of electrostatic and magnetic analyzer focusses both, ion angles and energy, a property called double focusing.

Precise Ca isotope ratio measurements require that ion beams are collected simultaneously in multiple Faraday detectors (also called Faraday collectors or cups). Multiple collection in Faraday cups takes care of ion beam fluctuations during the course of the analysis, but requires cross calibration of the gain of the attached amplifiers which is possible with accuracies of about 10 ppm. (Multiple) Ion counters are more sensitive, but cross calibration is less precise and prone to drift effects such that the isotope ratios obtained are not sufficiently precise for Ca stable isotope geochemistry. Ion beams generated by thermal ionization can be very stable, which allows ion beams to be collected sequentially in a single Faraday collector with the advantage, that ion beams for different Ca isotopes have identical flight paths. This provides a principle advantage in terms of accurate and reproducible analysis. However, longer analysis times, detector decay and drift issues are the downside of single-collector TIMS (see also Sect. 5.2).

Faraday collectors are commonly attached to high ohmic feedback resistors (typically  $10^{11} \Omega$ ) where the voltage measured across the resistor is representative of the ion beam intensity. According to Ohms law ( $I = V/R$ ), 1 V measured across a  $10^{11} \Omega$  resistor corresponds to  $10^{-11}$  A or 10 pA. Because 1 A equals  $6.241 \times 10^{18}$  elementary charges per second, 10 pA correspond to 62.41 million ions per second [million counts per second (Mcps)]. Faraday collectors within modern TIMS or MC-ICP-MS instruments equipped with  $10^{11} \Omega$  resistors may collect ion beam signals up to about 50 V (500 pA).

Using  $10^{10} \Omega$  resistors allows to collect ion beam currents that are ten times larger, which is particularly useful for the collection of  $^{40}\text{Ca}$  as it allows to detect the less abundant Ca isotopes at higher signal intensities which in turn leads to better isotope ratio precision (provided that sufficiently intense ion beams can be generated). On the other hand, ion currents of less than  $\sim 0.5$  pA may be better detected using higher ohmic (e.g.  $10^{12} \Omega$ ) resistors as a  $10^{12} \Omega$  resistor is characterized by higher signal/noise ratios (e.g. Wieser and Schwieters 2005; Koornneef et al. 2013). According to Ohms law, the voltage measured across  $10^{10}$  ( $10^{12} \Omega$ ) resistor is by a factor of 10 lower (higher) than across a  $10^{11} \Omega$  resistor. However, for the ease of users, signals intensities reported as voltages for amplifiers with  $10^{10}$  or  $10^{12} \Omega$  resistors are (inaccurately) reported as if  $10^{11} \Omega$  resistors were in place.

The inherited noise of the resistors attached to Faraday detectors requires that baselines are taken, usually before measurements (e.g. Schiller et al. 2012). The lower the signal intensities and the better the precision aimed at, the longer should the baseline be taken (Fig. 2).

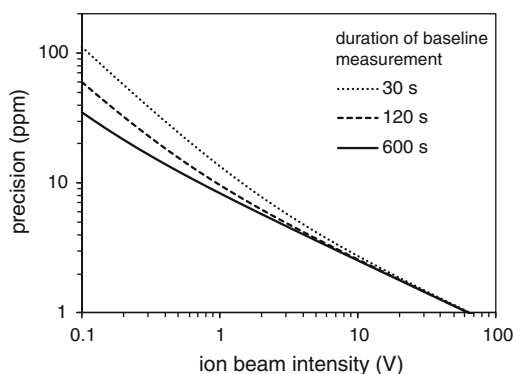


**Fig. 2** Calculated effect of signal intensity and duration of baseline measurements on the precision of isotope ratio measurements for an isotope ratio of one, 60 integrations of 8.4 s and Johnson noise for  $10^{11} \Omega$  resistors. Drift effects and/or additional uncertainty introduced by the mass discrimination correction procedure are ignored. The figure shows that longer baseline readings are required for small signal intensities where the noise contribution becomes increasingly significant and hints at the signal intensities needed to achieve the precision requirements. See Ludwig (1997) for a thorough discussion of signal versus baseline measurement times

Collected isotope ratios finally need to be corrected online or offline for interferences and mass discrimination and possibly for background contributions and eventually referenced to the Ca isotope standards (e.g. using the  $\delta$ -notation) that are usually run along with the samples.

## 5.2 Thermal Ionization Mass Spectrometry (TIMS)

Because the most abundant isotope ( $^{40}\text{Ca}$ ) can be analyzed by TIMS, but not usually by MC-ICP-MS, TIMS remains the method of choice for most geochemists. Several articles have reviewed TIMS measurement techniques (Platzner 2000; Holmden 2005; Fantle and Bullen 2009; Boulyga 2010; Carlson 2014).

### 5.2.1 Mass Discrimination in TIMS and the Exponential Law Correction

During the course of the measurement, progressive mass dependent fractionation of Ca isotopes occurs. Light Ca isotopes are preferably evaporated from the hot filament, which results in an enrichment of heavy Ca isotopes in the Ca pool remaining on the filament. Thus, the ratio of light to heavy Ca isotopes is decreasing with time during the analysis.

A viable measure for the progressive isotope fractionation in thermal ion sources is the relative (%) fractionation per mass unit:

$$\left[ \frac{\left( \frac{^X\text{Ca}}{^Y\text{Ca}} \right)_{\text{sample}}}{\left( \frac{^X\text{Ca}}{^Y\text{Ca}} \right)_{\text{reference}}} - 1 \right] \times 100 / (X - Y) \quad (35)$$

where  $^X\text{Ca}$  is the light Ca isotope with mass  $X$  and  $^Y\text{Ca}$  is the heavy Ca isotope with mass  $Y$ . For normalization to the reference value, either natural reference ratios or ratios of double spike (Sect. 5.4) compositions are used.

Figure 3 shows a typical evolution path for  $^{43}\text{Ca}/^{48}\text{Ca}$  during a run. However, reverse fractionation may sometimes be observed if new Ca reservoirs at the filament are tapped. This is a

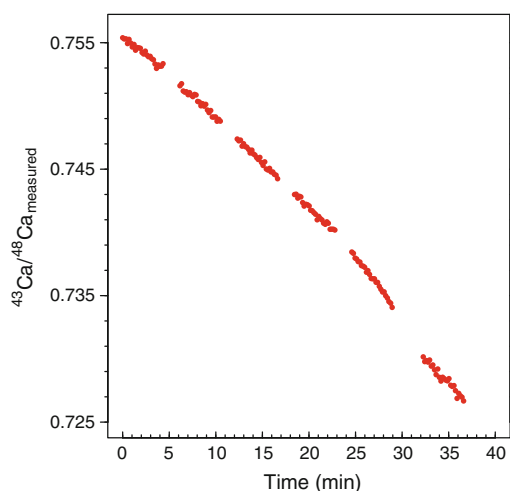


**Fig. 3** Typical progressive mass fractionation of  $^{43}\text{Ca}/^{48}\text{Ca}$  during TIMS analysis

critical issue as the “mixed” ion beam signals from variably fractionated reservoirs are not accurately described by the exponential law (see below) that is commonly used for mass fractionation correction (Hart and Zindler 1989; Fantle and Bullen 2009; Upadhyay et al. 2008; Andreassen and Sharma 2009; Lehn and Jacobson 2015). This observation highlights the importance of reproducible filament loading and heating procedures.

The continuous mass fractionation during TIMS measurements needs to be accurately corrected. As in most cases, natural stable isotope variations are investigated no “true” reference value can be assumed for mass fractionation correction. Therefore, a double spike technique (Sect. 5.4) has to be applied to accurately correct for instrumental mass discrimination.

The so called exponential mass (or isotope) fractionation law (Russell et al. 1978) is widely applied for mass discrimination correction in TIMS as well as MC-ICP-MS. It is commonly applied in double-spike data reduction procedures for stable isotope analysis and for the determination of radiogenic isotope compositions. The exponential law of Russell et al. (1978) has been shown to provide an accurate and suitable description for the progressive Ca isotope discrimination in TIMS (Russell et al. 1978; Hart and Zindler 1989; Schiller et al. 2012), but

Caro et al. (2010), Schiller et al. (2012) and Naumenko-Dèzes et al. (2015) observed small deviations from the exponential law with increasing fractionation. The latter authors applied an empirical second order correction, while Schiller et al. (2012) fitted the generalized power law (Maréchal et al. 1999; Wombacher and Rehkämper 2003) for individual measurement sessions to slightly improve the results.

Below the exponential law is given along with an example that uses the values employed for the correction of mass discrimination for the determination of the radiogenic  $^{40}\text{Ca}$  ( $\epsilon_{\text{Ca}}$ ). First the fractionation coefficient  $f$  is determined:

$$f = \frac{\ln\left(\frac{R_B}{r_B}\right)}{\ln\left(\frac{m_3}{m_1}\right)} \text{ e.g. } f = \ln\left(\frac{0.31221}{(^{42}\text{Ca}/^{44}\text{Ca})_{\text{measured}}}\right) / \ln\left(\frac{41.9586183}{43.955481}\right) \quad (36)$$

Using the fractionation coefficient  $f$ , all other isotope ratios can be corrected:

$$R_A = r_A \left(\frac{m_2}{m_1}\right)^f \text{ e.g. } (^{40}\text{Ca}/^{44}\text{Ca})_{\text{corrected}} = (^{40}\text{Ca}/^{44}\text{Ca})_{\text{measured}} * \left(\frac{39.9625912}{43.955481}\right)^f \quad (37)$$

$R_A$  refers to the mass discrimination corrected isotope ratio and  $R_B$  refers to the reference value for the isotope ratio used for normalization;  $r_A$  and  $r_B$  refer to the measured (fractionated) values of the same isotope ratios as  $R_A$  and  $R_B$ . The mass of the denominator isotope common to both isotope ratios is denoted  $m_1$ , while the numerator isotope of the corrected ratio B is denoted  $m_2$  and the mass of the numerator isotope for the normalizing isotope ratio B is  $m_3$ .

Note that some authors used  $^{40}\text{Ca}/^{42}\text{Ca}$  and  $^{44}\text{Ca}/^{42}\text{Ca}$  for ratio A and ratio B, respectively, in order to determine the radiogenic  $^{40}\text{Ca}$  excess. For samples, the deviation of the corrected  $^{40}\text{Ca}/^{44}\text{Ca}$  (or  $^{40}\text{Ca}/^{42}\text{Ca}$ ) ratio from a reference

value in parts per ten thousand (pptt) is then calculated as  $\epsilon_{\text{Ca}}$  based on Eqs. 12 or 13.

The exponential law is identical to the kinetic law discussed in Chapter “Introduction”, but presented here in a more convenient form with the fractionation coefficient  $f$  that is obtained from the properties of the normalizing isotope ratio (cf. Hart and Zindler 1989; Wombacher and Rehkämper 2003). The advantage of this form is that once  $f$  is determined from the normalizing isotope ratio, all other isotope ratios can be corrected using Eq. 3. The fractionation coefficient ( $f$ ) is called  $\beta$  in most publications. This is unfortunate, however, because  $\beta$  also denotes (i) the slope in three isotope plots defined by different isotope fractionation laws, (ii) the exponent used to describe isotope fractionation associated with kinetic transport processes and (iii) reduced partition function ratios (cf. Chapter “Introduction”).

### 5.2.2 Analysis of Radiogenic $^{40}\text{Ca}$ by TIMS

Two data reduction procedures for radiogenic  $^{40}\text{Ca}$  excesses have been reported up to now, both based on TIMS analysis.

In the first procedure, unspiked isotope ratios are measured and mass fractionation corrections are performed using Eqs. 36 and 37 above. The accuracy of the correction depends on the precision with which the isotope ratios can be measured (DePaolo 2004). Earlier studies using Finnigan MAT 262 TIMS instruments were able to achieve external reproducibilities of about one  $\epsilon_{\text{Ca}}$  (Marshall and DePaolo 1982, 1989; Marshall et al. 1986; Nelson and McCulloch 1989). New generation TIMS instruments are able to improve this value below one  $\epsilon_{\text{Ca}}$  (Kreissig and Elliott 2005; Simon et al. 2009; Caro et al. 2010; Simon and DePaolo 2010). Caro et al. (2010) were able to decrease the external reproducibility down to 0.34  $\epsilon_{\text{Ca}}$  by using a multi-dynamic mode and a low-resolution dual source-exit slit assembly. They observed significant deviation from the exponential law (up to 4  $\epsilon_{\text{Ca}}$  bias) if the instrumental mass fractionation of the analyses was

below  $-2$  ‰/amu. In order to avoid artifacts they filtered out data that was not comprised between  $-2$  and  $2$  ‰/amu and tightly controlled the amount of Ca loaded onto the filament.

The correction for instrumental mass discrimination also means that natural stable isotope fractionation effects are simultaneously corrected along with the instrumental mass discrimination and therefore natural stable isotope effects should be irrelevant for  $\epsilon_{\text{Ca}}$ . However, this is true only to the extent that the exponential (=kinetic) law corrects accurately for the commonly small natural mass-dependent isotope fractionation. We can use the difference between the mass-scaling of the equilibrium and kinetic/exponential law to estimate the potential error that can be introduced by inappropriate mass discrimination correction of natural stable isotope fractionations. For any ‰/amu natural Ca isotope fractionation with a mass-scaling according to the equilibrium law (Chapter “[Introduction](#)”), the systematic error in  $\epsilon_{\text{Ca}}$  corresponds to  $-1$  (pptt). It is difficult to estimate the true error in  $\epsilon_{\text{Ca}}$  introduced by an inappropriate correction of natural stable isotope fractionation as it requires that the mass-dependence for the natural fractionation process is precisely known. However, the above evaluation leads to two important conclusions:

- (1) for the determination of precise (better than  $\sim \pm 0.5$  ‰Ca)  $\epsilon_{\text{Ca}}$  values, samples that possibly display a large ( $\gg 0.1$  ‰/amu) natural stable isotope fractionation should be avoided. Fortunately, most high-temperature samples will not show large Ca stable isotope variations.
- (2) If potentially large stable isotope fractionations cannot be avoided, the stable isotope fractionation need to be determined and potential errors on  $\epsilon_{\text{Ca}}$  must be evaluated.

The determination of radiogenic  $^{40}\text{Ca}$  excesses has been combined with the determination of mass dependent fractionation effects. To this end,  $\delta^{44/40}\text{Ca}$  and  $\delta^{44/42}\text{Ca}$  are first determined as described in Sect. 5.2.3, using either one protocol (Schmitt et al. 2003a, b; Schmitt and Stille 2005; Huang et al. 2010, 2011; Hindshaw et al. 2011) or two measurement protocols with two different double spikes in order to improve the

external reproducibility of  $\delta^{44/42}\text{Ca}$  (Ryu et al. 2011). The  $\epsilon_{\text{Ca}}$  excess can be visualized by plotting  $\delta^{44/40}\text{Ca}$  versus  $\delta^{44/42}\text{Ca}$  in a diagram. Samples that plot below the mass fractionation line defined by Eqs. 38 or 39 display  $^{40}\text{Ca}$  excesses. The amount of the excess can be evaluated using following equations, depending either on the equilibrium fractionation law:

$$\epsilon_{\text{Ca}} = \left[ \left( \delta^{44/42}\text{Ca} \times 2.0995 \right) - \delta^{44/40}\text{Ca} \right] * 10 \quad (38)$$

or on the kinetic fractionation law:

$$\epsilon_{\text{Ca}} = \left[ \left( \delta^{44/42}\text{Ca} \times 2.0483 \right) - \delta^{44/40}\text{Ca} \right] * 10 \quad (39)$$

No detectable  $^{40}\text{Ca}$  enrichments were recordable in most studies (Schmitt et al. 2003a, b; Schmitt and Stille 2005; Hindshaw et al. 2011) due to low reproducibilities of  $\epsilon_{\text{Ca}}$  ( $\sim 3$  ‰Ca; Hindshaw et al. 2011) and/or because of young crystallization ages of the studied granite bedrocks ( $\sim 300$  Ma; Schmitt et al. 2003b; Hindshaw et al. 2011). Farkaš et al. (2011) and Ryu et al. (2011), who studied old granodiorites (of Precambrian age and of 1.7 Ga, respectively), recorded  $^{40}\text{Ca}$  enrichments (see Sect. 3 in Chapter “[High Temperature Geochemistry and Cosmochemistry](#)”).

Although insignificant in many cases, studies of mass-dependent Ca isotope fractionation effects that rely on  $^{44}\text{Ca}/^{40}\text{Ca}$  isotope ratios need to be aware of potential biases introduced by radiogenic contributions. The effect of  $^{40}\text{K}$  decay on the  $\delta^{44/40}\text{Ca}$  as a function of the  $^{40}\text{K}/^{44}\text{Ca}$  ratio and sample age is illustrated in Fig. 4, demonstrating that radiogenic ingrowth of  $^{40}\text{Ca}$  is small in young rocks, even in those with relatively high K/Ca ratios, and it is insignificant in rocks with low K/Ca, irrespective of their formation ages.

### 5.2.3 Calcium Stable Isotope Analysis by TIMS

Table 3 highlights that there exists no consensus on filament loading techniques among different laboratories and each laboratory has developed

**Fig. 4** Effect of  $^{40}\text{K}$  decay on the  $\delta^{44/40}\text{Ca}$  of a rock or mineral, depending on the  $^{40}\text{K}/^{44}\text{Ca}$  ratio and formation age

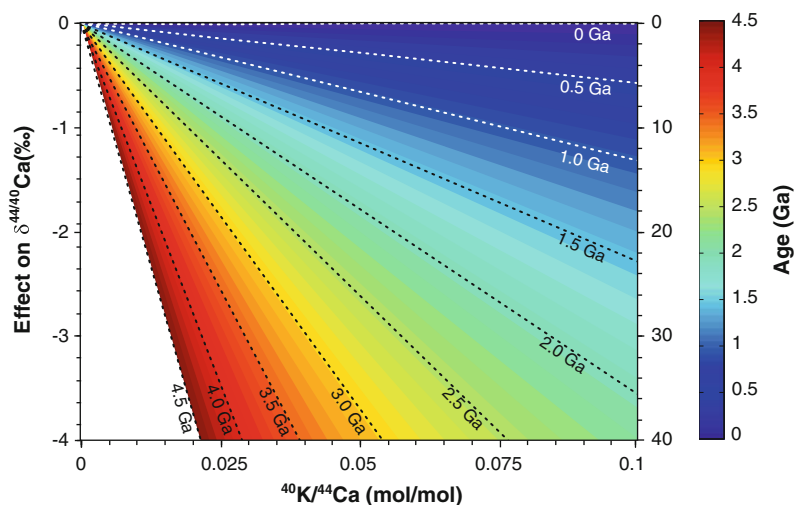


**Table 3**  $\delta^{44/40}\text{Ca}$  of selected rock standards from the literature

Reference material	Rock type	$\delta^{44/40}\text{Ca}$ (‰)	References
BHVO-1	Basalt	0.98	Huang et al. (2010, 2011)
BHVO-2	Basalt	0.87	Magna et al. (2015), Amini et al. (2008), Valdes et al. (2014)
BIR-1	Basalt	0.83	Amini et al. (2008), Wombacher et al. (2009), Valdes et al. (2014)
BIR-2	Basalt	0.99	Valdes et al. (2014)
AGV-2	Andesite	0.77	Valdes et al. (2014)
ATHO-G	Rhyolite	0.87	Amini et al. (2008)
BCR-1	Basalt	0.82	Simon and DePaolo (2010)
BCR-2	Basalt	0.89	Wombacher et al. (2009), Amini et al. (2008), Valdes et al. (2014)
SRM688	Basalt	0.86	Valdes et al. (2014)
JP-1	Peridotite	1.15	Magna et al. (2015)
PCC-1	Peridotite	1.14	Amini et al. (2008)
DTS-1	Dunite	1.54	Amini et al. (2008), Huang et al. (2010)
J-Dol	Dolomite	0.70	Wang et al. (2013)
J-Cp1	Coral	0.63	Wombacher et al. (2009)

its own measurement protocol. Samples are loaded onto a filament in the chloride, nitrate or iodide form, with or without an activator, i.e. a supplementary solution increasing the ionisation efficiency. Calcium isotope analysis is then carried out using a single, double or triple Ta, Re or W filament configuration.

Given the configuration of the TIMS present in the different laboratories, Ca isotope ratios have been measured using either single or

multi-collection. The most striking analytical challenge is to obtain the best possible external reproducibility and accuracy for Ca isotope ratios.

In single-collector peak-hopping, individual ion beams are collected sequentially (Russell et al. 1978; Skulan et al. 1997; DeLaRocha et al. Nägler and Villa 2000; Schmitt et al. 2001, 2003a, b; Lemarchand et al. 2004; Schmitt and Stille 2005; Fantle and DePaolo 2005, 2007;



Gopalan et al. 2006). The advantage of this technique is that the measured ion beam intensities remain unaffected by ion optical effects. However it requires a correction of the drift in ion beam intensity between succeeding measurement cycles. Thus time-interpolated Ca isotope ratios may be subject to large uncertainties if the ion beam is not perfectly stable and short ion beam integration times are necessary (1–3 s). Short integration times however render high precision Ca isotope analysis difficult. This is due to counting statistics as Ca is composed of one highly abundant ( $^{40}\text{Ca}$ ) and five minor isotopes ( $^{42}\text{Ca}$ ,  $^{43}\text{Ca}$ ,  $^{44}\text{Ca}$ ,  $^{46}\text{Ca}$ ,  $^{48}\text{Ca}$ ; see Table 3; Chapter “[Introduction](#)”). It is therefore necessary to generate high intensity ion beams to boost the signal intensity for the low abundance isotopes.

In multi-collection all ion beams are either collected simultaneously (static measurement) or split between alternating measurement cycles (dynamic measurements) (Heuser et al. 2002, 2011; Clementz et al. 2003; Gussone et al. 2003, 2004, 2007, 2010, 2011; Holmden 2005; Kasemann et al. 2005; Böhm et al. 2006; Farkaš et al. 2006, 2007; Amini et al. 2008, 2009; Ewing et al. 2008; Heuser and Eisenhauer 2008, 2010; Cenko-Tok et al. 2009; Schmitt et al. 2009; Simon et al. 2009; Huang et al. 2010; Simon and DePaolo 2010; Cobert et al. 2011a, b; Ryu et al. 2011). So far, the mass difference of 20 % between  $^{48}\text{Ca}$  and  $^{40}\text{Ca}$  exceeds the mass dispersion of TIMS instruments, thus not all six Ca isotopes can be simultaneously detected. However, Naumenko-Dèzes et al. (2015) report data obtained on a Triton plus with a special Faraday cup array with extended mass dispersion that enables simultaneous collection of all six Ca isotopes without the use of zoom lenses.

In principle,  $^{48}\text{Ca}$  only needs to be taken into account if it is chosen as one of the double spike isotopes (see Sect. 5.4), but as the fourth most abundant isotope it is advantageous to be included in any multicollection routine for the comparison of results from different Ca isotope ratios. Ion optical effects due to the large mass difference between Ca isotopes and the resulting wide dispersion of the different ion beams are major obstacles to ameliorate the external precision.

Wide dispersion of Ca ion beams have been accused to cause peak-shape defects with asymmetric peaks at the outermost cup positions (Fletcher et al. 1997; Heuser et al. 2002), which was responsible for the lack of improvement in internal precision for multi-collection over single-collection peak hopping. Holmden (2005) suggested to decrease the imprecision generated by ion optical effects in the mass spectrometer by decreasing the relative mass separation from  $\sim 10$  to 5 %. To attain this objective, he dynamically collected only four ion beams ( $^{40}\text{Ca}$ ,  $^{42}\text{Ca}$ ,  $^{43}\text{Ca}$ , and  $^{44}\text{Ca}$ ) in three collectors (L1, Axial, H1) on a Triton. Finally, damage to individual Faraday collectors have been reported, linked to  $^{40}\text{Ca}$  measurements that poison collector cups (Andreasen and Sharma 2006; Simon et al. 2009; Holmden and Bélanger 2010; Simon and DePaolo 2010). These authors have indeed shown that Faraday cup graphite liners degradation with use can affect efficiencies and thus  $^{40}\text{Ca}$  abundances. This can be avoided by replacing the graphite liners for example every 18 months, depending on usage.

## 5.3 Multiple Collector Inductively Coupled Plasma Mass Spectrometry (MC-ICP-MS)

### 5.3.1 Basics of MC-ICP-MS

In this section, we first briefly introduce issues that are characteristic for MC-ICP-MS, such as the sample introduction, plasma and interface processes. We then discuss the fundamental problems in MC-ICP-MS: interferences, mass discrimination and matrix effects on mass discrimination. This will be followed by a brief overview centered on key publications where MC-ICP-MS was used for the analysis of Ca isotopes. Note that isotope ratio measurements by (MC-)ICP-MS in general have been reviewed extensively in the past (Halliday et al. 2000; Rehkämper et al. 2001, 2004; Albarède and Beard 2004; Albarède et al. 2004; Vanhaecke et al. 2009; Yang 2009; Epov et al. 2011; Baxter et al. 2012).

The first MC-ICP-MS introduced was the VG Plasma54 (Waldner and Freedman 1992), followed by Nu Instruments NuPlasma, the Micro-mass IsoProbe, the VG Axiom and the Finnigan Neptune MC-ICP-MS. Note that in most cases, the names of the companies change quicker than authors can adjust. Currently, only the NuPlasma and the Neptune MC-ICP-MS are manufactured, with options and modifications that differ from the first models. Nu Instruments also manufactures a large geometry high-resolution MC-ICP-MS, the Nu Plasma 1700 but only a few instruments have been installed and so far no Ca isotope data are published.

If the MC-ICP-MS is coupled to a laser ablation system, samples can potentially be analyzed for Ca isotope compositions *in situ*, at the tenth of  $\mu\text{m}$  scale without further preparation (e.g. Tacail et al. 2016). However, since the plasma source efficiently ionizes all elements, matrix effects and interferences related to matrix elements (e.g.  $^{88}\text{Sr}^{++}$  on  $^{44}\text{Ca}^+$ ) cause severe problems if present.

The vast majority of Ca isotope studies carried out by MC-ICP-MS were based on sample and standard Ca dissolved in dilute acid (typically  $\text{HNO}_3$ ) with matrix elements commonly separated by ion chromatography beforehand. The solutions are usually aspirated at a rate of about  $100\ \mu\text{L}\ \text{min}^{-1}$  and dispersed using a microconcentric nebulizer commonly made of PFA or borosilicate glass. Within the nebulizer, an Ar gas stream of about  $1\ \text{L}\ \text{min}^{-1}$  passes along the tip of the capillary tubing. This results in a lower pressure at the capillary tip and hence self-aspiration. The aspirated solution is then sprayed into a fine aerosol. If the resulting droplets enter the plasma, the solvent evaporates, the remaining solids are atomized and eventually ionized. Because large droplets of about  $>10\ \mu\text{m}$  diameter would not dry down completely during the short passage through the plasma, they need to be sorted out by the use of a spray chamber. Therefore, only a few % of the sample and standard solution will make it to the plasma. To improve the delivery of the analyte (i.e. Ca) to

the plasma and thus improve sensitivity, most isotope analysis by MC-ICP-MS employs desolvators such as the Cetac Aridus or the Elemental Scientific Apex. In both systems, the aerosol generated by a microconcentric nebulizer is sprayed into a heated spray chamber to evaporate the solvent. Since too much water vapor would overload the plasma, the vapor must be removed before the Ar gas and analyte enters the plasma. In the Apex, this is facilitated by passing the sample gas through a Peltier cooled condenser. In the Aridus, the solvent vapor diffuses through a heated membrane where it is taken up and removed by a counter flow of Ar gas. The removal of water has the added benefit of reducing oxide and other solvent related interferences. In both desolvators, a small amount of  $\text{N}_2$  may be admixed to the dry aerosol to boost the signal further. However, polyatomic interferences containing nitrogen (e.g.  $^{14}\text{N}_3^+$  and  $^{14}\text{N}_2^{16}\text{O}^+$  on *mas* 42 and 44) may become more abundant.

The coupling of an efficient Ar plasma ion source, which operates at atmospheric pressure, to a mass spectrometer that needs to be maintained under vacuum in order to prevent high detector noise and collisions between ions and background gas is realized by a water cooled interface. This interface allows extracting the ions generated in the plasma into the mass spectrometer. It consists of a set of two cones made of Ni (or Al or Pt) with orifices of 0.5–1 mm. The cones serve as the inlet and outlet of an expansion chamber which is pumped to achieve a transitional vacuum at a few mbar. The sampler cone “samples” the ions generated in the plasma. The ions then expand into the vacuum of the expansion chamber where the March disk is the region where the ions attain ultrasonic speed. The skimmer cone “skims” the ions from a region slightly before the March disk. At the rear of the skimmer cone, positive ions are accelerated into the mass spectrometer by the negative potential applied to the extraction lens. Ions within the positively charged ion beam (dominated by  $^{40}\text{Ar}^+$ ) repel each other. This space

charge effect may be responsible for the pronounced mass discrimination in MC-ICP-MS.

### 5.3.2 Mass Discrimination and Matrix Effects in (MC-)ICP-MS

Mass discrimination or mass bias in MC-ICP-MS is much larger than in TIMS, but far more stable. This is not surprising, since the analyte elements are introduced to the plasma and mass spectrometer under stable and reproducible conditions as long as tuning parameters (gas flow, lens settings, torch position, RF power) are not changed. The fact that the instrumental mass bias drifts only slightly with time allows for stable isotope analysis without the use of double spikes, using the standard-sample-standard bracketing technique. Analyses of samples are simply alternated with the analysis of standards and  $\delta$ -values are then calculated for samples relative to the average of the preceding and succeeding standard analysis.

The downside of the sample bracketing technique is the possibility that the mass bias changes in response to sample matrices being different than that of the standard. Together with the need to remove interfering ions, this makes chemical separation of Ca a prerequisite for MC-ICP-MS. Fitzke et al. (2004) noted large matrix effects in the per mill range under cool plasma conditions, if samples were measured in different acid matrices. Stürup (2004) observed a matrix related decrease of the ionization rate in urine samples with high Na and K contents. Matrix tests for Mg isotope measurements by MC-ICP-MS showed a memory of the matrix induced mass bias in succeeding matrix element free standard solutions, likely due to depositions on the cone (Wombacher et al. 2009). This hints at the possibility to detect sample matrix effects on mass bias by the matrix related drift induced between the bracketing standards. That the state of the cones is important for stable measurement has been frequently observed. For example, Schiller (2012) analyzed Ca isotopes with high ion beam intensities ( $\sim 100$  V on  $^{44}\text{Ca}^+$ ). During the first hour of analysis they observed large mass bias drift after cone cleaning that could be avoided by conditioning the cones with Ca during tuning.

Shiel et al. (2009) detected the influence of ion exchange resin derived organics on the mass bias of Zn and Cd isotope measurements by MC-ICP-MS. For Ca isotope analysis organic matter from the ion exchange resin may not be a common problem, as Ca is a major element and is usually separated in sufficient quantity to allow for significant dilution of organic matrix contributions. This can be tested by running a Ca standard through chemistry using an amount of Ca similar or below that of samples.

So far no Ca double spike has been applied for mass bias correction during MC-ICP-MS measurements. This is because the use of a double spike requires that four interference free isotopes can be reliably measured and possibly also because MC-ICP-MS generally consumes more sample Ca and thus double spike than TIMS (Wieser et al. 2004).

Many studies of isotope ratios by ICP-MS use element additions for mass bias drift correction, for example Tl, added to both samples and standards, were used to monitor the mass bias drift in Pb isotopes ratios (Longerich et al. 1987) and Cu isotopes were used for Zn and vice versa (Maréchal et al. 1999). At least potentially, mass bias drift for ratios of  $^{42}\text{Ca}$ ,  $^{43}\text{Ca}$  and  $^{44}\text{Ca}$  could likewise be corrected using  $^{49}\text{Ti}/^{47}\text{Ti}$ .

### 5.3.3 Interferences in (MC-)ICP-MS

The biggest disadvantage of Ca isotope analysis using ICP-MS is the occurrence of various and often significant isobaric interferences. Table 4 presents a selection of possible isobaric interferences on Ca isotopes.

Several ways exist to deal with these isobaric interferences: (1) chemical purification of the sample, (2) high mass resolution (3) mathematical correction for interfering ions, and (4) suppression of interfering ions by cold (or cool) plasma or collision cell technology.

Purification of the sample via ion chromatography (Sect. 4.2) provides an efficient way to avoid interferences introduced by the sample matrices, e.g.  $^{40}\text{K}^+$ ,  $^{48}\text{Ti}^+$ ,  $^{26}\text{Mg}^{16}\text{O}^+$  or  $^{88}\text{Sr}^{2+}$ , but cannot remove interferences that are introduced by the Ar gas and its impurities ( $^{40}\text{Ar}^+$ ;

**Table 4** Potential interferences on Ca isotopes

Ca isotope	Interference	$\Delta m$	Required resolution	Ca isotope	Interference	$\Delta m$	Required resolution
$^{40}\text{Ca}$	$^{80}\text{Kr}^{++}$	-0.0044	9076	$^{44}\text{Ca}$	$^{88}\text{Sr}^{++}$	-0.0027	16,448
	$^{80}\text{Se}^{++}$	-0.0043	9228		$^{43}\text{CaH}^+$	0.0111	3956
	$^{40}\text{Ar}^+$	-0.0002	193,149		$^{28}\text{Si}^{16}\text{O}^+$	0.0164	2687
	$^{40}\text{K}^+$	0.0014	28,378		$^{32}\text{S}^{12}\text{C}^+$	0.0166	2650
	$^{39}\text{KH}^+$	0.0089	4469		$^{30}\text{Si}^{14}\text{N}^+$	0.0214	2058
	$^{24}\text{Mg}^{16}\text{O}^+$	0.0174	2301		$^{26}\text{Mg}^{18}\text{O}^+$	0.0263	1673
	$^{20}\text{Ne}_2^+$	0.0223	1793		$^{27}\text{Al}^{16}\text{OH}^+$	0.0288	1526
	$^{23}\text{Na}^{16}\text{OH}^+$	0.0299	1336		$^{12}\text{C}^{16}\text{O}_2^+$	0.0343	1280
$^{42}\text{Ca}$				$^{46}\text{Ca}$	$^{14}\text{N}_2^{16}\text{O}^+$	0.0456	964
	$^{84}\text{Kr}^{++}$	-0.0029	14,627				
	$^{84}\text{Sr}^{++}$	-0.0019	21,993		$^{92}\text{Zr}^{++}$	-0.0012	39,297
	$^{41}\text{KH}^+$	0.0110	3805		$^{46}\text{Ti}^+$	-0.0011	43,504
	$^{30}\text{Si}^{12}\text{C}^+$	0.0151	2770		$^{92}\text{Mo}^{++}$	-0.0003	161,524
	$^{26}\text{Mg}^{16}\text{O}^+$	0.0189	2221		$^{30}\text{Si}^{16}\text{O}^+$	0.0150	3064
	$^{40}\text{ArH}_2^+$	0.0194	2161		$^{32}\text{S}^{14}\text{N}^+$	0.0215	2142
	$^{40}\text{CaH}_2^+$	0.0196	2139		$^{29}\text{Si}^{16}\text{OH}^+$	0.0255	1799
	$^{28}\text{Si}^{14}\text{N}^+$	0.0214	1962		$^{14}\text{N}^{16}\text{O}_2^+$	0.0392	1172
	$^{24}\text{Mg}^{18}\text{O}^+$	0.0256	1640	$^{48}\text{Ca}$			
$^{43}\text{Ca}$	$^{25}\text{Mg}^{16}\text{OH}^+$	0.0300	1401		$^{48}\text{Ti}^+$	-0.0046	10,458
	$^{14}\text{N}_3^+$	0.0506	829		$^{96}\text{Mo}^{++}$	-0.0002	246,860
					$^{96}\text{Ru}^{++}$	0.0013	37,877
					$^{96}\text{Zr}^{++}$	0.0016	29,896
	$^{86}\text{Sr}^{++}$	-0.0041	10,392	$^{43}\text{Ca}$	$^{32}\text{S}^{16}\text{O}^+$	0.0145	3317
	$^{86}\text{Kr}^{++}$	-0.0035	12,404		$^{36}\text{Ar}^{12}\text{C}^+$	0.0150	3194
	$^{42}\text{CaH}^+$	0.0077	5596		$^{24}\text{Mg}_2^+$	0.0176	2731
	$^{27}\text{Al}^{16}\text{O}^+$	0.0177	2429		$^{34}\text{S}^{14}\text{N}^+$	0.0184	2605
	$^{31}\text{P}^{12}\text{C}^+$	0.0150	2865		$^{31}\text{P}^{16}\text{OH}^+$	0.0240	2000
	$^{26}\text{Mg}^{16}\text{OH}^+$	0.0266	1617		$^{16}\text{O}_3^+$	0.0322	1489
	$^{14}\text{N}_3\text{H}^+$	0.0583	737				

Interferences with  $\Delta m < 0$  have masses lighter than the respective Ca isotope, interferences with  $\Delta m > 0$  have heavier masses

To fully resolve the Ca and interfering ion beams and achieve a flat plateau region, the resolving power of the instrument  $R(5, 95 \%)$  should be about a factor of two better than the nominally required resolution given in the table

$^{86}\text{Kr}^{2+}$ ), the solvent ( $\text{H}$  in  $\text{ArH}_2^+$ ) or the N-gas flow of desolvators ( $\text{N}_2\text{O}^+$ ) (Table 4).

Many interferences on Ca isotopes can be avoided by the use of high mass resolution. In the low resolution mode, Ca and interference ion beams overlap significantly, even though their mass is slightly different due to variable mass defects. If ion beams are sufficiently clipped by a

narrow source slit in the mass spectrometer, the interference and Ca isotope ion beams can be resolved at the focal plane where the multi collector array is positioned, obviously at the cost of sensitivity which may only be 5 % at high mass resolution. The two currently available MC-ICP-MS instruments, the Nu Instruments Plasma HR and the ThermoScientific Neptune

Plus have the possibility to choose between three different predefined low, medium and high mass resolution modes.

Precise isotope ratio measurements require flat-topped peaks. Flat topped peaks are obtained by the width of the ion beam being significantly smaller than the collector width. In single collector sector field ICP-MS instruments, ion beams of slightly different mass are completely resolved by narrow source and detector slit which commonly results in triangular peaks that are not suitable for precise isotope ratio measurements. In MC-ICP-MS, interferences (most of which are of higher mass than the analyte ions) are screened out at the low mass edge of the Faraday collector. The resolving power  $R$  quantifies the ability of the mass spectrometer to resolve ion beams of slightly different mass. Resolving power is commonly determined as the ion beam width at 5 and 95 % peak height:  $R_{(5, 95 \%)} = m/\Delta m$  with  $\Delta m$  being the mass at the left hand side peak slope at 5 % peak height minus the mass at 95 % peak height (Weyer and Schwieters 2003; see illustration further below). Because of this definition and the associated ion beam tailing, full resolution between the Ca ion beam and the interfering ion beam requires a resolving power that is about double that given as required resolution in Table 4, in particular, a higher resolving power is needed if interferences display high intensities.

It is possible to eliminate the most significant *polyatomic* interferences from Ca isotope masses using mid or high resolution mode, as these interferences require mass resolutions ranging from  $\sim 740$  ( $^{14}\text{N}_3\text{H}^+$ ) to  $\sim 3300$  ( $^{32}\text{S}^{16}\text{O}^+$ ) (Table 4).

Atomic interferences like  $^{48}\text{Ti}^+$  or  $^{88}\text{Sr}^{2+}$  on  $^{48}\text{Ca}^+$  and  $^{44}\text{Ca}^+$  cannot be resolved as this would need resolving powers much larger than 10,000. Furthermore, their mass is lighter than that of the Ca isotopes (Table 4). Therefore, they would have to be resolved on the high mass side peak shoulder where the heavier polyatomic interferences cannot be resolved. Atomic and also some polyatomic isobaric interferences can be handled by mathematical interference corrections, where the contribution of the interfering element is stripped from the measured intensity of the Ca ion beam as shown in the example for the  $^{48}\text{Ti}$  interference correction:

$$I_{48\text{Ca}} = I_{48\text{Ca}+48\text{Ti}} - I_{48\text{Ti}} \quad (40)$$

where  $I_{48\text{Ca}}$  denotes the signal intensity for  $^{48}\text{Ca}$  after the interference correction. The contribution of  $^{48}\text{Ti}$  ( $I_{48\text{Ti}}$ ) to the measured intensity  $I_{48\text{Ca}+48\text{Ti}}$  can be determined by monitoring  $^{47}\text{Ti}$  during the analysis:

$$I_{48\text{Ti}} = I_{47\text{Ti}} \times \left( \frac{^{48}\text{Ti}}{^{47}\text{Ti}} \right)_{\text{biased}} \quad (41)$$

During analysis,  $^{48}\text{Ti}/^{47}\text{Ti}$  ( $\approx 0.7372/0.0744$ ) is affected by the instrumental mass bias; therefore the measured ratio may be by about 5 % higher than in the sample solution. Hence, the interference correction can be much improved if this mass bias is simulated using the exponential law (Eqs. 36 and 37):

$$\left( \frac{^{48}\text{Ti}}{^{47}\text{Ti}} \right)_{\text{biased}} = \left( \frac{^{48}\text{Ti}}{^{47}\text{Ti}} \right)_{\text{nature}} \times \left( \frac{47.9479471}{46.9517638} \right)^{-f_{\text{Ca}}} \quad (42)$$

with  $f$  taken from Ca isotope ratios as given in Eq. 36 above. Natural Ca isotope fractionation will affect  $f_{\text{Ca}}$  and stable isotope fractionation of Ti in nature and during chemical separation will also affect the accuracy of the correction. Furthermore, the natural isotope ratios assumed for  $^{48}\text{Ti}/^{47}\text{Ti}$  and in the determination of  $f_{\text{Ca}}$  may not be accurate. However all these uncertainties are expected to be about an order of magnitude less significant than the large effect of the instrumental mass discrimination in MC-ICP-MS. Interference corrections obviously work best if the correction is of minor significance. The Ti correction shown in the example above is unfortunate, as the abundance of the monitor isotope  $^{47}\text{Ti}$  is about 10 times less than that of  $^{48}\text{Ti}$ . As a result, noise recorded by the monitor isotope  $^{47}\text{Ti}$  will be amplified to the signal on mass 48 by an order of magnitude. Thus, if the Ti correction is insignificant (which has to be shown) it may better be avoided. For example in TIMS analysis, ionization of Ti is not expected and application of the Ti correction would only induce additional scatter. A further pitfall results from the possible presence of unresolved interferences on the interference monitor mass, e.g.  $^{31}\text{P}^{16}\text{O}^+$  on  $^{47}\text{Ti}^+$ , which would lead to overcorrection.

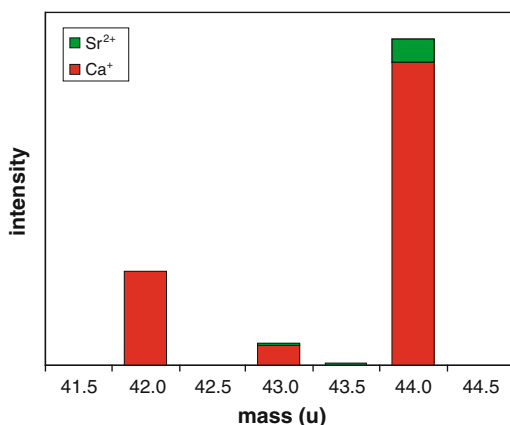


**Fig. 5** Schematic illustration of the  $\text{Sr}^{2+}$ -interference correction

For many Ca isotope measurements interference correction of  $^{46}\text{Ti}$  and  $^{48}\text{Ti}$  does not play a role as masses  $^{46}\text{Ca}$  and  $^{48}\text{Ca}$  are commonly not measured.

In analogy to the Ti correction,  $\text{Sr}^{2+}$ -ions interfering on the masses 42, 43 and 44 can be corrected by measuring  $^{87}\text{Sr}^{2+}$  on mass 43.5. Using the known isotopic composition of Sr and assuming a mass bias being similar to that of Ca it may be possible to calculate the intensity of  $^{84}\text{Sr}^{2+}$ ,  $^{86}\text{Sr}^{2+}$  and  $^{88}\text{Sr}^{2+}$  (Fig. 5) and correct the measured intensities on masses 42, 43 and 44. However, the exponential law fractionation coefficient  $f_{\text{Ca}}$  may not be perfectly suitable for Sr isotopes and the  $^{87}\text{Sr}$  abundance in natural samples is somewhat variable (e.g. Hirata et al. 2008). Therefore, Sr isotope corrections should be carefully implemented and large corrections are best avoided by chemical separation.

A similar procedure could be used for the correction of  $\text{Kr}^{2+}$  ions (monitoring  $^{83}\text{Kr}^{2+}$  on mass 41.5). As the Ar gas usually only contains traces of Kr, and given the high second ionization potential of Kr (24.36 eV), it may not be possible to reliably monitor  $^{83}\text{Kr}^{2+}$  at mass 41.5 and the Kr interferences can possibly be neglected or may be subtracted along with the background anyway.

Because large interferences are more difficult to resolve, to correct for, or to be subtracted

based on background measurements, interferences should be kept to a minimum. Apart from desolvation and chemical separation, cool plasma techniques and collision cells offer additional interference suppression, such that even  $^{40}\text{Ca}$  may be analyzed by MC-ICP-MS. These approaches will be discussed in the next section.

### 5.3.4 Calcium Isotope Analysis by (MC-)ICP-MS

Several studies applied ICP-MS for Ca isotope analysis and in most cases multiple collector arrays were used (Halicz et al. 1999; Fietzke et al. 2004; Wieser et al. 2004; Steuber and Buhl 2006; Tipper et al. 2006, 2008a, b, 2010; Sime et al. 2007; Hirata et al. 2008; Morgen et al. 2011; Schiller et al. 2012; Tacail et al. 2016; Martin et al. 2015). From the above discussion, it is expected that (i) multi-collection, (ii) chemical separation and (iii) high mass resolution is generally required in order to obtain sufficiently precise and accurate Ca stable isotope data by (MC-)ICP-MS. In the following, published methods for Ca isotope analysis by ICP-MS are discussed, beginning with the pioneering study by Halicz et al. (1999), including methods that aim at the suppression of interferences (*cold plasma and reaction/collision cell technology*) and summarizing first attempts for in situ Ca isotope analysis by *laser ablation*.

Halicz et al. (1999) used a NuPlasma instrument for the first Ca isotope ratio measurements by MC-ICP-MS. Analyzed were  $^{42}\text{Ca}$ ,  $^{43}\text{Ca}$  and  $^{44}\text{Ca}$  for commercial Ca reagents and a few natural  $\text{CaCO}_3$  samples, including speleothems and coral aragonite. The sensitivity was 0.3 V for  $^{44}\text{Ca}$  at an uptake rate of  $\sim 70 \mu\text{l min}^{-1}$ . Sample and standard solutions containing 20–30 ppm Ca in 0.1 M  $\text{HNO}_3$  were introduced into the plasma using a Cetac MCN6000 membrane desolvator (the predecessor of the Cetac Aridus) and analyzed for 10 min. Membrane desolvation was used to reduce polyatomic interferences such as  $^{14}\text{N}_2^{16}\text{O}^+$  and  $^{12}\text{C}^{16}\text{O}_2^+$  on  $^{44}\text{Ca}^+$  and  $\text{ArH}_2^+$  on  $^{42}\text{Ca}^+$  to low levels. About half of the elevated background levels of about 1.5 mV were attributed to scattered  $^{40}\text{Ar}^+$  and  $^{40}\text{Ca}^+$  ions, respectively. This background component was



monitored on additional masses (42.5, 43.25, and 44.5) and subtracted from the corresponding Ca ion beam signals. Doubly charged Sr ion interferences on all three Ca isotope masses were corrected based on the background corrected  $^{87}\text{Sr}^{++}$  signal monitored at mass 43.5. Mass bias was corrected for by bracketing sample solutions with analysis of NIST SRM 915a Ca. Precision assessed from repeated sample analysis ranges from 0.04 for a coral sample ( $n = 3$ ) to 0.40 for a calcrete sample ( $n = 5$ ) for  $\delta^{44/42}\text{Ca}$  (2 sd).

Cool plasma conditions also allow for the reduction of interfering molecular as well as elemental ion formation. Under normal operating conditions the RF (radio frequency) power coupled into the plasma is set between 1200 and 1400 W. Decreased RF power results in a plasma with a lower degree of ionization and temperature and therefore is called “cool plasma” or “cold plasma”. Thus elements or molecules with a high first ionization potential are ionized to a much lesser degree. Since the ionization of Ar and the formation of oxides and argides is suppressed, cool plasma conditions provide a reasonable approach for Ca isotope analysis (Fietzke et al. 2004). Several publications report the measurements of Ca isotopes using cool plasma. Most of the published cool plasma Ca measurements (e.g. Patterson et al. 1999, Murphy et al. 2002) are tracer experiments in humans without the need of high precision data and measurement of  $^{40}\text{Ca}$ . In addition these studies have been performed using Q-ICP-MS which is not suitable for high precision Ca isotope measurements. Fietzke et al. (2004), however, conducted Ca isotope measurements using cool plasma MC-ICP-MS. Using a VG AXIOM MC-ICP-MS, they set the RF power as low as 400 W, resulting in a  $^{40}\text{Ar}$  background decrease from about  $2.5 \times 10^7$  cps (0.4 V with  $10^{11} \Omega$  resistors) to  $1.0 \times 10^6$  cps (Fig. 6). The rather low  $^{40}\text{Ar}^+$  background even in hot plasma probably also reflects a narrow source slit that was used to screen out interferences at the high mass edge of the detector at high mass resolution as described in more detail below. Along with  $^{40}\text{Ar}^+$ , the formation of  $^{40}\text{ArH}^+$ ,  $^{40}\text{ArD}^+$  and to some degree  $^{14}\text{NO}_2^+$  ions decreased (Fig. 6). On

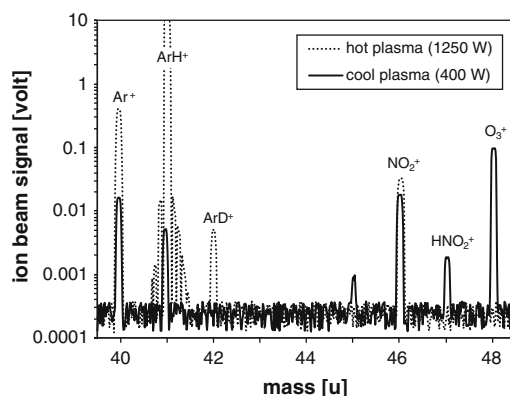
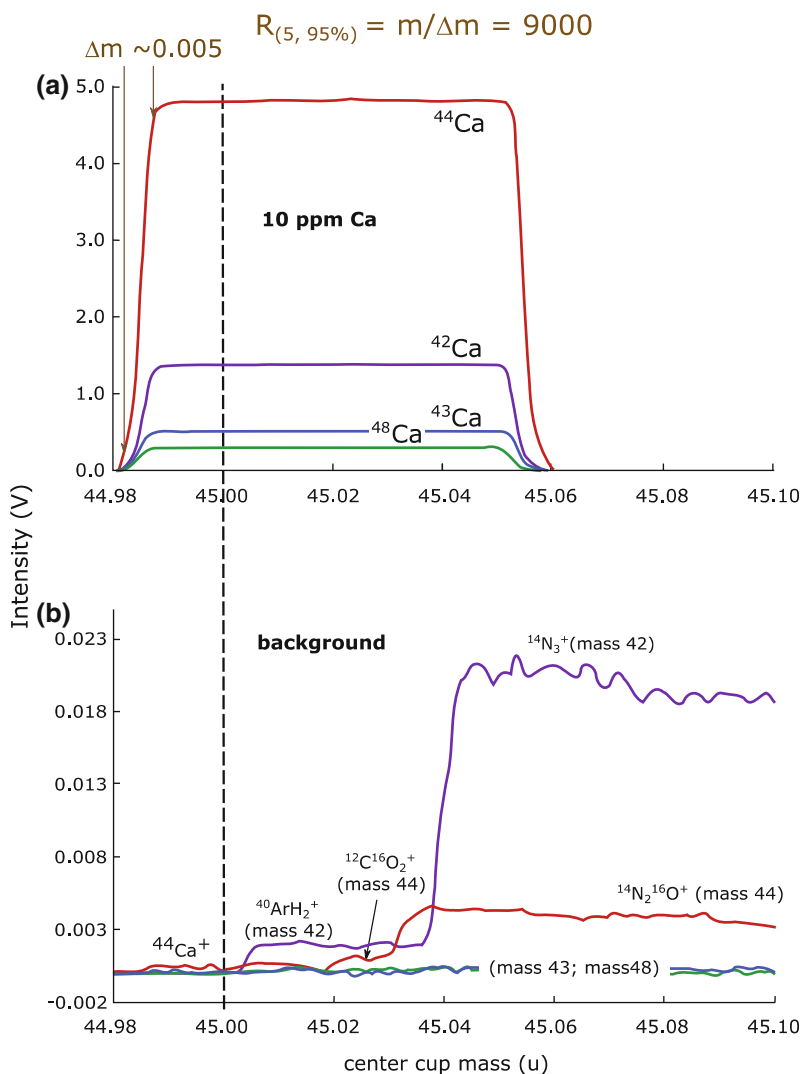


**Fig. 6** Comparison of the background spectrum under hot and cool plasma conditions using the VG Axiom MC-ICP-MS. Figure modified from Fietzke et al. (2004)

the other hand the use of cool plasma increased the production of  $^{14}\text{N}^{16}\text{O}_2\text{H}^+$  and  $^{16}\text{O}_3^+$  ions. As the study aimed to measure  $^{44}\text{Ca}/^{40}\text{Ca}$  values, interferences on  $^{42}\text{Ca}$ ,  $^{43}\text{Ca}$ ,  $^{46}\text{Ca}$  and  $^{48}\text{Ca}$  were less relevant. However, masses 42 and 43 were not affected by significant interferences, while mass 46 and 48 were. As the  $^{40}\text{Ca}$  signal was about 500 times higher compared to the  $^{40}\text{Ar}$  background, drift in the Ar background was considered negligible. Fietzke et al. (2004) reported a RSD of about 0.14 ‰, thus the precision of the  $\delta^{44/40}\text{Ca}$  data generated by cool plasma MC-ICP-MS is comparable to TIMS measurements. The downside of the cool plasma method were large matrix related shifts in  $\delta^{44/40}\text{Ca}$  if the acid molarity was not precisely matched between standards and samples. Other reasons why the cool plasma technique has not become widely adopted may be that (1) the production of AXIOM MC-ICP-MS was stopped in 2002 and currently available MC-ICP-MS may not be able to set the RF power and thereby reduce the  $^{40}\text{Ar}^+$  ion beam to such a low level and (2)  $\delta^{44/42}\text{Ca}$  and other ratios measured using conventional MC-ICP-MS may be considered sufficient for Ca isotope geochemistry. Since cool plasma MC-ICP-MS and the apparent matrix sensitivity is not well investigated, further studies on other instruments would be of interest, perhaps in conjunction with a suitable double-spike which may be able to correct for residual matrix effects.

**Fig. 7** Simultaneous peak scan for  $^{42}\text{Ca}$ ,  $^{43}\text{Ca}$ ,  $^{44}\text{Ca}$  and  $^{48}\text{Ca}$  in high resolution. Panel **a** displays the overlapping Ca ion beams for a 10 ppm solution and shows the resolving power  $R = m/\Delta m$  with  $\Delta m$  defined as the ion beam width at 5 and 95 % peak height; panel **b** shows the interferences observed in a Ca free background solution. An interference free measurement position (as indicated by the *stippled line*) that is sufficiently distant from the low mass peak edge needs to be identified. Figure modified from Wieser et al. (2004)



Wieser et al. (2004) determined  $\delta^{44/42}\text{Ca}$ ,  $\delta^{48/42}\text{Ca}$ ,  $\delta^{44/43}\text{Ca}$  and  $\delta^{48/43}\text{Ca}$  with external reproducibilities of  $\pm 0.11$ ,  $\pm 0.33$ ,  $\pm 0.12$  and  $\pm 0.28$  (2 sd;  $n = 54$ ) respectively, using a Neptune MC-ICP-MS at hot (1200 W) plasma conditions and high mass resolution (Fig. 7). Data for  $\text{CaCO}_3$  reference samples were measured relative to seawater Ca. The sample Ca was first separated by cation exchange. Mass bias, which amounts to 5 % per atomic mass unit, was corrected for by bracketing sample solutions with seawater Ca analysis. Background determinations were alternated with sample and standard analysis and background values were subtracted

from sample and standard measurements. The  $^{40}\text{Ar}^+$  ion beam corresponds to about 8000 V ( $10^{11} \Omega$  resistor). While scattering of Ar ions was not observed, analysis of  $^{40}\text{Ca}$  is obviously impossible under these conditions. The  $^{46}\text{Ca}$  signal was too low for meaningful analysis. Sample solutions, containing 10 ppm Ca in 3.5 %  $\text{HNO}_3$ , were analyzed for two minutes followed by a 120 s rinse. Sample and standard solutions were introduced using an Apex-Q coupled to a Cetac Aridus membrane desolvator. This combination offers a thoroughly dried aerosol which is expressed in a further reduction of the  $^{40}\text{ArH}_2^+$  interference down to 2 mV,

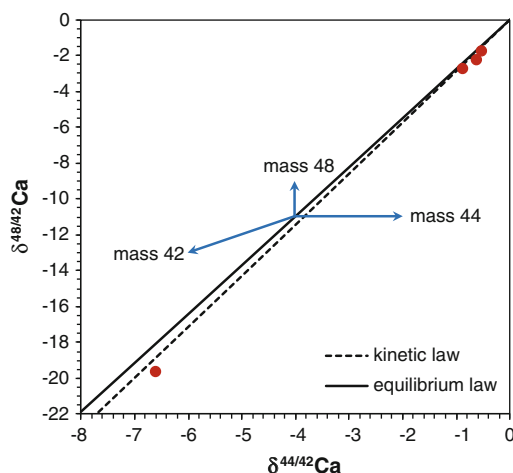


**Fig. 8** Three isotope plot featuring data obtained by high-resolution MC-ICP-MS for Ca carbonate samples relative to seawater (Wieser et al. 2004). The size of the symbols roughly corresponds to the precision of the measurements (2 sd). Fractionation curves correspond to the equilibrium and kinetic laws (see Chapter “Introduction”). Arrows indicate 2 ‰ interferences on the masses indicated. The data plots closer to the slope of the kinetic law than that defined by the equilibrium law. At a first glance, this may suggest kinetic isotope fractionation. However, the samples are not related to the zero-delta material (IAPSO seawater) with the possible exception of the least fractionated sample, a modern bivalve shell. Furthermore, the interpretation of kinetic and equilibrium law slopes may not always be straight forward (Chapter “Introduction”) and the offset from the reference slopes could also indicate the effects of interferences. For example, the samples could be affected by small interferences on mass 44. Likewise, the seawater reference sample analysis could be compromised by small interferences on mass 42 or 48

compared to 30 mV using the Apex-Q with an Aero Naphion membrane. With this set-up,  $^{44}\text{Ca}$  ion beams of 4.8 V were obtained. Due to the large internal volume of the coupled desolvating introduction systems, very stable ion beams are achieved. While the multi-collector array corrects very well for somewhat unstable signals in isotope ratio analysis, unstable ion beam signals impede the precise peak shape tuning needed for high resolution analysis. Three isotope plots were used to constrain the absence of significant interferences (Fig. 8).

Schiller et al. (2012) combined high resolution MC-ICP-MS (Neptune with sensitive jet and

x-cones) analysis of  $^{42}\text{Ca}$ ,  $^{43}\text{Ca}$ ,  $^{44}\text{Ca}$ ,  $^{46}\text{Ca}$  and  $^{48}\text{Ca}$  with TIMS (Triton) analysis for  $^{40}\text{Ca}$ ,  $^{42}\text{Ca}$ ,  $^{43}\text{Ca}$  and  $^{44}\text{Ca}$  in order to measure all stable Ca isotopes in their terrestrial test samples. The method presented was developed with the aim to study nucleosynthetic Ca isotope anomalies in meteorites and their components (Chapter “High Temperature Geochemistry and Cosmochemistry”) by high precision analysis. For this reason, no double spike was applied in TIMS analysis, thus no  $\delta$ -values for mass dependent isotope fractionations were calculated. However,  $\delta$ -values were obtained from MC-ICP-MS analysis of rock and seawater reference samples from which Ca was chemically separated after acid digestions. Pooled  $\delta^{42/44}\text{Ca}$ ,  $\delta^{43/44}\text{Ca}$ ,  $\delta^{46/44}\text{Ca}$  and  $\delta^{48/44}\text{Ca}$  values measured relative to NIST SRM 915b yielded typical uncertainties for the mean, corresponding to  $\pm 0.03$ ,  $\pm 0.01$ ,  $\pm 0.04$ ,  $\pm 0.05$  per mil (2se;  $n = 10$ ). The data agreed very well with TIMS analysis by Heuser and Eisenhauer (2008), Amini et al. (2009) and Wombacher et al. (2009). For mass bias correction, samples were bracketed by analysis of NIST SRM915b. The instrumental background was carefully monitored and subtracted.

To reveal (mass-independent) nucleosynthetic anomalies, the MC-ICP-MS and TIMS data were internally normalized to  $^{42}\text{Ca}/^{44}\text{Ca} = 0.31221$ . Results are expressed using a  $\mu$ -notation, which gives deviations in normalized  $^x\text{Ca}/^{44}\text{Ca}$  from the same value in NIST SRM 915b in parts per million (ppm). The  $\mu^{43/44}\text{Ca}$ ,  $\mu^{46/44}\text{Ca}$ ,  $\mu^{48/44}\text{Ca}$  values obtained by MC-ICP-MS display uncertainties of  $\pm 2$ ,  $\pm 45$  and  $\pm 13$  ppm (2se;  $n = 10$ ). The main reasons for the high precision achieved, besides internal normalization and clean chemical separation, are the high ion beam intensities for the smaller isotopes ( $\sim 0.15$  V for  $^{46}\text{Ca}$ ;  $\sim 100$  V for  $^{44}\text{Ca}$ ) that are possible if  $^{40}\text{Ca}$  is omitted, and the lengthy measurement times (10 analysis, each lasting 14 min.). The downside of the high signal intensities are the loss in sensitivity over time due to deposition onto the cones and the degradation of the aperture lens and resolution slits, such that the slits had to be replaced after 150 h of measurement. Furthermore, with increasing Ca ion beam intensities, a non-linear increase of the background between

mass 42 and 43 and between mass 47 and 48 up to 300  $\mu\text{V}$  was observed. Effects of this elevated background were minimized by precisely matching the signal intensities between samples and standards.

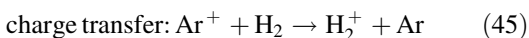
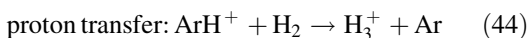
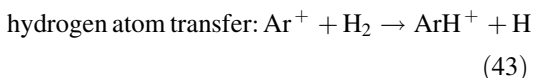
Sample introduction was facilitated using an Elemental Scientific APEX with an attached ACM membrane for desolvation. Measurements were carried out either in medium or high resolution mode with a resolving power  $>5000$ . Before analysis, Ca isotope ratios were measured at slightly different positions at the low mass side of the flat topped peak in order to obtain a measurement position that is interference free, but not too close to the peak edge. This position was typically located about 0.024 amu from the center of the calcium peak. A peak center was conducted prior to every standard analysis. Sensitivity ranged from 6 to 17 V for  $^{44}\text{Ca}$  per ppm Ca in solution. Samples and standard solutions contained between 8 and 16 ppm Ca in 2 %  $\text{HNO}_3$ . Because every sample was analyzed ten times, a total of 250–500  $\mu\text{g}$  Ca was consumed, while 10  $\mu\text{g}$  were consumed during single TIMS analysis.

Schiller et al. (2012) also discuss problems related to the correction of Ti interferences on  $^{46}\text{Ca}$  and  $^{48}\text{Ca}$  that were corrected based on the monitoring of  $^{47}\text{Ti}$  employing a  $10^{12}\Omega$  resistor. However, because of difficulties related to the scattered Ca ion beam, Ti intensities were checked for most samples using a secondary electron multiplier equipped with a retarding potential quadrupole filter to avoid scattered ions.

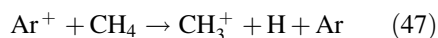
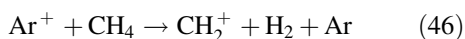
Another way to remove polyatomic interferences and even the  $^{40}\text{Ar}$  interference is provided by the use of a collision and reaction cell or a dynamic reaction cell. Reaction cells contain a quadrupole, hexapole or octopole, placed off-axis behind the skimmer cone. Introducing different reaction gases (He, Xe,  $\text{N}_2$ ,  $\text{O}_2$ ,  $\text{NH}_3$  or  $\text{CH}_4$ ) into the cell leads to a fragmentation or neutralization of the interfering atomic and polyatomic ions.

Feldmann et al. (1999) used He as a buffer gas and  $\text{H}_2$  as the reaction gas. They state that three

different processes play a major role for the neutralization of  $\text{Ar}^+$ -ions:



Boulyga and Becker (2001) used a HEX-ICP-QMS (Micromass “Platform ICP”) with He and H as collision gases within the hexapole. They noticed a reduction of  $^{40}\text{Ar}^+$  by about three to four orders of magnitude. Stürup et al. (2006) used  $\text{CH}_4$  as a reaction gas for their measurements with a dynamic reaction cell (DRC) ICP-MS (Elan DRC-e). They quote three reactions leading to a neutralization of  $\text{Ar}^+$ -ions:



Boulyga et al. (2007) used a DRC-ICP-MS (Elan DRC-II) with  $\text{NH}_3$  as reaction gas and compared their results with TIMS measurements of the same reference materials (in-house standard, SRM 915a and SRM 1486). They argue that the obtained reproducibilities are in the same order of magnitude and the  $\delta^{44/40}\text{Ca}$  values of their lab ICP standard and SRM 1486 relative to SRM 915a are comparable. They concluded that using DRC-ICP-MS seems to be a good alternative to MC-ICP-MS and TIMS measurements of Ca isotopes. However, the reported  $\delta^{44/40}\text{Ca}$  value of SRM 1486 of ca. +3 ‰ (rel. to SRM 915a) is about 4 ‰ heavier than the reported SRM 1486 value of Heuser and Eisenhauer (2008) (Sect. 3.1). As SRM 1486 is a bone meal and bones are normally enriched in the light Ca isotopes (Chapter “Biomedical Application of Ca

Stable Isotopes”), it is unlikely that SRM1486 exhibits a strong enrichment in  $^{44}\text{Ca}$ . Although the use of a collision and reaction cell enables the analysis of  $^{40}\text{Ca}$  and suppresses the formation of atomic and polyatomic interfering ions, the precision of published single-collector methods is about one order of magnitude worse compared to MC-ICP-MS or TIMS measurements.

The IsoProbe and a few VG Axiom MC-ICP-MS were equipped with a collision cell. Cecil and Ducea (2011) determined radiogenic  $^{40}\text{Ca}$  enrichment in K-rich authigenic minerals using a GV IsoProbe and gas-phase reactions in a hexapole collision cell to minimize isobaric Ar interference. A new attempt is currently made by Elliott et al. (2015). They coupled the front end, i.e. the interface and collision cell, from the Thermo Fisher Scientific iCAP Q (a quadrupole single collector ICP-MS) to the double-focusing Neptune mass analyzer.

Laser ablation (LA)-MC-ICP-MS offers the potential for in situ analysis of Ca isotope compositions without chemical separation. The sample (e.g. a thin or thick section, crystal or shell specimen) or standard material is ablated with a laser beam. The resulting aerosol is then transport into the mass spectrometer and analyzed. LA-ICP-MS is more frequently used for concentration determinations and radiogenic isotope systems (Sr, U/Pb). Currently, two published LA-ICP-MS studies on Ca stable isotope fractionation are published.

Santamaria-Fernandez and Wolff (2010) tried to determine the Ca isotopic composition in pharmaceutical packaging for discriminatory purposes. Their study nicely shows that precise and accurate LA-ICP-MS analyses of Ca isotopes are very challenging. The main problems relate to the mass bias correction and interferences. While it is possible to get rid of isobaric atomic interferences in solution analysis by a chemical purification prior to the measurement this is not possible for in situ analyses. Standard-sample bracketing has to be applied for the mass bias correction. This method usually requires that the composition of samples and standard materials are similar for matrix effects to be negligible.

Santamaria-Fernandez and Wolff (2010) used a 213 nm laser ablation system (NewWave UP-213) attached to a Neptune MC-ICP-MS for their Ca isotope measurements with the aim to identify counterfeit pharmaceuticals by comparing the packaging. Cardboard and ink of packaging have high concentrations of Ca mainly due to the use of kaolinite, calcium carbonate, chalk or china clay as coating material. In order to correct the instrumental mass bias relative to standards, Santamaria-Fernandez and Wolff (2010) prepared solid pressed pellets from NIST SRM 915a and 915b calcium carbonates using a KBr press without adding KBr to the pellets. The Ca isotopic composition of both carbonate standards has been characterized previously. Thus standard sample bracketing of both reference materials with SRM 915a being the standard and SRM 915b being the sample allows to detect problems. As both materials are chemically not very different, matrix effects should be negligible.

Santamaria-Fernandez and Wolff report a  $\delta^{44/42}\text{Ca}$  of  $1.2 \pm 0.2 \text{ ‰}$  for the SRM 915b relative to SRM 915a. This value is not in agreement with previously reported  $\delta^{44/42}\text{Ca}$  of  $0.35 \pm 0.04$  to  $0.42 \pm 0.02$  for SRM 915b relative to SRM 915a obtained by either TIMS or MC-ICP-MS (Heuser and Eisenhauer 2008; Wombacher et al. 2009; Schiller et al. 2012). They also report a  $\delta^{44/43}\text{Ca}$  value, which should be about half the  $\delta^{44/42}\text{Ca}$  value, i.e. 0.6. But their  $\delta^{44/43}\text{Ca}$  value for SRM 915b is 0.2, which better matches the  $\delta^{44/43}\text{Ca}$  of 915b expected from previously published data. Figure 3 of their study also clearly shows serious analytical problems: the  $^{42}\text{Ca}/^{44}\text{Ca}$  should be highly correlated to the  $^{43}\text{Ca}/^{44}\text{Ca}$  but both ratios vary independently. This lack of correlation is a typical indication for an isobaric interference affecting at least one of the isotopes used. The extent of this interference varies between the two very similar samples, leading to the observed lack of correlation between  $^{43}\text{Ca}/^{44}\text{Ca}$  and  $^{42}\text{Ca}/^{44}\text{Ca}$ . Possibly doubly charged ions interfere on masses 42, 43 and 44; a correction for interferences of  $\text{Sr}^{2+}$  ions was not carried out.

Tacail et al. (2016) used an Exite 193 nm Photon machines laser ablation system coupled to a Neptune MC-ICP-MS in high resolution mode to measure  $\delta^{44/42}\text{Ca}$  and  $\delta^{43/42}\text{Ca}$  in igneous apatite and modern tooth enamel samples. Matrix matched standard materials were prepared by sintering NIST SRM 1400 bone ash which was used for sample bracketing and two synthetic apatites, in one case with Sr added. The samples were also analyzed by solution mode and good agreement between solution and laser data was obtained for  $\delta^{44/42}\text{Ca}$  for the three sintered standards and tooth enamel samples, but igneous apatites were significantly displaced from the 1:1 correlation line. Moreover,  $\delta^{43/42}\text{Ca}$  from LA analysis was systematically higher than expected from their  $\delta^{44/42}\text{Ca}$  and this is also observed when the  $\delta^{43/42}\text{Ca}$  data obtained by laser ablation is compared with results from solution analysis. This suggests an uncorrected interference on mass 43, likely related to the  $\text{Sr}^{++}$  interference that is difficult to correct accurately (Tacail et al. 2016). This study was in part successful in as much that  $\delta^{44/42}\text{Ca}$  values that are consistent with solution analysis could be obtained for tooth enamel samples. The precision quoted for repeated analysis of about  $\pm 0.7\text{‰}$  for  $\delta^{44/42}\text{Ca}$  (2sd) as judged from repeated analysis of laser ablation data appears insufficient to reveal internal variations in Ca isotope compositions in most samples. Yet, with further improvements, LA-ICP-MS may find its way to the Ca isotope community, especially in regard to Ca dominated materials such as  $\text{CaCO}_3$ , gypsum or apatite. Improvements may result from higher sensitivity e.g. due to modifications on the plasma interface. The use of fs lasers may also reduce the need for near perfect matrix matching (e.g. Horn et al. 2006; Shaheen et al. 2012). Finally, if reintroduced to MC-ICP-MS, collision cells may allow to reduce interferences during laser ablation work (cf. Elliott et al. 2015).

## 5.4 Double Spike Approach for Stable Isotope Analysis

### 5.4.1 Basic Principles

As already mentioned it is not possible to correct measurements for the isotope fractionation occurring during measurement without knowing the extent of natural isotope fractionation, i.e. no Ca isotope ratio is fixed. A fractionation correction which is done using a static reference ratio e.g. fractionation of Sr isotopes is corrected using a  $^{86}\text{Sr}/^{88}\text{Sr}$  of 0.1194, also corrects for any natural isotope fractionation. While this is desirable for the determination of radiogenic ingrowth by radioactive decay it is not possible to determine the natural fractionation. This problem can be solved by addition of a double spike to the sample before its measurement or chemical preparation. A double spike is a solution consisting of two isotopes of an element which both are enriched compared to their natural abundances. The ratio of the two enriched isotopes has to be well known and the ratio of double spike/sample has to be high enough so that natural isotope variations of the spiked isotopes become negligible.

Two general requirements for the use of the double spike technique exist: (1) the element must have four or more stable isotopes or long-lived artificial isotopes (two isotopes for the double spike and two isotopes representing the isotopic composition of a sample), and (2) enriched isotopes with a sufficient enrichment are

**Table 5** Commercially available enriched Ca isotopes

Isotope	Natural abundance (atom %)	Enrichment (atom %) <sup>a</sup>	Enrichment factor
<sup>40</sup> Ca	96.97	>99.9	1.03
<sup>42</sup> Ca	0.64	>93	145.31
<sup>43</sup> Ca	0.145	>79	544.83
<sup>44</sup> Ca	2.086	>98.5	47.22
<sup>46</sup> Ca	0.004	>43	10750
<sup>48</sup> Ca	0.187	>97	518.72

<sup>a</sup>Data from isotope services, Oak Ridge National Laboratory



available. Table 5 compares natural abundances of Ca isotopes with commercially available enriched isotopes.

Beside these general requirements some more prerequisites for a good working double spike exist: (1) the spike isotopes should be as pure as possible, i.e. high enrichment of the isotope, (2) the enrichment/natural abundance ratio of the used isotopes should be high, (3) by adding a double spike solution the abundance differences between the isotopes in the sample/spike mixture should be small and (4) the mass difference (in u) between double spike isotopes and “sample” isotopes should be similar. As can be seen from Table 5 enriched  $^{40}\text{Ca}$ ,  $^{44}\text{Ca}$  and  $^{48}\text{Ca}$  have enrichments >97 atomic-% but  $^{40}\text{Ca}$  and  $^{44}\text{Ca}$  at the same do not show high enrichment/natural abundance ratios. Therefore it is not advisable to use  $^{40}\text{Ca}$  and  $^{44}\text{Ca}$  as a double spike. Combinations of two of the remaining four Ca isotopes are suited better for the use as a double spike.

The use of a double spike solution to correct for the instrumentally driven isotope fractionation requires also a correction for the shift in isotopic composition caused by the double spike addition, because commercially available enriched isotopes are not pure, affecting thus to the measured isotope ratio of interest. The double spike deconvolution methods are not Ca isotope specific and generally valid for different isotope systems. Different approaches to correct for the added double spike are published (e.g. Compston and Oversby 1969; Gale 1970; Hamelin et al. 1985; Powell et al. 1998; Johnson and Beard 1999; Galer 1999; Siebert et al. 2001).

### 5.4.2 Double Spike Calibration

The progressive mass dependent Ca-isotope fractionation during thermal ionization mass spectrometry, equally affects the sample and double spike Ca.

Therefore, the isotope composition of the double spike cannot be directly determined by TIMS. Instead, the double spike can be either calibrated by exact weighing of the two enriched Ca salts, or calibrated against a standard of known isotopic composition. As weighing of small amounts of powder can be difficult due to

electrostatic effects, Ca-double spikes are typically calibrated against a standard. In Fig. 10 we illustrate the basic principle of the Ca double spike calibration following the approach for the Pb-double spike calibration of Galer (1999). This correction algorithm is a three dimensional approach and the isotope fractionation is described in a three dimensional vector space. As an example we show the calibration of a  $^{43}\text{Ca}/^{48}\text{Ca}$  double spike, using a 3D-vector space, which is defined by three Ca isotope ratios  $^{40}\text{Ca}/^{48}\text{Ca}$ ,  $^{44}\text{Ca}/^{48}\text{Ca}$  and  $^{43}\text{Ca}/^{48}\text{Ca}$ . For this calibration, the isotope ratios published for  $\text{CaF}_2$  by Russell et al. (1978) are used as a fix point.

For the double spike calibration, analyses of the pure spike and a mixture of spike and standard are required. The isotopic fractionation trends ( $^{40}\text{Ca}/^{48}\text{Ca}$ ,  $^{44}\text{Ca}/^{48}\text{Ca}$  and  $^{43}\text{Ca}/^{48}\text{Ca}$ ) of the individual runs are fitted in a 3D vector space with one additional isotope ratio (e.g. the  $^{42}\text{Ca}/^{48}\text{Ca}$ ) as a running parameter. For practical reasons a linear instead of an exponential fractionation trend can be used, if the quality of the fit is sufficiently good and allows for this simplification. The fractionation trends of the spike and the mixture are shown in Fig. 9 as dashed lines. A basic principle of the 3D fractionation correction is that the fractionation trend depends on the isotope composition of the analyzed material, i.e. the fractionation trends of the spike-sample mixture and of the pure spike are not parallel which means that the vector product

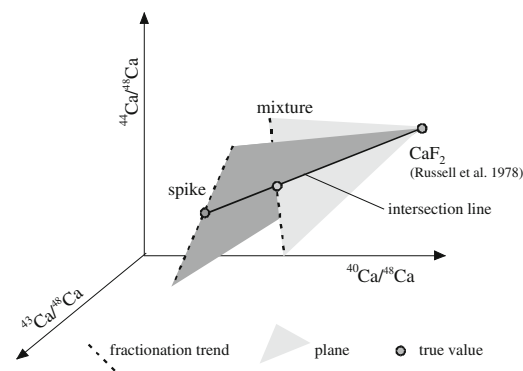


**Fig. 9** Schematic illustration of a  $^{43}\text{Ca}/^{48}\text{Ca}$ -double spike calibration, following the Pb-double spike approach of Galer (1999)

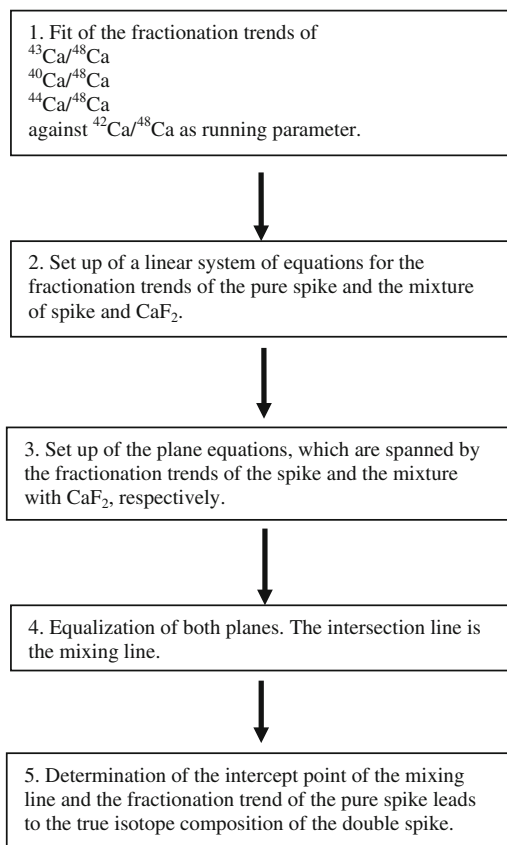


**Fig. 10** Flow chart of the Ca-double spike calibration

of the spike-fractionation trend and mix-fractionation trend is unequal to 0 ( $MxS \neq 0$ ) (Galer 1999). The planes, which are spanned by the spike-fractionation trend and the  $\text{CaF}_2$  (dark gray plane) and the mixture-fractionation trend and the  $\text{CaF}_2$  (light grey plane), intersect in an intersection line, which is also the mixing line of all spike— $\text{CaF}_2$  mixtures. Consequently, the true isotope compositions of the mixture and of the pure spike lie on this line. The true isotope composition of the spike is in the intercept of the mixing line and the spike fractionation trend. To correct for potential deviations between linear and exponential fractionation law, the obtained isotope ratios can numerically optimized using ‘Solver’ or similar functions. The general procedure is schematically illustrated in a flow sheet (Fig. 10).

### 5.4.3 Used Double Spikes

#### $^{42}\text{Ca}/^{48}\text{Ca}$ and $^{43}\text{Ca}/^{48}\text{Ca}$ double spike

Russell et al. (1978) were the first who used a double spike ( $^{42}\text{Ca}/^{48}\text{Ca}$ ) for Ca isotope measurements. The main advantage of using a  $^{42}\text{Ca}/^{48}\text{Ca}$  or  $^{43}\text{Ca}/^{48}\text{Ca}$  is that all used isotopes have a low natural abundance combined with a high enrichment factor (cf. Table 5). The mass difference of a  $^{42,43}\text{Ca}/^{48}\text{Ca}$  double spike well matches the mass difference of the Ca isotope ratio used ( $^{44}\text{Ca}/^{40}\text{Ca}$ ). As the fractionation per mass unit is needed for the correction of the double spike, a greater mass difference allows a more precise determination of the fractionation per mass unit. One major disadvantage of such a double spike has to be seen in the fact that it results in a high mass dispersion which is still a problem for modern mass spectrometers although some improvements have been made. The relative mass difference of about 20 % between  $^{40}\text{Ca}$  and  $^{48}\text{Ca}$  exceeds the mass dispersion of most instruments which are constructed for a maximum mass difference of about 17 % ( $^6\text{Li}$  and  $^7\text{Li}$ ). So far no Ca isotopes data is published using  $^{42}\text{Ca}$  or  $^{43}\text{Ca}/^{48}\text{Ca}$  double spike and mass spectrometers capable of a 20 % relative mass difference.

#### $^{42}\text{Ca}/^{43}\text{Ca}$ double spike

A  $^{42}\text{Ca}/^{43}\text{Ca}$  double spike also makes use of two minor Ca isotopes with reasonably high enrichment (cf. Table 5). But the mass difference of the used isotope does not well match the difference of the isotope ratio reported for TIMS measurements ( $^{44}\text{Ca}/^{40}\text{Ca}$ ). But for TIMS measurements this double spike has the big advantage that works pretty well for a static Ca isotope measurement ( $^{40}\text{Ca}$ ,  $^{42}\text{Ca}$ ,  $^{43}\text{Ca}$ ,  $^{44}\text{Ca}$ ). For ICPMS Ca isotope analyses which normally determine  $^{44}\text{Ca}/^{42}\text{Ca}$  the use of a  $^{42}\text{Ca}/^{43}\text{Ca}$  double spike is not possible.

#### $^{43}\text{Ca}/^{46}\text{Ca}$ -double spike

During the past years a number of researches tried to make use of a  $^{43}\text{Ca}/^{46}\text{Ca}$  double spike.  $^{46}\text{Ca}$  has the lowest natural abundance of all Ca isotopes but the highest enrichment factor (cf. Table 5). This high enrichment factor makes

enriched  $^{46}\text{Ca}$  very expensive. On the other hand only small amounts of  $^{46}\text{Ca}$  in a  $^{43}\text{Ca}/^{46}\text{Ca}$  double spike are needed to establish a fixed ratio in the sample double spike mixture.

## 5.5 Other Instrumentation

Especially in the field of analytical chemistry several other instrumentations for the measurement of stable Ca isotopes have been developed. However, most of these techniques are not suitable for isotope geochemistry as precision and accuracy of these techniques are not sufficient. Some of these instrumentations and methods used either special or unique and even ‘home’ made instruments. The list below gives a short overview of some of these techniques:

- LD-TOFMS (laser desorption time of flight mass spectrometry, e.g. Koumenis et al. 1995)
- RIMS (resonant ionization mass spectrometry, e.g. Nicolussi et al. 1997)
- FABMS (fast atom bombardment, e.g. Smith 1983)
- MIP-TOFMS (microwave induced plasma time of flight mass spectrometry, Duan et al. 2001)

Some other instrumentations, described below, have either the potential to become a valuable tool in Ca isotope geochemistry (ion microprobe), are an often used tool for several studies of Ca isotopes in the pre-TIMS and pre-ICPMS times (INAA) or are used outside the field of isotope geochemistry (radionuclides).

### 5.5.1 Ion Microprobe

As with laser ablation ICP-MS, Ca isotope ratios have been determined in situ by secondary ion mass spectrometry (SIMS). Rollion-Bard et al. (2007) and Kasemann et al. (2008) applied SIMS to investigate the spatial variations of Ca isotope ratios in biogenic carbonates. The spatial resolution was 15–20  $\mu\text{m}$  and about 25  $\mu\text{m}$  which is smaller than that reasonably applied in LA-ICP-MS, e.g. Tacail et al. (2016) used a laser beam diameter of 85  $\mu\text{m}$ . Both SIMS studies focused on heterogeneities of

Ca isotope ratios in tests of foraminifers. These unicellular calcifiers are of particular interest, since earlier results obtained by conventional TIMS and MC-ICP-MS methods revealed a complex isotope fractionation behavior in these organisms, and indicating that isotope analysis with high spatial resolution might contribute to a better understanding of biomineralization related Ca isotope fractionation effects and their consequences for paleo proxy applications. Both studies indicated a heterogeneous distribution of Ca isotope ratios in foraminifer tests. In particular Kasemann et al. (2008) showed systematic differences between different generations of biogenic calcite (ontogenetic and gametogenetic calcite). The difference between both calcite generations is not consistent for the two different species analyzed, as they show variable magnitudes and different signs of isotope fractionation.

Both Ca isotope studies used a Cameca IMS 1270 multicollector secondary ion mass spectrometer with a primary oxygen ion-beam. Calcium isotopes were analyzed with a spatial resolution of  $\sim 10$  and 25  $\mu\text{m}$  spot-diameter. With count rates on  $^{44}\text{Ca}$  of about  $8\text{--}10 \times 10^6$  cps Rollion-Bard et al. (2007) reported internal errors 0.2 ‰ 2 S.E. and external reproducibility of 0.25–0.50 ‰ (2 S.D.) and found intra-test variation in foraminifer shells of about 1.5 ‰ ( $\delta^{44/40}\text{Ca}$ ).

Kasemann et al. (2008) operated with slightly smaller count rates of about  $4\text{--}9 \times 10^6$  cps and report internal errors of about 0.4 ‰ (2 S.E.) and an external reproducibility of standard and samples of  $\sim 1$  and 0.4 ‰, respectively. The intra-test variability of the foraminifer tests account to 1.6 and  $-3.7$  ‰ between gametogenetic and ontogenetic calcite in different species. The observed overall variability of Ca isotope ratios within single foraminifer tests is compatible in both studies indicating the potential of SIMS for Ca isotope analysis. Nevertheless both studies also point to challenges that need to be resolved. These are mainly related to matrix effects, interferences and the availability of appropriate standard materials. Presently, there are no certified homogenous Ca isotope

standards available that are suited for SIMS. These complications include matrix-matching between samples and standards or structural or chemical/isotopical heterogeneities of standards leading to different fractionation effects or background/signal-ratio of samples and standards. Possible interference include (e.g.  $^{12}\text{C}^{16}\text{O}_2$ ,  $^{24}\text{Mg}^{16}\text{O}$ ,  $^{88}\text{Sr}^{2+}$ ,  $^{86}\text{Sr}^{2+}$ ).

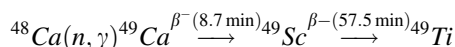
Calcium isotope analysis by SIMS has been frequently applied to minerals (hibonites, oldhamite (CaS) in chondritic meteorite samples (Zinner et al. 1986; Ireland et al. 1990; Lundberg et al. 1994 and Weber et al. 1995). The main focus was on nucleosynthetic  $^{48}\text{Ca}$  isotope anomalies and mass-dependent Ca isotope fractionation in CAIs. Beside these geoscientific oriented studies other studies on Ca isotopes exist (Roy et al. 1995; Bushinsky et al. 1990). Both studies used  $^{44}\text{Ca}$  for labeling of bone (Bushinsky et al. 1990) and for determination of Ca deposition at the cell walls of apple fruit. As both studies are tracer studies working with high amounts of  $^{44}\text{Ca}$  enrichment these studies did not need a precision needed to investigate natural Ca isotope variations.

SIMS has also been used to determine the radiogenic  $^{40}\text{Ca}$  ingrowth in K-rich minerals. In order to suppress the K intensities relative to Ca, Harrison et al. (2010) analysed doubly charged  $\text{K}^{++}$  and  $\text{Ca}^{++}$  ions. With this technique the authors were able to reconcile K–Ar and K–Ca systematics in alkali feldspars from the Klokken syenite (1166 Ma) in southern Greenland and to unravel complex genetic relations.

### 5.5.2 Neutron Activation Analysis INAA

Mass dependent Ca isotope fractionation effects were also approached by methods other than mass spectrometry. One of the applied analytical methods was neutron activation analysis (INAA) (Corless 1966, 1968). The basic concept of neutron activation is that certain nuclides are selectively activated by neutron-radiation. To analyze Ca isotope fractionation effects with this methods, the ratio of  $^{48}\text{Ca}$  and the total Ca concentration ( $^{48}\text{Ca}/\text{Ca}_{\text{total}}$ ) is determined. The  $^{48}\text{Ca}$

is measured indirectly on the basis of the nuclear reaction:



The total Ca concentration is precisely determined for instance by acid EDTA titration (ethylenediaminetetraacetic) in wet chemistry. The results obtained by neutron activation analysis showed large variations of up to 10 ‰ (Corless 1966, 1968), which were, however, not reproduced by subsequent studies.

### 5.5.3 Determination of Mass Dependent Ca Isotope Fractionation by Radionuclide Tracers

A further non-mass spectrometric approach to investigate mass dependent calcium isotope fractionation effects was the application of radiotracers. For instance, Möller and Papendorff (1971) used a  $^{45}\text{Ca}$  tracer ( $t_{1/2} = 163 \text{ d}$ ) during calcium carbonate precipitation experiments. Their experiments revealed that Ca isotope fractionation between solution and precipitated  $\text{CaCO}_3$  is smaller than 0.3 ‰/amu. Based on their results, Möller and Papendorff (1971) proposed that the hydration of the  $\text{Ca}^{2+}$ -ion may hinder a larger degree of Ca isotope fractionation and that fractionation in  $\text{Ca}^{2+}$ -diffusion processes may exceed 0.3 ‰/amu. Although this method was not sensitive enough to quantify the degree of Ca isotope fractionation during  $\text{CaCO}_3$  precipitation, their results are still consistent with recent studies.

## 5.6 Error Representation

An overview of existing external reproducibilities of Ca isotopic measurements shows that the long-term 2 standard deviation (2SD) is comprised between 0 and 0.50 ‰ for  $\delta^{44/40}\text{Ca}$  (Table 6). Usually reproducibility is calculated from full procedural replicates on reference material. However, samples present different matrixes than standards and thus react differently during ionization. As a result, some authors proposed to take

**Table 6** Summary of different TIMS measurement protocols for Ca isotopes and associated external reproducibilities

Continent	Country	Laboratory	Instrument	Collection	Filament	Loaded with	Activator	Amount of Ca loaded	<sup>40</sup> Ca peak intensity	Sequence of measurement	Number of scans	±2 SD <sup>a</sup>	References
Australia	Australia	Curtin	Modified VG 354	Multi	Triple zone-refined Re	HI				<sup>140</sup> Ca, <sup>41</sup> K, <sup>42</sup> Ca; <sup>242</sup> Ca, <sup>43</sup> Ca, <sup>44</sup> Ca; <sup>344</sup> Ca, <sup>46</sup> Ca		0.40	Fletcher et al. (1997)
North America	Canada	Saskatchewan	Thermo Triton	Multi	Double Re	HNO <sub>3</sub>		3–5 µg	8 V	<sup>140</sup> Ca, <sup>42</sup> Ca, <sup>43</sup> Ca, <sup>44</sup> Ca; <sup>246</sup> Ca, <sup>41</sup> K, <sup>42</sup> Ca	180	0.10	Holmden (2005)
		Saskatchewan	Thermo Triton	Multi	Single Ta (using parafilm dams)	HNO <sub>3</sub>	H <sub>3</sub> PO <sub>4</sub>	3–8 µg	8–20 V	<sup>140</sup> Ca, <sup>41</sup> K, <sup>42</sup> Ca; <sup>242</sup> Ca; <sup>43</sup> Ca; <sup>343</sup> Ca, <sup>44</sup> Ca	130–180	0.07–0.10	Jacobson and Holmden (2008), Anini et al. (2009), Holmden (2009), Holmden and Bélanger (2010), Ryu et al. (2011)
	USA	Caltech	Lunatic I	Single	Single V-shaped zone refined Ta	HCl, HNO <sub>3</sub>	Oxidized filament	5–10 µg	4 V	<sup>40</sup> Ca, <sup>42</sup> Ca, <sup>44</sup> Ca, <sup>48</sup> Ca	200	0.12–0.50	Russel et al. (1978), Lemarchand et al. (2004)
	USA	Scripps	VG54-A	Single	Single W		Ta <sub>2</sub> O <sub>5</sub> (sandwich technique)	300–600 ng	5.4–6.6 V	<sup>40</sup> Ca, <sup>42</sup> Ca, <sup>43</sup> Ca, <sup>44</sup> Ca, <sup>48</sup> Ca	2 Independent measurements (spiked and not spiked)	0.10–0.20	Zhu and MacDougall (1998)
USA	USA	Santa Cruz univ.	VG 54/WARP	Multi	Single Re	HNO <sub>3</sub>	Ta <sub>2</sub> O <sub>5</sub> , H <sub>3</sub> PO <sub>4</sub>	1 µg		<sup>40</sup> Ca, <sup>42</sup> Ca, <sup>44</sup> Ca, <sup>48</sup> Ca	100–200	0.10–0.30	Clementz et al. (2003)
		IGGRC, Carleton univ.	Thermo Triton	Multi	Zone-refined double Re	HNO <sub>3</sub>	H <sub>3</sub> PO <sub>4</sub> , taken to dull red	3 µg	10 V	<sup>140</sup> Ca, <sup>41</sup> K, <sup>42</sup> Ca, <sup>43</sup> Ca, <sup>44</sup> Ca; <sup>244</sup> Ca, <sup>48</sup> Ca	100	0.15	Farkaš et al. (2006, 2007)
	USA	Berkely	modified VG 354 with one large Faraday bucket collector	Single	Single Ta		H <sub>3</sub> PO <sub>4</sub>	3–8 µg	6–9 V			0.10–0.20	Skulan et al. (1997), DeLa Rocha and DePaolo (2000), Fanile and DePaolo (2005, 2007)
		Berkely	VG Sector 54		Single Ta		H <sub>3</sub> PO <sub>4</sub>	8 µg		<sup>40</sup> Ca, <sup>42</sup> Ca, <sup>44</sup> Ca, <sup>48</sup> Ca	100–200		Skulan and DePaolo (1999)
		Berkely	Thermo triton	Multi	Double Re	HNO <sub>3</sub>	H <sub>3</sub> PO <sub>4</sub>	3 µg	20 V	<sup>39</sup> K, <sup>40</sup> Ca, <sup>42</sup> Ca, <sup>43</sup> Ca	200	0.14	Ewing et al. (2008), Simon et al. (2009),

(continued)

Table 6 (continued)

Continent	Country	Laboratory	Instrument	Collection	Filament	Loaded with	Activator	Amount of Ca loaded	<sup>40</sup> Ca peak intensity	Sequence of measurement	Number of scans	±2 SD <sup>a</sup>	References
Europe										<sup>44</sup> Ca, <sup>48</sup> Ca, <sup>49</sup> Ti			Simon and DePaolo (2010)
	USA	Stanford	Finnigan MAT 262		Single Ta		H <sub>3</sub> PO <sub>4</sub>			<sup>40</sup> Ca, <sup>42</sup> Ca, <sup>44</sup> Ca, <sup>48</sup> Ca	80	0.15	Wiegand et al. (2005)
	USA	Harvard	Isoprobe-T	Multi	Triple Re			5 µg		<sup>140</sup> Ca, <sup>42</sup> Ca, <sup>43</sup> Ca, <sup>44</sup> Ca, <sup>48</sup> Ca, <sup>244</sup> Ca		0.13	Huang et al. (2010)
	USA	North Western University	Thermo Triton	Multi	Single Ta	HNO <sub>3</sub>	H <sub>3</sub> PO <sub>4</sub>	10–16 µg	20 V	<sup>140</sup> Ca, <sup>41</sup> K, <sup>42</sup> Ca, <sup>242</sup> Ca, <sup>43</sup> Ca, <sup>343</sup> Ca, <sup>44</sup> Ca	90	0.04	Lehn et al. (2013)
	France	Strasbourg	VG Sector	Single	Single Ta	1.5 N HCl	H <sub>3</sub> PO <sub>4</sub>	10 µg	6 V	<sup>40</sup> Ca, <sup>41</sup> K, <sup>42</sup> Ca, <sup>43</sup> Ca, <sup>44</sup> Ca, <sup>48</sup> Ca	2 Independent measurements (spiked and not spiked)	0.20	Schmitt et al. (2001, 2003a, b), Schmitt and Stille (2005)
		Strasbourg	Thermo triton	Multi	Single Re	1.5 N HCl	Ta <sub>2</sub> O <sub>5</sub> , H <sub>3</sub> PO <sub>4</sub>	5 µg		<sup>140</sup> Ca, <sup>41</sup> K, <sup>42</sup> Ca, <sup>43</sup> Ca, <sup>44</sup> Ca, <sup>242</sup> Ca, <sup>48</sup> Ca		0.30	Cenki-Tok et al. (2009)
		Strasbourg	Thermo triton	Multi	Single Ta	1.5 N HCl	Filament oxidized in partial vacuum	5 µg	5 V	<sup>140</sup> Ca, <sup>41</sup> K, <sup>42</sup> Ca, <sup>243</sup> Ca, <sup>44</sup> Ca, <sup>342</sup> Ca, <sup>43</sup> Ca	130–200	0.12	Schmitt et al. (2009), Cobert et al. (2011a, b)
Germany		Geomar, Kiel	Finnigan MAT 262 RPQ <sup>+</sup>	Multi	Single zone-refined Re	2.5 N HCl	Ta <sub>2</sub> O <sub>5</sub> sandwich technique; sample heated to red	300 ng	4–5 V	<sup>140</sup> Ca, <sup>41</sup> K, <sup>42</sup> Ca, <sup>43</sup> Ca, <sup>244</sup> Ca, <sup>48</sup> Ca	154	0.20–0.50	Heuser et al. (2002), Gussone et al. (2003, 2004, 2005), Heuser and Eisenhauer (2008)
		Geomar, Kiel	Thermo triton	Multi	Single zone-refined Re	2.5 N HCl	Ta <sub>2</sub> O <sub>5</sub> sandwich technique; sample heated to red	300 ng		Static <sup>40</sup> Ca, <sup>41</sup> K, <sup>42</sup> Ca, <sup>43</sup> Ca, <sup>44</sup> Ca or <sup>140</sup> Ca, <sup>42</sup> Ca, <sup>43</sup> Ca, <sup>44</sup> Ca, <sup>243</sup> Ca, <sup>44</sup> Ca, <sup>245</sup> Ca, <sup>48</sup> Ca		0.13–0.16	Gussone et al. (2006, 2007), Böhm et al. (2006), Amiri et al. (2008), Griffith et al. (2008), Heuser and Eisenhauer (2008), Amiri et al. (2009), Gussone et al. (2009);

(continued)



Table 6 (continued)

Continent	Country	Laboratory	Instrument	Collection	Filament	Loaded with	Activator	Amount of Ca loaded	<sup>40</sup> Ca peak intensity	Sequence of measurement	Number of scans	±2 SD <sup>a</sup>	References
													<a href="#">(2010)</a> , <a href="#">Heuser and Eisenhauer (2010)</a>
	Germany	Münster	Thermo Triton	Multi	Single zone-refined Re	6N HCl	Ta <sub>2</sub> O <sub>5</sub>	300–400 ng	12–16 V	<sup>140</sup> Ca, <sup>41</sup> K, <sup>42</sup> Ca, <sup>43</sup> Ca, <sup>44</sup> Ca; ( <sup>27</sup> / <sup>43</sup> Ca, <sup>44</sup> Ca, <sup>48</sup> Ca)	180	0.02–0.21	<a href="#">Aming et al. (2008)</a> , <a href="#">Gussone et al. (2010, 2011)</a> , <a href="#">Heuser et al. (2011)</a>
	United Kingdom	Bristol	Thermo Triton	Multi	Double zone-refined Re	1 N HCl		2 µg		<sup>40</sup> Ca, <sup>41</sup> K, <sup>42</sup> Ca, <sup>43</sup> Ca, <sup>44</sup> Ca, <sup>46</sup> Ca	90	0.10–0.12	<a href="#">Kasemann et al. (2005)</a>
	Switzerland	Bern	modified AVCO equipped with a Thermoliner ion source	Single	Single Re	2.5 N HCl	Ta <sub>2</sub> O <sub>5</sub>	0.3–5 µg		<sup>48</sup> Ca, <sup>44</sup> Ca, <sup>43</sup> Si, <sup>43</sup> Ca, <sup>41</sup> K, <sup>40</sup> Ca		0.15–0.30	<a href="#">Nägler and Villa (2000)</a> , <a href="#">Nägler et al. (2000)</a> , <a href="#">Hippler et al. (2006, 2009)</a> , <a href="#">Silva-Tamayo et al. (2010)</a> , <a href="#">von Allmen et al. (2010b)</a>
	Switzerland	ETH, Zürich	Thermo triton	Multi	Single Re		Ta <sub>2</sub> O <sub>5</sub>	0.7–1 µg		Static <sup>40</sup> Ca, <sup>41</sup> K, <sup>42</sup> Ca, <sup>43</sup> Ca, <sup>44</sup> Ca, <sup>46</sup> Ca	280	0.07 <sup>b</sup>	<a href="#">Hindshaw et al. (2010)</a>

<sup>a</sup><sub>8</sub><sup>44/40</sup>Ca  
<sup>b</sup><sub>8</sub><sup>44/42</sup>Ca

into account repeated measurements of various sample materials (Teichert et al. 2005; Griffith et al. 2008; Gussone et al. 2009; Schmitt et al. 2009, 2013; Cobert et al. 2011a, b). A way to avoid this artifact is to process seawater standard, which is a matrix-rich standard through each measurement session and to process it similarly to samples (Lehn et al. 2013; du Vivier et al. 2015). In doing so, du Vivier et al. (2015) observed no difference between replicate sample and standard measurements. The Saskatchewan group (Holmden and Bélanger 2010) introduced drift corrections for each measurement session. They indeed observed an instrumental drift from about 0.3 ‰ over 2-years. In order to avoid this, they usually performed around 15–30 measurements in 1–2 weeks measurement sessions, including samples and standards. Then they adjusted the isotopic composition of their double spike using an exponential law in each measurement session, to achieve an average constant isotopic difference between two standards (seawater and  $\text{CaF}_2$ ). Similarly, Hindshaw et al. (2011) measured in each turret standards, which values were averaged and corrected to zero. This correction was then applied to all samples run on the same turret. As a result these authors (Hindshaw et al. 2011; Holmden and Bélanger 2010; Ryu et al. 2011) decreased their long-term external 2SD down to  $\pm 0.07$  ‰, compared to  $\pm 0.10$ – $0.15$  ‰ obtained by most other laboratories. More recently Lehn et al. (2013) decreased their long-term external reproducibility down to  $\pm 0.04$  ‰ by improving the measurement protocol and optimizing the  $^{43}\text{Ca}/^{42}\text{Ca}$  spike mixture. However, in doing so they also increased the amount of Ca loaded on the filament (10–16  $\mu\text{g}$ ), which may be limiting for samples very poor in Ca.

To improve the statistical significance of a single  $\delta^{44/40}\text{Ca}$  measurement, most of presently published Ca isotope data result from the combination of at least two individual measurements. These values and their corresponding errors are presented in different ways, trying to minimize the error, in order to be able to resolve the smallest  $\delta^{44/40}\text{Ca}$  variations. Thus, direct comparison between different laboratories is difficult.

However, the significance of the numbers is mostly clearly stated in the different articles dealing with Ca isotopes, so that the reader can judge their significance for themselves and recalculate the errors if necessary.

Five main ways of reporting replicate  $\delta^{44/40}\text{Ca}$  (or  $\delta^{44/42}\text{Ca}$ ) values and associated errors can be listed from the literature and are reported hereafter:

- (1) Mean  $\delta^{44/40}\text{Ca}$  (or  $\delta^{44/42}\text{Ca}$ ) values and 2SD (95 % confidence level) corresponding to N measurements of one given sample (Skulan et al. 1997; Soudry et al. 2004; Wieser et al. 2004; Fantle and DePaolo 2005, 2007; Immenhauser et al. 2005; Schmitt and Stille 2005; Steuber and Buhl 2006; Kasemann et al. 2008; Komiya et al. 2008; Gussone et al. 2009; Tipper et al. 2010; Reynard et al. 2011).
- (2) Mean  $\delta^{44/40}\text{Ca}$  (or  $\delta^{44/42}\text{Ca}$ ) values and 1SD (68 % confidence level) corresponding to N measurements of one given sample (e.g. Halicz et al. 1999; Heuser et al. 2002, 2005; Clementz et al. 2003; Fietzke et al. 2004; Wiegand et al. 2005; Chu et al. 2006; Rollion-Bard et al. 2007; Sime et al. 2007; Ewing et al. 2008; Page et al. 2008; Reynard et al. 2010).
- (3) Mean  $\delta^{44/40}\text{Ca}$  (or  $\delta^{44/42}\text{Ca}$ ) values and 2SE corresponding to N measurements of one given sample (e.g. Zhu and Macdougall 1998; Gussone et al. 2003, 2004; Schmitt et al. 2003a, b; Kasemann et al. 2005; Sime et al. 2005; Teichert et al. 2005; Böhm et al. 2006; Tipper et al. 2006; Amini et al. 2008; Griffith et al. 2008; Heuser and Eisenhauer 2008; Heuser et al. 2011).
- (4) Mean  $\delta^{44/40}\text{Ca}$  (or  $\delta^{44/42}\text{Ca}$ ) values corresponding to N measurements of one given sample and long-term 2SE calculated from replicates of different samples or standards (e.g. Marriott et al. 2004; Farkaš et al. 2007; Ewing et al. 2008; Jacobson and Holmden 2008; Cenki-Tok et al. 2009; Schmitt et al. 2009, 2013; Cobert et al. 2011a; b; Hindshaw et al. 2010; Farkaš et al. 2011; Bagard

**Table 7** Comparison of the way of reporting multiple isotopic measurements of one single sample

	$\delta^{44/40}\text{Ca}$	2SE <sub>int</sub>	N	Mean	Weighted average	2SD	1SD	2SD <sub>weighted</sub>	2SD <sub>long term</sub>	2SE	2SE <sub>weighted</sub>	2SE <sub>long term</sub>
<i>Replicates of different sample measurements</i>												
Sample 1	Rainwater	0.62	2	0.59	0.58	0.10	0.05	0.11	0.11	0.07	0.08	0.08
		0.55										
Sample 2	Rainwater	0.57	2	0.59	0.59	0.04	0.02	0.10	0.11	0.03	0.07	0.08
		0.60										
Sample 3	Swamp	0.08	2	0.02	0.01	0.17	0.08	0.08	0.11	0.12	0.06	0.08
		-0.04										
Sample 4	Nutritive solution	0.98	3	0.93	0.93	0.07	0.04	0.12	0.11	0.04	0.07	0.06
		0.91										
		0.91										
Sample 5	Carbonate	-0.63	2	-0.63	-0.63	0.00	0.00	0.11	0.11	0.00	0.08	0.08
		-0.63										
Sample 6	Carbonate	-1.16	2	-1.20	-1.21	0.10	0.05	0.11	0.11	0.07	0.07	0.08
		-1.23										
Sample 7	Granite	-1.36	2	-1.34	-1.33	0.06	0.03	0.10	0.11	0.04	0.07	0.08
		-1.32										
Sample 8	Apatite	0.77	2	0.84	0.84	0.18	0.09	0.08	0.11	0.13	0.06	0.08
		0.90										
Sample 9	Soil	-1.12	2	-1.14	-1.14	0.04	0.02	0.08	0.11	0.03	0.06	0.08
		-1.15										
Sample 10	Soil	-0.93	2	-1.01	-1.01	0.21	0.11	0.11	0.11	0.15	0.08	0.08
		-1.08										
Sample 11	Leave	0.15	2	0.25	0.20	0.27	0.13	0.07	0.11	0.19	0.05	0.08
		0.34										

(continued)

Table 7 (continued)

		$\delta^{44/40}\text{Ca}$	2SE <sub>int</sub>	N	Mean	Weighted average	2SD	1SD	2SD <sub>weighted</sub>	2SD <sub>long term</sub>	2SE	2SE <sub>weighted</sub>	2SE <sub>long term</sub>
Sample 12	Cotyledon	-0.36 -0.37	0.09 0.07	2	-0.37	-0.37	0.01	0.01	0.08	0.11	0.01	0.06	0.08
Sample 13	Tegument	-0.90 -0.99	0.11 0.07	2	-0.94	-0.96	0.13	0.07	0.08	0.11	0.09	0.06	0.08
Sample 14	Root	0.01 0.07	0.09 0.18	2	0.04	0.02	0.08	0.04	0.11	0.11	0.06	0.08	0.08
Sample 15	Stem	0.02 -0.16	0.16 0.12	2	-0.07	-0.10	0.25	0.13	0.14	0.11	0.18	0.10	0.08
Sample 16	Sap	-0.07 -0.16	0.09 0.05	2	-0.12	-0.14	0.13	0.06	0.06	0.11	0.09	0.04	0.08
Sample 17	Trunk	-1.92 -1.83	0.18 0.13	2	-1.88	-1.86	0.13	0.06	0.16	0.11	0.09	0.11	0.08
<i>Replicates of standards</i>													
E 5109	Seawater	1.83	0.16	6	1.86	1.79	0.12	0.06	0.12	0.11	0.05	0.05	0.04
		1.90	0.18										
		1.91	0.09										
		1.79	0.15										
		1.69	0.07										
NIST SRM 915a	Carbonate	1.67	0.03										
		-0.03	0.16	4	0.00	0	0.06	0.03	0.12	0.11	0.03	0.06	0.06
		0.00	0.15										
		-0.01	0.09										
		0.04	0.12										

(continued)

Table 7 (continued)

[illegible]

et al. 2013; Gangloff et al. 2014; Blättler et al. 2015; du Vivier et al. 2015)

- (5) Weighted  $\delta^{44/40}\text{Ca}$  and 2SE corresponding to  $N$  measurements of one given sample (e.g. Nägler et al. 2000; Hippler et al. 2003, 2006).

As it is widely known, statistically SD and SE do not have the same significance. The standard deviation (SD or  $\sigma$ ) says how widely scattered some measurements are. The standard error (SE or  $\sigma_{\text{mean}}$ ) indicates the uncertainty around the estimate of the mean measurement. Moreover, SE and SD are related by the following equation:

$$SE = \frac{SD}{\sqrt{n}}, \text{ with } n: \text{ number of replicates} \quad (49)$$

If the data follow a normal (or Gaussian) distribution, then about 68 % of the data values are within one standard deviation of the mean ( $\pm 1\text{SD}$ ). About 95 % are within two standard deviations ( $\pm 2\text{SD}$ ). It has also to be noted that, for small number of replicates, the mean values and corresponding errors are usually expressed using weighted values.

In order to check the differences induced by the multiple ways of reporting replicate measurements of  $\delta^{44/40}\text{Ca}$  values and corresponding errors, we have applied all the existing calculations to replicate analysis of samples (Table 7). It can especially be observed that for the presented dataset up to 50 % relative difference can be observed between mean and weighted average  $\delta^{44/40}\text{Ca}$  values, with an average difference of  $3 \pm 41$  % (2SD;  $N = 17$ ). For a limited number of replicates, weighted average values are statistically closer to the “true” value than mean ones. However, when only few replicates are available this method accords more weight to a sample measured with a good internal error, with no glance at the accuracy.

Given the small number of replicates usually performed in Ca isotopic studies, 2SD, 2SE and 1SD are statistically not robust. Indeed, when we consider for instance samples 5 or 12, which are measured twice and give each time similar  $\delta^{44/40}\text{Ca}$  values, internal 2SE values, external SD or SE would be close to zero, which makes no

sense. We can deduce from Table 7 that the variation between weighted 2SE (rep. weighted 2SD) and long-term 2SE (resp. long-term 2SD) differ but are in the same order of magnitude. Weighted errors refer to replicates of the same sample and reflect the way the measurement is completed. Long-term errors average short-term instabilities and show how the measurement reproduces over a long period of time. Each method presents its highlights and drawbacks; no optimal method exists for small replicates (2–3). As a result caution should be exercised in drawing conclusions over small differences in samples when comparing data from one laboratory to another without recalculating the  $\delta^{44/40}\text{Ca}$  values and corresponding errors.

## References

- Albarède F, Beard B (2004) Analytical methods for non-traditional isotopes. In: Johnson CM, Beard BL, Albarède F (eds) *Geochemistry of non-traditional stable isotopes*, Reviews in mineralogy and geochemistry Mineralogical Society of America, Washington, pp 113–152
- Albarède F, Telouk P, Blichert-Toft J et al (2004) Precise and accurate isotopic measurements using multiple-collector ICPMS. *Geochim Cosmochim Acta* 68:2725–2744
- Amini M, Eisenhauer A, Böhm F et al (2008) Calcium Isotope ( $\delta^{44/40}\text{Ca}$ ) fractionation along hydrothermal pathways, logatchev field (mid-atlantic ridge,  $14^\circ 45'\text{N}$ ). *Geochim Cosmochim Acta* 72:4107–4122
- Amini M, Eisenhauer A, Böhm F et al (2009) Calcium isotopes ( $\delta^{44/40}\text{Ca}$ ) in MPI-DING reference glasses, USGS rock powders and various rocks: evidence for Ca isotope fractionation in terrestrial silicates. *Geostand Geoanal Res* 33:231–247
- Andreasen R, Sharma M (2006) Solar nebula heterogeneity in P-process samarium and neodymium isotopes. *Science* 314:806–809
- Andreasen R, Sharma M (2009) Fractionation and mixing in a thermal ionization mass spectrometer source: implications and limitations for high-precision Nd isotope analyses. *J Anal At Spec* 285:49–57
- Baadsgaard H (1987) Rb–Sr and K–Ca isotope systematics in minerals from potassium horizons in the prairie evaporite formation, Saskatchewan, Canada. *Chem Geol Isotope Geosci Sect* 66:1–15
- Bagard ML, Schmitt AD, Chabaux F et al (2013) Biogeochemistry of stable Ca and radiogenic Sr isotopes in a larch-covered permafrost-dominated



- watershed of Central Siberia. *Geochim Cosmochim Acta* 114:169–187
- Baxter DC, Rodushkin I, Engström E (2012) Isotope abundance ratio measurements by inductively coupled plasma-sector field mass spectrometry. *J Anal At Spec* 27:1355–1381
- Blättler CL, Jenkyns HC, Reynard LM et al (2011) Significant increases in global weathering during oceanic anoxic events 1a and 2 indicated by calcium isotopes. *Earth Planet Sci Lett* 309. doi:[10.1016/j.epsl.2011.06.029](https://doi.org/10.1016/j.epsl.2011.06.029)
- Blättler CL, Miller NR, Higgins JA (2015) Mg and Ca isotope signatures of authigenic dolomite in siliceous deep-sea sediments. *Earth Planet Sci Lett* 419:32–42
- Blum JD et al (2008) Use of foliar Ca/Sr discrimination and  $^{87}\text{Sr}/^{86}\text{Sr}$  ratios to determine soil Ca sources to sugar maple foliage in a northern hardwood forest. *Biogeochem* 87:287–296
- Böhm F, Gussone N, Eisenhauer A et al (2006) Calcium isotope fractionation in modern scleractinian corals. *Geochim Cosmochim Acta* 70:4452–4462
- Boulyga SF (2010) Calcium isotope analysis by mass spectrometry. *Mass Spectrom Rev* 29:685–716
- Boulyga SF, Becker JS (2001) ICP-MS with hexapole collision cell for isotope ratio measurements of Ca, Fe, and Se. *Fresen J Anal Chem* 370:618–623
- Boulyga SF, Klötzli U, Stingeder G et al (2007) Optimization and application of ICPMS with dynamic reaction cell for precise determination of  $^{44}\text{Ca}/^{40}\text{Ca}$  isotope ratios. *Anal Chem* 79:7753–7760
- Brazier JM et al (2015) Calcium isotope evidence for dramatic increase of continental weathering during the Toarcian oceanic anoxic event (Early Jurassic). *Earth Planet Sci Lett* 411:164–176
- Breit GN, Simmons EC, Goldhaber MB (1985) Dissolution of barite for the analysis of strontium isotopes and other chemical and isotopic variations using aqueous sodium carbonate. *Chem Geol Isot Geosci Sect* 52:333–336
- Bullen TD et al (2004) Calcium stable isotope evidence for three soil calcium pools at a granitoid chrono-sequence. In: Wanty RB, Seal RR (eds) *Water-rock interaction, proceedings of the 11th international symposium on water-rock interaction*, vol 1. Saratoga Springs/Taylor & Francis, New York/London, July 2004, pp 813–817
- Bushinsky DA, Chabala JM, Levi-Setti R (1990) Comparison of in vitro and in vivo  $^{44}\text{Ca}$  labeling of bone by scanning ion microprobe. *Am J Physiol* 259:586–592
- Carlson RW (2014) 15.18—thermal ionization mass spectrometry. In: Holland HD, Turekian KK (eds) *Treatise on geochemistry* (2nd Edn), 337–54. Elsevier, Oxford. <http://www.sciencedirect.com/science/article/pii/B978008080959757014273>
- Caro G, Papanastassiou DA, Wasserburg GJ (2010)  $^{40}\text{K}$ – $^{40}\text{Ca}$  isotopic constraints on the oceanic calcium cycle. *Earth Planet Sci Lett* 296:124–132
- Cecil MR, Ducea MN (2011) K–Ca ages of authigenic sediments: examples from Paleozoic glauconite and applications to low-temperature thermochronometry. *Int J Earth Sci* 100:1783–1790
- Centi-Tok B, Chabaux F, Lemarchand D et al (2009) The impact of water-rock interaction and vegetation on calcium isotope fractionation in soil- and stream waters of a small, forested catchment (the Strengbach case). *Geochim Cosmochim Acta* 73: 2215–2228
- Chang VTC, Williams RJP, Makishima A et al (2004) Mg and Ca isotope fractionation during  $\text{CaCO}_3$  biomineralisation. *Biochem Bioph Res Co* 323:79–85
- Channon MB, Gordon GW, Morgan JLL et al (2015) Using natural, stable calcium isotopes of human blood to detect and monitor changes in bone mineral balance. *Bone* 77:69–74. doi:[10.1016/j.bone.2015.04.023](https://doi.org/10.1016/j.bone.2015.04.023)
- Chu N-C, Henderson GM, Belshaw NS et al (2006) Establishing the potential of Ca isotopes as proxy for consumption of dairy products. *Appl Geochem* 21:1656–1667
- Church TM (1979) Marine barite. In: Burns RG (ed) *Marine minerals*. Mineralogical Society of America, Washington D.C., pp 175–209
- Clementz MT, Holden P, Koch PL (2003) Are calcium isotopes a reliable monitor of trophic level in marine settings? *Int J Osteoarchaeol* 13:29–36
- Cobert F et al (2011a) Biotic and abiotic experimental identification of bacterial influence on Ca isotopic signatures. *Rapid Commun Mass Spectrom* 25:2760–2768
- Cobert F, Schmitt AD, Bourgeade P et al (2011b) Experimental identification of Ca isotopic fractionations in higher plants. *Geochim Cosmochim Acta* 75:5467–5482
- Compston W, Oversby VM (1969) Lead isotopic analysis using a double spike. *J Geophys Res* 74(17):4338–4348
- Coplen TB (2011) Guidelines and recommended terms for expression of stable-isotope-ratio and gas-ratio measurement results. *Rapid Commun Mass Sp* 25:2538–2560
- Coplen TB, Hopple JA, Böhlke JK et al (2002) Compilation of minimum and maximum isotope ratios of selected elements in naturally occurring terrestrial materials and reagents. USGS, Reston, Virginia. 01–4222, 98 p
- Corless JT (1966) Determination of calcium-48 in natural calcium by neutron activation analysis. *Anal Chem* 38:810–813
- Corless JT (1968) Observations on the isotopic geochemistry of calcium. *Earth Planet Sci Lett* 4:475–478
- De La Rocha CL, DePaolo DJ (2000) Isotopic evidence for variations in the marine calcium cycle over the Cenozoic. *Science* 289:1176–1178
- DePaolo DJ (2004) Calcium isotopic variations produced by biological, kinetic, radiogenic and nucleosynthetic processes. *Rev Mineral Geochem* 55:255–288
- Du Vivier ADC, Jacobson AD, Lehn GO et al (2015) Ca isotope stratigraphy across the Cenomanian-Turonian OAE 2: links between volcanism, seawater geochemistry, and the carbonate fractionation factor. *Earth Planet Sci Lett* 416:121–131
- Duan Y, Su Y, Jin Z et al (2001) Measurements of calcium isotopes and isotope ratios: a new method

- based on helium plasma source “off-cone” sampling time-of-flight mass spectrometry. *J Anal At Spec* 16:756–761
- Eisenhauer A, Nögler TF, Stille P et al (2004) Proposal for an international agreement on Ca notation as result of the discussions from the workshops on stable isotope measurements in Davos (Goldschmidt 2002) and nice (EGS-AGU-EUG 2003). *Geostand Geoanal Res* 28:149–151
- Elliot T, Wehrs H, Coath C et al (2015) Collision cell MC-ICPMS. *Goldschmidt Abstr* 2015:824
- Epov VN, Malinovsky D, Vanhaecke F et al (2011) Modern mass spectrometry for studying mass-independent fractionation of heavy stable isotopes in environmental and biological sciences. *J Anal At Spec* 26:1142–1156
- Ewing SA, Yang W, DePaolo DJ et al (2008) Non-biological fractionation of stable Ca isotopes in soils of the Atacama Desert. *Chile Geochim Cosmochim Acta* 72:1096–1110
- Fantle MS, DePaolo DJ (2005) Variations in the marine Ca cycle over the past 20 million years. *Earth Planet Sci Lett* 237:102–117
- Fantle MS, DePaolo DJ (2007) Ca isotopes in carbonate sediment and pore fluid from ODP Site 807A: the  $\text{Ca}^{2+}(\text{aq})$ -calcite equilibrium fractionation factor and calcite recrystallization rates in Pleistocene sediments. *Geochim Cosmochim Acta* 71:2524–2546
- Fantle MS, Bullen TD (2009) Essentials of iron, chromium, and calcium isotope analysis of natural materials by thermal ionization mass spectrometry. *Chem Geol* 258:50–64
- Farkaš J, Buhl D, Blenkinsop J et al (2006) Evolution of the oceanic calcium cycle during the late Mesozoic: evidence from  $\delta^{44/40}\text{Ca}$  of marine skeletal carbonates. *Earth Planet Sci Lett* 253:96–111
- Farkaš J, Böhm F, Wallmann K et al (2007) Calcium isotope record of Phanerozoic oceans: implications for chemical evolution of seawater and its causative mechanisms. *Geochim Cosmochim Acta* 71:5117–5134
- Farkaš J et al (2011) Calcium isotope constraints on the uptake and sources of  $\text{Ca}^{2+}$  in a base-poor forest: a new concept of combining stable ( $\delta^{44/42}\text{Ca}$ ) and radiogenic ( $\epsilon\text{Ca}$ ) signals. *Geochim Cosmochim Acta* 75:7031–7046
- Feldmann I, Jakubowski N, Stuewer D (1999) Application of a hexapole collision and reaction cell in ICP-MS Part I: instrumental aspects and operational optimization. *Fresen J Anal Chem* 365:415–421
- Fietzke J, Eisenhauer A, Gussone N et al (2004) Direct measurement of  $^{44}\text{Ca}/^{40}\text{Ca}$  ratios by MC-ICP-MS using the cool plasma technique. *Chem Geol* 206:11–20
- Fletcher IR, Maggi AL, Rosman KJ et al (1997) Isotopic abundance measurements of K and Ca using a wide-dispersion multi-collector mass spectrometer and low-fractionation ionization techniques. *Int J Mass Spec Ion Proc* 163:1–17
- Gale NH (1970) A solution in closed form for lead isotopic analysis using a double spike. *Chem Geol* 6:305–310
- Galer SJG (1999) Optimal double and triple spiking for high precision lead isotopic measurement. *Chem Geol* 157:255–274
- Gangloff S et al (2014) Impact of bacterial activity on Sr and Ca isotopic compositions ( $^{87}\text{Sr}/^{86}\text{Sr}$  and  $\delta^{44/40}\text{Ca}$ ) in soil solutions (the Strengbach CZO). *Procedia Earth Planet Sci* 10:109–113
- Gopalan K, Macdougall D, Macisaac C (2006) Evaluation of a  $^{42}\text{Ca}$ – $^{43}\text{Ca}$  double-spike for high precision Ca isotope analysis. *Int J Mass Spectrom* 248:9–16
- Griffith EM, Schauble EA, Bullen TD et al (2008) Characterization of calcium isotopes in natural and synthetic barite. *Geochim Cosmochim Acta* 72:5641–5658
- Gussone N, Filipsson HL (2010) Calcium isotope ratios in calcitic test of benthic foraminifers. *Earth Planet Sci Lett* 290:108–117
- Gussone N, Eisenhauer A, Heuser A et al (2003) Model for kinetic effects on calcium isotope fractionation ( $\delta^{44}\text{Ca}$ ) in inorganic aragonite and cultured foraminifer (orbulina universa and globigerinoides sacculifer). *Geochim Cosmochim Acta* 67:1375–1382
- Gussone N, Eisenhauer A, Tiedemann R et al (2004) Reconstruction of caribbean sea surface temperature and salinity fluctuations in response to the pliocene closure of the central american gateway and radiative forcing, using  $\delta^{44/40}\text{Ca}$ ,  $\delta^{18}\text{O}$  and Mg/Ca ratios. *Earth Planet Sci Lett* 227:201–214
- Gussone N, Böhm F, Eisenhauer A et al (2005) Calcium isotope fractionation in calcite and aragonite. *Geochim Cosmochim Acta* 69:4485–4494
- Gussone N, Langer G, Thoms S et al (2006) Cellular calcium pathways and isotope fractionation in emiliania huxleyi. *Geology* 34:625–628
- Gussone N, Langer G, Riebesell U et al (2007) Calcium isotope fractionation in coccoliths of cultured calcidiscus leptoporus, helicosphaera carteri, syracosphaera pulchra and umbilicosphaera foliosa. *Earth Planet Sci Lett* 260:505–515
- Gussone N, Höhnisch B, Heuser A et al (2009) A critical evaluation of calcium isotope ratios in tests of planktonic foraminifers. *Geochim Cosmochim Acta* 73:7241–7255
- Gussone N, Zonneveld K, Kuhnert H (2010) Minor element and Ca isotope composition of calcareous dinoflagellate cysts of cultured thoracosphaera heimii. *Earth Planet Sci Lett* 289:180–188
- Gussone N, Nehrke G, Teichert BMA (2011) Calcium isotope fractionation in ikaite and vaterite. *Chem Geol* 285:194–202
- Halicz L, Galy A, Belshaw NS et al (1999) High-precision measurement of calcium isotopes in carbonates and related materials by multiple collector inductively coupled plasma mass spectrometry. *J Anal At Spec* 14:1835–1838
- Halliday AN, Christensen JN, Lee DC et al (2000) Multiple-collector inductively coupled plasma mass spectrometry. In: Barshick CM, Duckworth DC, Smith DH (eds) *Inorganic mass spectrometry—fundamentals and applications*. M. Dekker, Inc, New York, Basel, pp 291–327

- Hamelin B, Manhès G, Albarede F et al (1985) Precise lead isotopic measurements by the double spike technique: a reconsideration. *Geochim Cosmochim Acta* 49:173–182
- Harouaka K, Eisenhauer A, Fantle MS (2014) Experimental investigation of Ca isotopic fractionation during abiotic gypsum precipitation. *Geochim Cosmochim Acta* 129:157–176
- Harrison TM, Heizler MT, McKeegan KD et al (2010) In situ  $^{40}\text{K}$ – $^{40}\text{Ca}$  “double-plus” SIMS dating resolves Klokken feldspar 40 K–40Ar paradox. *Earth Planet Sci Lett* 299:426–433
- Hart SR, Zindler A (1989) Isotope fractionation laws: a test using calcium. *Int J Mass Spectrom Ion Process* 89:287–301
- Hensley TM (2006) Calcium isotopic variation in marine evaporites and carbonates: applications to late miocene mediterranean brine chemistry and late cenozoic calcium cycling in the oceans. PhD thesis, University of California
- Heumann KG, Gindner F, Klöppel H (1977) Abhängigkeit des calcium-isotopieeffekts von der elektrolytkonzentration bei der Ionenaustausch-chromatographie. *Angew Chem Ger Ed* 89:753–754
- Heumann KG, Kubassek E, Schwabenbauer W et al (1979) Analytical method for the K/Ca age determination of geological samples. *Fresen Z Anal Chem* 297:35–43
- Heuser A, Eisenhauer A (2008) The calcium isotope composition ( $\delta^{44/40}\text{Ca}$ ) of NIST SRM 915b and NIST SRM 1486. *Geostand Geoanal Res* 32:311–315
- Heuser A, Eisenhauer A (2010) A pilot study on the use of natural calcium isotope ( $^{44}\text{Ca}/^{40}\text{Ca}$ ) fractionation in urine as a proxy for the human body calcium balance. *Bone* 46:889–896
- Heuser A, Eisenhauer A, Gussone N et al (2002) Measurement of calcium isotopes ( $\delta^{44}\text{Ca}$ ) using a multicollector TIMS technique. *Int J Mass Spectrom* 220:387–399
- Heuser A, Eisenhauer A, Böhm F et al (2005) Calcium isotope ( $\delta^{44/40}\text{Ca}$ ) variations of neogene planktonic foraminifera. *Paleoceanography* 20, doi:10.1029/2004PA001048
- Heuser A, Tütken T, Gussone N et al (2011) Calcium isotopes in fossil bones and teeth—diagenetic versus biogenic origin. *Geochim Cosmochim Acta* 75:3419–3433
- Hindshaw RS, Reynolds BC, Wiederhold JG et al (2011) Calcium isotopes in a proglacial weathering environment: damma glacier, Switzerland. *Geochim Cosmochim Acta* 75:106–118
- Hindshaw RS, Reynolds BC, Wiederhold JG et al (2012) Calcium isotope fractionation in alpine plants. *Biogeochem* 112:373–388. doi:10.1007/s10533-012-9732-1
- Hindshaw RS, Bourdon B, Pogge von Strandmann PA et al (2013) The stable calcium isotopic composition of rivers draining basaltic catchments in Iceland. *Earth Planet Sci Lett* 374:173–184
- Hippler D, Schmitt A-D, Gussone N et al (2003) Calcium isotopic composition of various reference materials and seawater. *Geostand Geoanal Res* 27:13–19
- Hippler D, Eisenhauer A, Nägler TF (2006) Tropical atlantic SST history inferred from Ca isotope thermometry over the last 140 ka. *Geochim Cosmochim Acta* 70:90–100
- Hippler D, Kozdon R, Darling KF et al (2009) Calcium isotopic composition of high-latitude proxy carrier *Neoglobobulimina papyrifera* (sin.) *Biogeosc* 6:1–14
- Hirata T, Tanoshima M, Suga A et al (2008) Isotopic analysis of calcium in blood plasma and bone from mouse samples by multiple collector-ICP-mass spectrometry. *Anal Sci* 24:1501–1507
- Holmden C (2005) Measurement of  $\delta^{44}\text{Ca}$  using a  $^{43}\text{Ca}$ – $^{42}\text{Ca}$  double-spike TIMS technique; in summary of investigations 2005, Volume 1, Saskatchewan geological survey, Sask. Industry Resources, Misc Rep 2005-1, CD-ROM, Paper A-4, 7 p
- Holmden C (2009) Ca isotope study of Ordovician dolomite, limestone, and anhydrite in the Williston Basin: implications for subsurface dolomitization and local Ca cycling. *Chem Geol* 268:180–188
- Holmden C, Bélanger N (2010) Ca isotope cycling in a forested ecosystem. *Geochim Cosmochim Acta* 74:995–1015
- Holmden C et al (2012) Tightly coupled records of Ca and C isotope changes during the Hinuanian glaciations event in an epeiric sea setting. *Geochim Cosmochim Acta* 98:94–106
- Horn I, von Blanckenburg F, Schoenberg R et al (2006). In situ iron isotope ratio determination using UV-Femtosecond laser ablation with application to hydrothermal ore formation processes. *Geochimica Et Cosmochimica Acta* 70:3677–3688. doi:10.1016/j.gca.2006.05.002
- Huang S, Farkaš J, Jacobsen SB (2010) Calcium isotopic fractionation between clinopyroxene and orthopyroxene from; mantle peridotites. *Earth Planet Sci Lett* 292:337–344
- Huang S, Farkas J, Jacobsen SB (2011) Stable calcium isotopic compositions of hawaiian shield lavas: evidence for recycling of ancient marine carbonates into the mantle. *Geochim Cosmochim Acta* 75(17): 4987–4997
- Immenhauser A, Nägler TF, Steuber T, Hippler D (2005) A critical assessment of mollusk 18O/16O, Mg/Ca, and 44Ca/40Ca ratios as proxies for Cretaceous seawater temperature seasonality. *Palaeogeogr Palaeoclimatol Palaeoecol* 215:221–237
- Ireland TR (1990) Presolar isotopic and chemical signatures in hibonite-bearing refractory inclusions from the Murchison carbonaceous chondrite. *Geochim Cosmochim Acta* 54:3219–3237
- Jacobson AD, Holmden C (2008)  $\delta^{44}\text{Ca}$  evolution in a carbonate aquifer and its bearing on the equilibrium isotope fractionation factor for calcite. *Earth Planet Sci Lett* 270:349–353
- John T, Gussone N, Podladchikov YY et al (2012) Volcanic arcs fed by rapid pulsed fluid flow through subducting slabs. *Nat Geosci* 5:489–492
- Johnson CM, Beard BL (1999) Correction of instrumentally produced mass fractionation during isotopic

- analysis of Fe by thermal ionization mass spectrometry. *Int J Mass Spectrom* 193:87–99
- Kasemann SA, Hawkesworth CJ, Prave AR et al (2005) Boron and calcium isotope composition in Neoproterozoic carbonate rocks from Namibia: evidence from extreme environmental change. *Earth Planet Sci Lett* 231:73–86
- Kasemann SA, Schmidt DN, Pearson PN et al (2008) Biological and ecological insights into Ca isotopes in planktic foraminifers as a paleotemperature proxy. *Earth Planet Sci Lett* 271:292–302
- Komiya T, Suga A, Ohno T et al (2008) Ca isotopic compositions of dolomite, phosphorite and the oldest animal embryo fossils from the Neoproterozoic in Weng'an, South China. *Gondwana Res* 14:209–218
- Koornneef JM, Bouman C, Schwieters JB et al (2013) Use of 1012 Ohm current amplifiers in Sr and Nd isotope analyses by TIMS for application to sub-nanogram samples. *J Anal At Spec* 28:749–54. doi:[10.1039/C3JA30326H](https://doi.org/10.1039/C3JA30326H)
- Koumenis IL, Vestal ML, Yergey AL et al (1995) Quantitation of metal isotope ratios by laser desorption time-of-flight mass spectrometry. *Anal Chem* 67:4557–4564
- Kreissig K, Elliott T (2005) Ca isotope fingerprints of early crust-mantle evolution. *Geochim Cosmochim Acta* 69:165–176
- Lehn GO, Jacobson AD (2015) Optimization of a  $^{48}\text{Ca}$ – $^{43}\text{Ca}$  double-spike MC-TIMS method for measuring Ca isotope ratios ( $\delta^{44/40}\text{Ca}$  and  $\delta^{44/42}\text{Ca}$ ): limitations from filament reservoir mixing. *J Anal At Spectrom* 30:1571–1581
- Lehn GO, Jacobson AD, Holmden C (2013) Precise analysis of Ca isotope ratios ( $\delta^{44/40}\text{Ca}$ ) using an optimized  $^{43}\text{Ca}$ – $^{42}\text{Ca}$  double-spike MC-TIMS method. *Int J Mass Spectrometry* 351:69–75
- Lemarchand D, Wasserburg GJ, Papanastassiou DA (2004) Rate-controlled calcium isotope fractionation in synthetic calcite. *Geochim Cosmochim Acta* 68 (22):4665–5678
- Longerich HP, Fryer BJ, Strong DF (1987) Determination of lead isotope ratios by inductively coupled plasma-mass spectrometry (ICP-MS). *Spectrochim Acta, Part B* 42:39–48. doi:[10.1016/0584-8547\(87\)80048-4](https://doi.org/10.1016/0584-8547(87)80048-4)
- Ludwig KR (1997) Optimization of multicollector isotope-ratio measurement of strontium and neodymium. *Chem Geol* 135:325–334. doi:[10.1016/S0009-2541\(96\)00120-9](https://doi.org/10.1016/S0009-2541(96)00120-9)
- Lundberg LL, Zinner E, Crozaz G (1994) Search for isotopic anomalies in oldhamite (CaS) from unequilibrated (E3) enstatite chondrites. *Meteoritics* 29: 384–393. doi:[10.1111/j.1945-5100.1994.tb00602.x](https://doi.org/10.1111/j.1945-5100.1994.tb00602.x)
- Magna T, Gussone N, Mezger K (2015) The calcium isotope systematics of mars. *Earth Planet Sci Lett* 430:86–94
- Maréchal CN, Télouk P, Albarède F (1999) Precise analysis of copper and zinc isotopic compositions by plasma-source mass spectrometry. *Chem Geol* 156:251–273
- Marriott CS, Henderson GM, Belshaw NS et al (2004) Temperature dependence of  $\delta^7\text{Li}$ ,  $\delta^{44}\text{Ca}$  and Li/Ca during growth of calcium carbonate. *Earth Planet Sci Lett* 222:615–624
- Marshall BD, DePaolo DJ (1982) Precise age determinations and petrogenetic studies using the K–Ca method. *Geochim Cosmochim Acta* 46:2537–2545
- Marshall BD, DePaolo DJ (1989) Calcium isotopes in igneous rocks and the origin of granite. *Geochim Cosmochim Acta* 53:917–922
- Marshall BD, Woodard HH, Krueger HW et al (1986) K–Ca–Ar systematics of authigenic sanidine from Wakau, Wisconsin, and the diffusivity of argon. *Geology* 14:936–938
- Martin JE, Tacail T, Adnet S et al (2015) Calcium isotopes reveal the trophic position of extant and fossil elasmobranchs. *Chem Geol* 415:118–125. doi:[10.1016/j.chemgeo.2015.09.011](https://doi.org/10.1016/j.chemgeo.2015.09.011)
- Möller P, Papendorf H (1971) Fractionation of calcium isotopes in carbonate precipitates. *Earth Planet Sci Lett* 11:192–194
- Morgan JLL, Gordon GW, Arrua RC et al (2011) High-precision measurement of variations in calcium isotope ratios in urine by multiple collector inductively coupled plasma mass spectrometry. *Anal Chem* 83:6956–6962. doi:[10.1021/ac200361t](https://doi.org/10.1021/ac200361t)
- Morgan JLL, Skulan JL, Gordon GW et al (2012) Rapidly assessing changes in bone mineral balance using natural stable calcium isotopes. *Proc Nat Acad Sci* 109:9989–9994
- Murphy KE, Long SE, Rearick MS et al (2002) The accurate determination of potassium and calcium using isotope dilution inductively coupled “cold” plasma mass spectrometry. *J Anal At Spec* 17:469–477
- Nägler T, Villa I (2000) In pursuit of the  $^{40}\text{K}$  branching ratios: K–Ca and  $^{39}\text{Ar}$ – $^{40}\text{Ar}$  dating of gem silicates. *Chem Geol* 169:5–16
- Nägler TF, Eisenhauer A, Müller A et al (2000) The  $\delta^{44}\text{Ca}$ -temperature calibration on fossil and cultured globigerinoides sacculifer. *Geochim Geophys Geosyst* 1: doi:[10.1029/2000GC000091](https://doi.org/10.1029/2000GC000091)
- Naumenko-Dèzes MO, Bouman C, Nægler ThF et al (2015) TIMS measurements of full range of natural Ca isotopes with internally consistent fractionation correction. *Int J Mass Spectrom* 387:60–68. doi:[10.1016/j.ijms.2015.07.012](https://doi.org/10.1016/j.ijms.2015.07.012)
- Nelson DR, McCulloch MT (1989) Petrogenic applications of the  $^{40}\text{K}$ – $^{40}\text{Ca}$  radiogenic decay scheme—a reconnaissance study. *Chem Geol* 79:275–293
- Nelson F et al (1964) Ion exchange procedures. I. Cation exchange in concentration HCl and  $\text{HClO}_4$  solutions. *J Chromatogr* 13:503–535
- Nezat CA, Blum JD, Driscoll ChT (2010) Patterns of Ca/Sr and  $^{87}\text{Sr}/^{86}\text{Sr}$  variation before and after a whole watershed  $\text{CaSiO}_3$  addition at the Hubbard Brook experimental forest, USA. *Geochim Cosmochim Acta* 74:3129–3142
- Nicolussi GK, Pellen MJ, Calaway WF et al (1997) Isotopic analysis of Ca from extraterrestrial micrometer-sized SiC by laser desorption and resonant ionization mass spectrometry. *Anal Chem* 69:1140–1146

- Page BD, Bullen TD, Mitchell MJ (2008) Influences of calcium availability and tree species on Ca isotope fractionation in soil and vegetation. *Biogeochemistry* 88:1–13
- Patterson KY, Veillon C, Hill AD et al (1999) Measurement of calcium stable isotope tracers using cool plasma ICP-MS. *J Anal At Spec* 14:1673–1677
- Paytan A, Kastner M, Martin EE et al (1993) Marine barite as a monitor of seawater strontium isotope composition. *Nature* 366:445–449
- Perakis SS, Maguire DA, Bullen TD et al (2006) Coupled nitrogen and calcium cycles in forests of the Oregon coast range. *Ecosystems* 9:63–74
- Platzner IT (2000) Modern isotope ratio mass spectrometry. Wiley, Chicester
- Powell R, Woodhead J, Hergt J (1998) Uncertainties on lead isotope analyses; deconvolution in the double-spike method. *Chem Geol* 148(1–2):95–104
- Rehkämper M, Schönbachler M, Stirling CH (2001) Multiple collector ICP-MS: introduction to instrumentation, measurement techniques and analytical capabilities. *Geostand News* 25:23–40
- Rehkämper M, Wombacher F, Aggarwal JK (2004) Chapter 31—stable isotope analysis by multiple collector ICP-MS. In: de Groot PA (eds) *Handbook of stable isotope analytical techniques*. Elsevier, Amsterdam, pp 692–725. <http://www.sciencedirect.com/science/article/pii/B9780444511140500338>
- Reynard LM, Henderson GM, Hedges REM (2010) Calcium isotope ratios in animal and human bone. *Geochim Cosmochim Acta* 74:3735–3750
- Reynard LM, Henderson GM, Hedges REM (2011) Calcium isotopes in archaeological bones and their relationships to dairy consumption. *J Archaeol Sci* 38:657–664
- Rollion-Bard C, Vigier N, Spezzaferri S (2007) In situ measurements of calcium isotopes by ion microprobe in carbonates and application to foraminifera. *Chem Geol* 244:679–690
- Romaniello SJ, Field M, Smith HB et al (2015) Fully automated chromatographic purification of Sr and Ca for isotopic analysis. *J Anal At Spectrom* 30:1906–1912. doi:10.1039/C5JA00205B
- Roy S, Gillen G, Conway WS et al (1995) Use of secondary ion mass spectrometry to image 44 calcium uptake in the cell walls of apple fruit. *Protoplasma* 189:163–172
- Russell WA, Papanastassiou DA (1978) Calcium isotope fractionation in ion-exchange chromatography. *Anal Chem* 50:1151–1154
- Russell WA, Papanastassiou DA, Tombrello TA (1978) Ca isotope fractionation on the earth and other solar system materials. *Geochim Cosmochim Acta* 42:1075–1090
- Ryu JS, Jacobson AD, Holmden C et al (2011) The major ion,  $\delta^{44/40}\text{Ca}$ ,  $\delta^{44/42}\text{Ca}$ , and  $\delta^{26/24}\text{Mg}$  geochemistry of granite weathering at pH = 1 and T = 25 °C: power-law processes and the relative reactivity of minerals. *Geochim Cosmochim Acta* 75:6004–6026
- Santamaria-Fernandez R, Wolff J-C (2010) Application of laser ablation multicollector inductively coupled plasma mass spectrometry for the measurement of calcium and lead isotope ratios in packaging for discriminatory purposes. *Rapid Comm Mass Sp* 24:1993–1999
- Schiller M et al (2012) Calcium isotope measurement by combined HR-MC-ICPMS and TIMS. *J Anal Atom Spectrom* 27:38–49
- Schmitt AD, Stille P (2005) The source of calcium in wet atmospheric deposits: Ca–Sr isotope evidence. *Geochim Cosmochim Acta* 69:3463–3468
- Schmitt AD, Bracke G, Stille P et al (2001) The calcium isotope composition of modern seawater determined by thermal ionisation mass spectrometry. *Geostand Newslett* 25:267–275
- Schmitt AD, Chabaux F, Stille P (2003a) The calcium riverine and hydrothermal isotopic fluxes and the oceanic calcium mass balance. *Earth Planet Sci Lett* 213:503–518
- Schmitt AD, Stille P, Vennemann T (2003b) Variations of the  $^{44}\text{Ca}/^{40}\text{Ca}$  ratio in seawater during the past 24 million years: evidence from  $\delta^{44}\text{Ca}$  and  $\delta^{18}\text{O}$  values of miocene phosphates. *Geochim Cosmochim Acta* 67:2607–2614
- Schmitt AD, Gangloff S, Cobert F et al (2009) High performance automated ion chromatography separation for Ca isotope measurements in geological and biological samples. *J Anal At Spec* 24:1089–1097
- Schmitt AD, Cobert F, Bourgeade P et al (2013) Calcium isotope fractionation during plant growth under a limiting nutrient supply. *Geochim Cosmochim Acta* 110:70–83
- Shaheen ME, Gagnon JE, Fryer BJ (2012) Femtosecond (fs) lasers coupled with modern ICP-MS instruments provide new and improved potential for in situ elemental and isotopic analyses in the geosciences. *Chem Geol* 330–331:260–273. doi:10.1016/j.chemgeo.2012.09.016
- Shiel AE, Barling J, Orians KJ et al (2009) Matrix effects on the multi-collector inductively coupled plasma mass spectrometric analysis of high-precision cadmium and zinc isotope ratios. *Anal Chim Acta* 633:29–37. doi:10.1016/j.aca.2008.11.026
- Shih C-Y, Nyquist LE, Bogard DD et al (1994) K–Ca and Rb–Sr dating of two lunar granites: relative chronometer resetting. *Geochim Cosmochim Acta* 58:3101–3116
- Siebert C, Nögler TF, Kramers JD (2001) Determination of molybdenum isotope fractionation by double-spike multicollector inductively coupled plasma mass spectrometry. *Geochem Geophys Geosyst* 2:2000GC000124
- Silva-Tamayo JC, Nögler TF, Villa IM et al (2010) Global Ca isotope variations in c. 0.7 Ga old post-glacial carbonate successions. *Terra Nova* 22:188–194
- Sime NG, De La Rocha CL, Galy A (2005) Negligible temperature dependence of calcium isotope fractionation in 12 species of planktonic foraminifera. *Earth Planet Sci Lett* 232:51–66



- Sime NG, De La Rocha CL, Tipper ET et al (2007) Interpreting the Ca isotope record of marine biogenic carbonates. *Geochim Cosmochim Acta* 71:3979–3989
- Simon JJ, DePaolo DJ (2010) Stable calcium isotopic composition of meteorites and rocky planets. *Earth Planet Sci Lett* 289:457–466
- Simon JJ, DePaolo DJ, Moynier F (2009) Calcium isotope composition of meteorites, earth and mars. *Astrophys J* 702:707–715
- Skulan JL, DePaolo DJ (1999) Calcium isotope fractionation between soft and mineralized tissues as a monitor of calcium use in vertebrates. *Proc Nat Acad Sci* 96:13709–13713
- Skulan JL, DePaolo DJ, Owens TL (1997) Biological control of calcium isotopic abundances in the global calcium cycle. *Geochim Cosmochim Acta* 61:2505–2510
- Smith DL (1983) Determination of stable isotopes of calcium in biological fluids by fast atom bombardment mass spectrometry. *Anal Chem* 55:2391–2393
- Soudry D, Glenn C, Nathan Y et al (2006) Evolution of tethyan phosphogenesis along the northern edges of the Arabian-African shield during the Cretaceous-Eocene as deduced from temporal variations of Ca and Nd isotopes and rates of P accumulation. *Earth Sci Rev* 78:27–57
- Steiger RH, Jäger E (1977) Subcommittee on geochronology: convention on the use of decay constants in geo- and cosmochemistry. *Earth Planet Sci Lett* 36:359–362
- Steinmann M, Stille P (1997) Rare earth element behavior and Pb, Sr, Nd isotope systematics in a heavy metal contaminated soil. *Appl Geochem* 12:607–624
- Steinmann M, Stille P (2006) Rare earth element transport and fractionation in small streams of a mixed basaltic-granitic catchment basin (Massif Central, France). *J Geoch Expl* 88:336–340
- Steuber T, Buhl D (2006) Calcium isotope fractionation in selected modern and ancient marine carbonates. *Geochim Cosmochim Acta* 70:5507–5521
- Stille P, Clauer N (1994) The process of glauconization: chemical and isotopic evidence. *Contrib Mineral Petrol* 117:253–262
- Stürup S (2004) The use of ICMPS for stable isotope tracer studies in humans: a review. *Anal Bioanal Chem* 378:273–282
- Stürup S, Bendahl L, Gammelgaard B (2006) Optimisation of dynamic reaction cell (DRC)-ICP-MS for the determination of  $^{42}\text{Ca}/^{43}\text{Ca}$  and  $^{44}\text{Ca}/^{43}\text{Ca}$  isotope ratios in human urine. *J Anal At Spec* 21:297–304
- Tacail T, Albalat E, Télouk P et al (2014) A simplified protocol for measurement of Ca isotopes in biological samples. *J Anal At Spectrom* 29:529–535
- Tacail T, Télouk P, Balter V (2016) Precise analysis of calcium stable isotope variations in biological apatites using laser ablation MC-ICPMS. *J At Anal Spectrom* 31:152–162
- Takano B, Watanuki K (1972) Strontium and calcium coprecipitation with lead-bearing barite from hot spring water. *Geochem J* 6:1
- Taylor SR, McLennan SM (1985) The continental crust. Its evolution and composition. Blackwell Science, Oxford
- Teichert BMA, Gussone N, Eisenhauer A et al (2005) Clathrites: archives of near-seafloor pore-fluid evolution ( $\delta^{44/40}\text{Ca}$ ,  $\delta^{13}\text{C}$ ,  $\delta^{18}\text{O}$ ) in gas hydrate environments. *Geology* 33:213–216
- Teichert BMA, Gussone N, Torres ME (2009) Controls on calcium isotope fractionation in sedimentary porewaters. *Earth Planet Sci Lett* 279:373–382
- Tera F et al (1970) Comparative study of Li, Na, K, Rb, Cs, Ca, Sr and Ba abundances in achondrites and in Apollo II lunar samples. *Proceedings of the Apollo II Lunar Conferences* 2:1637–1657
- Tipper ET, Galy A, Bickle MJ (2006) Riverine evidence for a fractionated reservoir of Ca and Mg on the continents: implications for the oceanic Ca cycle. *Earth Planet Sci Lett* 247:267–279
- Tipper ET, Galy A, Bickle MJ (2008a) Calcium and magnesium isotope systematics in rivers draining the Himalaya-Tibetan plateau region: lithological or fractionation control. *Geochim Cosmochim Acta* 72:1057–1075
- Tipper ET, Louvat P, Capmas F et al (2008b) Accuracy of stable Mg and Ca isotope data obtained by MC-ICP-MS using the standard addition method. *Chem Geol* 257:65–75
- Tipper ET, Gailiart J, Galy A et al (2010) Calcium isotope ratios in the world's largest rivers: a constraint on the maximum imbalance of oceanic calcium fluxes. *Global Biogeochem. Cy.* 24, doi:[10.1029/2009GB003574](https://doi.org/10.1029/2009GB003574)
- Upadhyay D, Scherer EE, Mezger K (2008) Fractionation and mixing of Nd isotopes during thermal ionization mass spectrometry: implications for high precision Nd-142/Nd-144 analyses. *J Anal At Spec* 23:561–568. doi:[10.1039/b715585a](https://doi.org/10.1039/b715585a)
- Valdes MC, Moreira M, Foriel J et al (2014) The nature of earth's building blocks as revealed by calcium isotopes. *Earth Planet Sci Lett* 394:135–145
- Vanhaecke F, Balcaen L, Malinovsky D (2009) Use of single-collector and multi-collector ICP-mass spectrometry for isotopic analysis. *J Anal At Spec* 24:863–886
- von Allmen K, Böttcher M, Samankassou E et al (2010a) Barium isotope fractionation in the global barium cycle: first evidence from barium minerals and precipitation experiments. *Chem Geol* 277:70–77
- von Allmen K, Nägler TF, Pettke et al (2010b) Stable isotope profiles (Ca, O, C) through modern brachiopod shells of *T. septentrionalis* and *G. vitreus*: implications for calcium isotope paleo-ocean chemistry. *Chem Geol* 269:210–219
- Walder AJ, Freedman PA (1992) Communication. Isotopic ratio measurement using a double focusing magnetic sector mass analyser with an inductively coupled plasma as an ion source. *J Anal At Spec* 7:571–575. doi:[10.1039/JA9920700571](https://doi.org/10.1039/JA9920700571)
- Wang S, Yan W, Magalhães HV et al (2012) Calcium isotope fractionation and its controlling factors over authigenic carbonates in the cold seeps of the northern South China Sea. *Chinese Sci Bull* 57:1325–1332



- Wang S, Yan W, Magalhães HV et al (2013) Factors influencing methane-derived authigenic carbonate formation at cold seep from southwestern Dongsha area in the northern South China. *Environ Earth Sci*. doi:[10.1007/s12665-013-2611-9](https://doi.org/10.1007/s12665-013-2611-9)
- Weber D, Zinner E, Bischoff A (1995) Trace element abundances and magnesium, calcium, and titanium isotopic compositions of grossite-containing inclusions from the carbonaceous chondrite acfer 182. *Geochim Cosmochim Acta* 59:803–823
- Weyer S, Schwieters JB (2003) High precision Fe isotope measurements with high mass resolution MC-ICPMS. *Int J Mass Spectrom* 226:355–368
- Wiegand BA, Schwendenmann L (2013) Sources in small tropical catchments (La Selva, Costa Rica). A comparison of Sr and Ca isotopes. *J Hydrol* 488:110–117
- Wiegand BA, Chadwick OA, Vitousek PM et al (2005) Ca cycling and isotopic fluxes in forested ecosystems in Hawaii. *Geophys Res Lett* 32:L11404
- Wieser ME, Schwieters JB (2005) The development of multiple collector mass spectrometry for isotope ratio measurements. *Int J Mass Spectrom* 242:97–115
- Wieser ME, Buhl D, Bouman C et al (2004) High precision calcium isotope ratio measurements using a magnetic sector multiple collector inductively coupled plasma mass spectrometer. *J Anal At Spec* 19:844–851
- Wombacher F, Rehkämper M (2003) Investigation of the mass discrimination of multiple collector ICP-MS using neodymium isotopes and the generalised power law. *J Anal At Spectrom* 18:1371–1375
- Wombacher F, Eisenhauer A, Heuser A et al (2009) Separation of Mg, Ca and Fe from geological reference materials for stable isotope ratio analyses by MC-ICP-MS and double-spike TIMS. *J Anal At Spec* 24:627–636
- Zinner EK, Fahey AJ, Goswami JN et al (1986) Large  $^{48}\text{Ca}$  anomalies are associated with  $^{50}\text{Ti}$  anomalies in Murchison and Murray hibonites. *Ap J* 311:L103–L107
- Yang L (2009) Accurate and precise determination of isotopic ratios by MC-ICP-MS: a review. *Mass Spectrom Rev* 28:990–1011. doi:[10.1002/mas.20251](https://doi.org/10.1002/mas.20251)
- Young ED, Galy A, Nagahara H (2002) Kinetic and equilibrium mass-dependent isotope fractionation laws in nature and their geochemical and cosmochemical significance. *Geochim Cosmochim Acta* 66:1098–1104
- Zhu P, Macdougall JD (1998) Calcium isotopes in the marine environment and the oceanic calcium cycle. *Geochim Cosmochim Acta* 62:1691–1698

Calcium Stable Isotope Geochemistry

Gussone, N.; Schmitt, A.-D.; Heuser, A.; Wombacher, F.;

Dietzel, M.; Tipper, E.; Schiller, M.

2016, X, 260 p. 102 illus., 37 illus. in color., Hardcover

ISBN: 978-3-540-68948-5